UNIVERSIDADE DE LISBOA
FACULDADE DE CIÊNCIAS
DEPARTAMENTO DE QUÍMICA E BIOQUÍMICA

Alpha-Synuclein Phosphorylation Role on Parkinson's Disease

Carolina da Silva Madaleno

Mestrado em Bioquímica

Especialização em Bioquímica

Dissertação orientada por:

Sandra Isabel Nogueira Tenreiro, PhD

Francisco Rodrigues Pinto, PhD

2017

Acknowledgments

In this gesture, I would like to mention and recognize the ones involved in this journey.

First and foremost, to my supervisor Dra. Sandra Tenreiro, whose dedication, patience and optimism were crucial during the development of this research project. I am sincerely grateful for the precious knowledge she transmitted, for her trust, for her effort in keeping me motivated and valuable guidance throughout this time, as well as for the treasured tools she acquainted me with, that made it possible to grow as a person and as a scientist. To my co-supervisor, Dr. Francisco Pinto, for his time and assistance during this project.

To *Cell and Molecular Neuroscience* group, to Dr. Tiago Fleming Outeiro, for this wonderful research opportunity in his lab group, for welcoming me and for his words of advice in the pursuing of a science path. Likewise, I am thankful to the members of the group I worked more closely with, Inês Brás, for her friendship, encouragement and help and to Dr. Hugo Miranda, for his insightful comments and availability.

To CEDOC community, for the sympathy shown by all researchers, for the interesting seminars and discussions organized and for the passion for science transmitted. A special gratitude goes for the kindness and help of the technical team and of the Flow Cytometry Unit.

To FCUL, for the assistance during the entire master's degree and for the nicely carried incorporation in the faculty.

To my friends for the endless emotional support and motivation given when I needed it the most, a special thank you to Vera Xistra, Mariana Caetano, Mariana Morais and Ricardo Morais.

For last but not the least important, to my family. To my parents, Salomé Madaleno and Manuel Madaleno, my brother Romeu Madaleno and my sister-in-law Marília Fernandes, for always supporting me in the dream of becoming a scientist, for believing in me, for their daily caring and unconditional support during this stage and throughout my entire life.

With these words I hope to return the affection and dedication you have always offered me during this time, each one of you shed a special light during my path.

Resumo

A incorreta aquisição da estrutura final e consequente agregação de proteínas são a principal causa para o desenvolvimento de patologias neuro-degenerativas, tais como a doença de Parkinson (DP), de Alzheimer (DA) e Huntington (DH).

A DP é a segunda mais comum doença neuro-degenerativa, afetando entre 1 a 2% da população acima dos 60 anos de idade nos países industrializados, sendo a Europa o continente mais afetado. Clinicamente, esta doença é caracterizada por tremor e rigidez musculares e instabilidade postural e de marcha. Eventualmente, há ainda o aparecimento de sintomas não-motores, tais como psicose e demência. Os sintomas motores, apenas detetados no momento do diagnóstico, ocorrem quando já uma significativa parte da população neuronal foi afetada e atualmente, a estratégia de tratamento é ainda paliativa, em vez de curativa. Patologicamente, a DP caracteriza-se pela acumulação da proteína α-Synucleína (αSyn), que forma inclusões intracelulares designadas por corpos de Lewis (CLs), causando a perda progressiva de neurónios dopaminérgicos na região cerebral da *Substantia Nigra* (SN) *pars compacta* e, em estádios mais avançados da doença, espalhando-se às restantes populações neuronais. Atualmente, é aceite que o papel pato-fisiológico da αSyn reside na sua agregação, no entanto, é ainda desconhecido quais os fatores que desencadeiam esse mesmo evento, assim como quais os mecanismos celulares e quais os intermediários proteicos responsáveis pela neuro-toxicidade.

A DP tem duas variantes, que têm como elo comum a agregação da αSyn: a esporádica e a familiar (menos de 10% dos casos). Assim, o estudo de uma das formas contribui para a compreensão do mecanismo patológico da outra. A forma esporádica da doença é desencadeada principalmente pela idade avançada e/ou fatores ambientais, enquanto a forma familiar ocorre prematuramente e com um fenótipo mais severo e é caracterizada pela existência de predisposições e mutações genéticas.

No caso da αSyn, mutações que originam duplicações e triplicações do gene que codifica esta proteína (gene *SNCA*), assim como as substituições de aminoácidos A30P, E46K, H50Q, G51D A53T e A53E na sequência da αSyn foram identificadas como associadas à forma familiar de DP. Adicionalmente, modificações pós-traducionais (MPTs) da αSyn, tais como a fosforilação do resíduo de serina S129, que em 90% da αSyn nos CLs se encontra fosforilada, em contraste com os 4% em condições fisiológicas, e recentemente, a identificação de aumento da fosforilação do resíduo de serina S87, estão associadas a ambas as formas esporádica e familiar da doença. No entanto, os mecanismos celulares e a toxicidade intrínseca pelos quais as mutações familiares contribuem para o papel neuropatológico da αSyn são ainda desconhecidos, assim como o papel neuro-protetor ou prejudicial da fosforilação da αSyn é ainda alvo de debate, já que diferentes modelos celulares apresentam diferentes efeitos na toxicidade da αSyn, quando fosforilada no resíduo S129. Em relação ao papel patológico da fosforilação do resíduo S87, este ainda não foi totalmente explorado, principalmente devido a duas principais limitações: este resíduo não é conservado entre espécies, o que dificulta o estabelecimento de conclusões de modelos de ratinhos para humanos, e é apenas fosforilável em humanos, o que evidencia um papel importante deste resíduo no desenvolvimento da DP.

A levedura *Saccharomyces cerevisiae (S. cerevisiae)* é um organismo unicelular que partilha um elevado grau de conservação de várias vias celulares básicas com outros eucariotas superiores, tais como o ser humano, como por exemplo o controlo de qualidade proteico. Este organismo foi estabelecido como um modelo celular para a compreensão de diversos mecanismos biológicos, assim como no estudo de doenças neuro-degenerativas. Nomeadamente, o estudo dos processos de fosforilação e agregação da αSyn, assim como a pato-biologia desta proteína são passíveis de ser estudados neste

organismo, uma vez que em levedura foi previamente demonstrado que a expressão da αSyn humana induz a formação de inclusões citoplasmáticas e confere toxicidade às células, de forma semelhante ao que ocorre não só noutros modelos biológicos, como ratinho e linhas celulares de mamífero, como também nos cérebros de pacientes com DP. Adicionalmente, a utilização deste organismo confere várias vantagens, como o a sua facilidade de manipulação, o curto tempo de geração, o genoma estar sequenciado e devidamente anotado em bases de dados e ser facilmente manipulável geneticamente.

Assim, utilizando a levedura como modelo celular, este projeto teve como objetivos abordar a pato-biologia da αSyn em ambas as vertentes esporádica e familiar da DP, nomeadamente A) na caracterização fenotípica da mais recentemente mutação identificada como associada a DP familiar, a mutação da αSyn A53E e B) o estudo da interação da fosforilação entre os resíduos S87 e S129. Para atingir os objetivos propostos, o fenótipo da mutação A53E foi caracterizado recorrendo à avaliação da viabilidade celular, formação de inclusões, expressão e fosforilação da αSyn, solubilidade dos agregados de αSyn e avaliação das alterações da rede mitocondrial. O efeito da fosforilação nos resíduos S129 e S87 foi estudado utilizando estirpes de levedura com o gene que codifica a proteína αSyn humana integrado no genoma, usando diferentes versões mutadas da αSyn, nomeadamente, mutantes que mimetizam e bloqueiam a fosforilação no resíduo S129, os mutantes S129D e S129A, respetivamente, o mutante que mimetiza a fosforilação no resíduo S87 (S87E) e um duplo mutante que mimetiza a simultânea fosforilação no resíduo S87 e S129 (S87E_S129D). Para este grupo de fosfo-mutantes foram avaliados os parâmetros de viabilidade celular, formação de inclusões, expressão, fosforilação e remoção intracelular da αSyn e a função dos mecanismos de manutenção da qualidade celular (função proteossomal e autofágica).

Resultante desta análise, foi observado que a expressão da proteína mutante A53E αSyn não resulta em diferenças significativas no fenótipo dos parâmetros avaliados, quando comparado com a expressão da proteína nativa (WT). De facto, a expressão da mutação A53E induz toxicidade e formação de inclusões, mas de forma equivalente à proteína WT, embora com tendência para diminuir o número de inclusões e ainda, relativamente à natureza das inclusões, a solubilidade das inclusões aparenta ser semelhante à proteína WT. Estes resultados estão em parte em concordância com estudos *in vitro* realizados, que descrevem um fenótipo da A53E de toxicidade celular semelhante à proteína WT.

Relativamente ao estudo da interação da fosforilação entre os resíduos S87 e S129, foi observado que quando a fosforilação no resíduo S87 é mimetizada (mutante S87E), a formação de inclusões e toxicidade conferidas pela αSyn aumentam significativamente (aproximadamente 80% de células com inclusões), causando a perda de função proteossomal e ativando a autofagia, quando comparando com a expressão da proteína WT. Surpreendentemente, quando a mutação S87E foi acoplada à mutação que mimetiza a fosforilação no resíduo S129 (mutante S87E_S129D), o fenótipo de toxicidade induzindo pelo mutante S87E é inexistente, prevalecendo um suposto efeito protetor da fosforilação no resíduo S129 (mutante S129D). Adicionalmente, é possível observar que o mutante S87E_S129D tem menos formação de inclusões e apresenta menos toxicidade que a expressão da proteína WT, o que permite inferir que não só prevalece o efeito protetor da mutação S129D sobre o efeito tóxico da mutação S87E, como também poderá existir um efeito sinérgico neuro-protetor quando ambos os resíduos se encontram fosforilados simultaneamente.

Explorar os mecanismos específicos com outros organelos assim como os eventos iniciais da agregação, nomeadamente aquando da presença de mutações familiares, é crucial para a determinação de como a αSyn induz toxicidade celular no caso da forma familiar de DP. Em relação ao papel da fosforilação na patogénese de PD, o presente estudo evidencia a importância do estudo de padrões de ativação/desativação de diferentes resíduos. Embora o presente trabalho suporte a ideia de um papel neuro-protetor da fosforilação do resíduo S129 da αSyn, assim como quando esta fosforilação é acoplada

à fosforilação no resíduo S87, outras abordagens relativamente a outros padrões de MPTs e outros resíduos de fosforilação, como os restantes resíduos de tirosina, assim como o efeito destes padrões em organelos celulares específicos devem ser seguidos no futuro.

As contribuições do presente trabalho, assim como um esforço futuro para a compreensão do efeito de alterações da αSyn no seu comportamento e na proteostase celular, são cruciais para o desenvolvimento de novas estratégicas terapêuticas, no contexto da DP e de outras synucleinopatias.

Palavras-chave: Doença de Parkinson, α-Synuclein, Agregação, Mutações Familiares, Fosforilação.

Abstract

Protein misfolding and aggregation is a pathological hallmark in neurodegenerative disorders, including the currently incurable and second most common age-related neurodegenerative disease, Parkinson's disease (PD). In both sporadic and familial cases (<10%) of PD, the protein α-Synuclein (αSyn) accumulates in intracellular inclusions, known as Lewy bodies (LBs), causing the progressive loss of dopaminergic neurons in the *Substantia Nigra* (SN) *pars compacta* and, ultimately spreading to non-dopaminergic neurons at later stages of the disease. In LBs, 90% of αSyn is phosphorylated at serine 129 (S129), in contrast with the 4% under physiological conditions. Nevertheless, whether this phosphorylation has a protective or detrimental effect is unclear and recently, additional phosphorylation sites of this protein, as serine 87 (S87) and three tyrosine residues (Y125, Y133 and Y136), have been identified. Furthermore, duplications and triplications of the αSyn coding gene (*SNCA* gene) and six missense mutations of αSyn (A30P, E46K, H50Q, G51D A53T and A53E) are associated with familial forms of PD, but how these mutations affect αSyn phosphorylation profile, as well as the overall cell mechanisms by which αSyn induces toxicity are not completely understood.

Given the high degree of conservation in basic cellular pathways between the budding yeast *Saccharomyces cerevisiae* (*S. cerevisiae*) and higher eukaryotes, yeast is an established model to study the process of αSyn phosphorylation and aggregation, as well as its pathobiology.

Therefore, the aims of this project were A) to phenotypically characterize the most recent PD familial linked mutation of αSyn, A53E and B) to study the phosphorylation interplay between the serine residues 129 and 87 on αSyn inclusion formation and toxicity. To achieve these objectives, the mutation A53E in αSyn was studied regarding cell viability, inclusion formation, protein expression and phosphorylation, solubility of aggregates and mitochondrial network alterations. The effect of phosphorylation at S129 and S87 was assessed using integrative transformed yeast strains encoding αSyn phospho-mutants, which were evaluated regarding cell viability, inclusion formation, protein expression, phosphorylation and clearance and proteasome and autophagy functions.

It was observed that the expression of the αSyn A53E mutant did not show any emerging phenotypic differences in yeast cells on the parameters evaluated, when compared to the wild-type (WT) protein expression. It was also found that mimicking phosphorylation at the S87 residue (S87E mutant), significantly increased αSyn toxicity and inclusion formation, caused proteasome impairment and up-regulated autophagy, when compared to the WT αSyn expression. Interestingly, when the S87E mutant was coupled with the S129 phosphomimic mutation (S87E_S129D mutant), the phenotype was lost and αSyn induced toxicity decreased, prevailing a supposedly protective effect of the phosphorylation at the S129 residue (S129D mutant).

Exploring the mechanism of αSyn toxicity to cells, including the impact of mutations and post-translational modifications (PTMs), are pivotal to understand PD etiology and new therapeutic strategies.

Overall, this study shed a light into the effect of both the phosphorylation state and missense point mutations of αSyn linked to early onset of PD, in its toxicity and aggregation tendency, as well as the impact in protein clearance and degradation systems and general cell homeostasis.

Keywords: Parkinson's disease, αSyn, Aggregation, Familial Mutations, Phosphorylation.

Communications of Intervention

Paper

Diana F Lázaro*, Mariana Castro Dias*, Anita Carija, Susanna Navarro, **Carolina Silva Madaleno**, Sandra Tenreiro, Salvador Ventura, Tiago F Outeiro, *The effects of the novel A53E alpha-synuclein mutation on its oligomerization and aggregation,* Acta Neuropathologica Communications, 2016 Dec 9, 4(1):128
*equal contribution

Abstract

Carolina Madaleno*, Inês Brás*, Sandra Tenreiro, Tiago F. Outeiro, *Molecular insights into the role of alpha-synuclein phosphorylation in synucleinopathies*. 1st CEDOC Symposium on Chronic Diseases (July 2016), NOVA Medical School, New University of Lisbon, Lisbon, Portugal.
*equal contribution

Index

List of Tables

List of Figures

List of Abbreviations

(E)GFP	(Enhanced) Green fluorescent protein
˚C	Degrees Celsius
αSyn	α-Synuclein/Alpha-synuclein
µg	Micrograms
µl	Microliters
A	Alanine
A30P	Alanine replacement to proline at the amino acid position 30
A53E	Alanine replacement to glutamic acid at the amino acid position 53
A53T	Alanine replacement to threonine at the amino acid position 53
ALP	Autophagy-lysosome pathway
APS	Ammonium persulphate
Ar	Argon
Atg	Autophagy related protein
ATP	Adenosine 5' triphosphate
BCA	Bicinchoninic acid assay
bp	Base pairs
BSA	Bovine serum albumin
C	Cytosine
C. elegans	*Caenorhabditis elegans*
Ca^{2+}	Calcium
CaM	Calmodulin
CCD	Charged coupled device
cDNA	Complementary deoxyribonucleic acid
CEDOC	Chronic Diseases Research Center
CG	Cytosine-Guanine Content
cHsc70	Cytosolic heat shock protein 70
CK1/2	Casein kinase 1/2
CMA	Chaperone-mediated autophagy
CTSD	Cathepsin D
Cu^{2+}	Copper
D. *melanogaster*	*Drosophila melanogaster*
DLB	Dementia with Lewy bodies
DNA	Deoxyribonucleic acid
E	Glutamic acid
E. coli	*Escherichia coli*
E46K	Glutamic acid replacement to lysine at the amino acid position 46
ECL	Enzyme linked chemiluminescence
ER	Endoplasmic reticulum
FACS	Fluorescence-activated cell sorting
FCUL	Faculty of Sciences – University of Lisbon
G	Guanine
G51D	Glycine replacement to aspartic acid at the amino acid position 51
GAL(1)	Galactose inducible promoter (1)
H50Q	Histidine replacement to glutamine at the amino acid position 30

HSPs	Heat shock proteins
JNK	c-Jun N-terminal kinases
Kbp	Kilo base pairs
kDa	Kilo Daltons
LAMP2A	Lysosome-associated membrane protein type 2A
LB	Luria Broth
LBDs	Dementias with Lewy bodies
LBs	Lewy bodies
lHsc70	Lysosome-associated heat shock protein 70
LiAc	Lithium acetate
LN	Lewy neurites
M	Molar
mA	Miliampers
MAMs	Mitochondria-associated endoplasmic reticulum membranes
MFI	Mean fluorescence intensity
ml	Milliliters
mM	Milimolar
mTOR	Mammalian target of rapamycin
mW	Miliwatts
NAC	Non-amyloid-β component
ng	Nanograms
nm	Nanometers
NMS-UNL	Nova Medical School - New University of Lisbon
OD	Optical density
OD_{600nm}	Optical density at 600 nm wavelength
ON	Overnight
PAGE	Sodium dodecyl sulfate polyacrylamide gel electrophoresis
PBS	Protein buffer sample
PBS 1X	Phosphate-buffered saline solution
PCR	Polymerase chain reaction
PD	Parkinson's disease
PDD	Parkinson's disease with dementia
PEG	Polyethylene glycol
PGK	Phosphoglycerate kinase
PI	Propidium iodide
PI^+	Propidium iodide positive cells
PI^+GFP^+	Propidium iodide positive and GFP positive cells
PKCδ	Protein kinase C δ
PLK2	Polo-like kinase 2
PP2A	Protein phosphatase 2
pS129	Phosphorylated S129 residue
pS87	Phosphorylated S87 residue
PTMs	Post-translational modifications
PUFA	Polyunsaturated fatty acid
ROS	Reactive Oxygen Species
Rpm	Revolutions per minute
S129	Serine 129
S129A	Serine replacement to alanine at the amino acid position 129

S129D	Serine replacement to aspartic acid at the amino acid position 129
S87	Serine 87
S87E	Serine replacement to glutamic acid at the amino acid position 87
SC	Selective synthetic minimum media
SDS	Sodium dodecyl sulfate
SN	*Substantia Nigra (pars compacta)*
TAE	Tris-acetate-EDTA
TBS	Tris-buffered saline solution
TCA	Trichloroacetic acid
TE	Tris-EDTA buffer
TEMED	Tetramethylethylenediamine
TH	Tyrosine hydroxylase
TI	Insoluble protein fraction
T_m	Temperature of melting
TOM20	Translocase of the outer membrane 20
TP	Total protein fraction
TRP/TRP1/*trp1*	Tryptophan/Tryptophan prototrophy/Tryptophan auxotrophy
TS	Soluble protein fraction
uGFP	Unstable green fluorescent protein
UPRs	Unfolded protein response
UPS	Ubiquitin-proteasome system
URA/URA3/*ura3*	Uracil/Uracil prototrophy/Uracil auxotrophy
V	Volume
V	Volt
WT	Wild-type
Y125	Tyrosine 125
Y133	Tyrosine 133
Y136	Tyrosine 136
YEP	Yeast extract peptone media
YPD	Yeast extract peptone dextrose media

1. Introduction

1.1. Parkinson's disease and synucleinopathies

Parkinson's disease (PD) is the second most common age-related neurodegenerative disorder, has an average of onset of 60 years old [Marques *et al*, 2011] and according to the *Parkinson's Disease Foundation* it affects between 7 to 10 million people worldwide. The prevalence of PD in industrialized countries is approximately 1 to 2% of the population over 60 years of age, which increases to 3 to 5% in people above 85 years old [de Lau and Breteler, 2006], being the most affected men, in Europe, North America and Australia [Pringsheim *et al*, 2014].

This slow and progressive neurodegenerative disorder is clinically characterized by the following motor symptoms: slow and decreased movement (bradykinesia), rest tremor or rigidity, gait and postural instability [Weintraub *et al*, 2008]. These motor symptoms, detected only at the time of diagnosis, occur when patients already have undergone significant neurodegeneration (approximately 70% of nigral dopaminergic neurons are lost) [Chaudhuri *et al*, 2016], [Huang *et al*, 2004]. Furthermore, at later stages of the disease, PD is widespread to non-dopaminergic neurons and other non-motor symptoms arise, such as depression, dementia, psychosis, constipation, neurogenic bladder disturbance, fatigue, insomnia, apathy, anxiety and excessive daytime sleepiness [Todorova *et al*, 2014], [Chaudhuri *et al*, 2016].

The current treatment for this disease is palliative rather than curative and its effectiveness is still far from satisfactory, since it is based on the administration of L-DOPA, by which the non-motor symptoms are neglected [Chaudhuri *et al*, 2016], [Taschenberger *et al*, 2012]. Thus, tremendous efforts are underway to elucidate the causes underlying this disorder and to find a cure as well as a viable early-stage biomarker [Chaudhuri *et al*, 2016].

In the past decades, α-Synuclein (αSyn) protein has been the center of focus in understanding the etiology of a group of overlapping neurodegenerative disorders called *Lewy body* diseases (LBDs), in which PD, PD with dementia (PDD) and dementia with Lewy bodies (DLB) are included [Kim *et al*, 2014]. LBDs are mainly characterized pathologically by the progressive cytoplasmic accumulation of the protein αSyn in eosinophilic intracellular inclusions composed of amyloid-like fibers, known as *Lewy bodies* (LBs) or *Lewy neurites* (LNs) [Weintraub *et al*, 2008], [Lashuel *et al*, 2013]. Hence LBDs are also referred to as Synucleinopathies or α-Synucleinopathies [Lashuel *et al*, 2013]. These protein aggregates lead to degeneration of neocortical, limbic and nigrostriatal circuitries [Braak and Braak, 2000], [Vekrellis *et al*, 2011] and, in the case of PD, patients show loss of dopaminergic neurons in the *substantia nigra* (SN) *pars compacta* and the consequential attenuation of dopaminergic innervation to the *striatum*, with the surviving neurons bearing signs of Lewy pathology and exhibiting abrogated levels of neuromelanin pigmentation (Figure 1.1) [Simuni and Sethi, 2008].

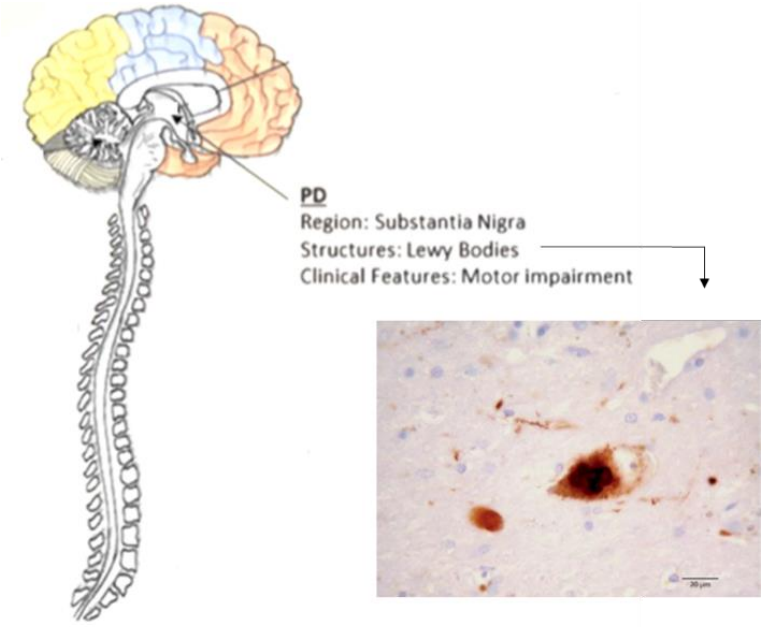

Figure 1.1. Schematic representation of PD pathology. On the right, light microscopy of a neuronal cell containing LBs (dark stain) [Lees *et al*, 2009]. On the left, brain localization of the neuronal cells primarily affected in PD, region of the SN. Adapted from [Wales *et al*, 2013].

The development of PD is described according to the Braak staging hypothesis that postulates that the pathology evolves in 6 stages [Braak *et al*, 2003a]. This staging suggests a pre-motor period in which the typical pathological changes, LNs and LBs, spread from the olfactory bulb and vagus nerve to the lower brainstem regions (stages 1 to 2), followed by a symptomatic period when pathological changes involve the midbrain, including the SN (stage 3), mesocortex (stage 4) and, eventually, the neocortex (stages 5 to 6) [Braak *et al*, 2003a]. Interestingly, morphological studies reveal a pattern of this hypothesis with αSyn pathology and LBs formation in the brains of patients with a clinical diagnosis of PD [Marques *et al*, 2011], [Braak *et al*, 2003a], [Braak *et al*, 2003b]. The study of *post-mortem* human brain tissue from PD patients suggests that αSyn progresses throughout the brain in a pattern that follows the progression of clinical symptoms stated by the Braak's staging for PD, being now considered the first evidence of the hypothesis of the prion-like spreading of αSyn pathology [Lopes da Fonseca *et al*, 2015].

1.2. Etiology of PD

Although the cause of PD remains unknown [Marques *et al*, 2011], emerging evidence has provided support for the hypothesis that this disorder is the result of interactions between genetic abnormalities, environmental toxins, mitochondrial dysfunction and other cellular processes and for this reason, it is considered a complex disorder, since it includes, genetic, epigenetic and environmental causes [Bertram and Tanzi, 2005], [Feng *et al*, 2015]. Nevertheless, the identity of most of these factors, the nature of their interaction, and the molecular pathways of neurodegeneration that they initiate remain poorly understood [Pringsheim *et al*, 2014]. In addition, αSyn toxicity is related with both familial (rare) and non-familial/idiopathic/sporadic (common) forms of PD, evidencing the strong dichotomy between both types [Marques *et al*, 2011], [Lopes da Fonseca *et al*, 2015]. Therefore, investigating the genes and proteins involved in PD is pivotal, in terms of their normal physiological role and contribution to the disease and, hence, provide critical insights of the molecular basis underlying the pathogenesis, in order to develop strategies to treat and prevent the disease [Mbefo *et al*, 2015].

1.2.1. Sporadic PD

Sporadic/Idiopathic PD, the most frequent form of parkinsonism, accounting for 90 to 95% of the cases, usually refers to a syndrome characterized by late-onset, largely non-heritable parkinsonism [Marques *et al*, 2011]. Although, environmental toxins, physical activity, dietary habits and the presence of other diseases have been suggested to play an impact on PD risk [de Lau and Breteler, 2006], [Hindle, 2010], [Nussbaum, 2003], [Gasser, 2010], aging is still the major risk factor in the pathology development [Elbaz and Moisan, 2008]. Furthermore, polymorphisms in the promotor region of *SNCA* gene [Edwards *et al*, 2010], [Fuchs *et al*, 2008], [Maraganore *et al*, 2006], [Mizuta *et al*, 2006], [Satake *et al*, 2009] as well as an increased expression of the *MAPT* gene (encoding for Tau, the protein involved in Alzheimer's disease) [Tobin *et al*, 2008], [Edwards *et al*, 2010] have also been identified as susceptibility factors for sporadic PD.

1.2.2. Familial PD

In 5 to 10% of cases, PD has mainly a genetic component, with both recessive and dominant modes of inheritance [Marques *et al*, 2011]. Although the genetic/familial cases represent a minority part of PD patients, the understanding of the molecular mechanisms underpinning the genetic forms of the disease has already provided insights into the pathogenesis of the sporadic forms, as well [Fujioka *et al*, 2014]. Several genes and chromosomal *loci* have been linked to familial forms of parkinsonism and are designated as PARK1 to PARK18 [Marques *et al*, 2011], [Klein and Westenberger, 2012]. These *loci* are associated with autosomal dominant, recessive and X-linked forms of the disease [Marques *et al*, 2011]. To date, four genes are identified as associated with autosomal dominant PD: *SNCA*, *LRRK2*, *VPS35* and *EIF4G1* [Sundal *et al*, 2012] (Table 1.1).

Table 1.1. Genes and chromosomal *loci* identified and linked to familial forms of PD, PARK1 to PARK18. Genes are organized in three groups: associated with PD with conclusive evidence, with unknown relevance to PD and associated with atypical parkinsonism. Adapted from [Corti *et al*, 2011] and [Sundal *et al*, 2012].

Loci	**Gene**	**Map Position**	**Type of Inheritance/Onset**
PD associated *loci* and genes with conclusive evidence			
PARK1/ PARK4	*SNCA*	4q22	Dominant/Early onset
PARK8	*LRRK2*	12q12	Dominant (Sporadic)/Late onset
PARK2	*PARKIN*	6q25-q27	Recessive (Sporadic)/Early onset
PARK6	*PINK1*	1p35-p36	Recessive/Early onset
PARK7	*DJ-1*	1p36	Recessive/Early onset
PARK9	*ATP13A2*	1p36	Recessive/Early onset
PARK17	*VPS35*	16q11.2	Dominant/Late onset
PARK18	*EIF4G1*	3q27.1	Dominant/Late onset
PD associated *loci* and genes with unknown relevance			
PARK3	*Unknown*	2p13	Dominant/Late onset
PARK5	*UCHL1*	4p14	Dominant/Late onset
PARK10	*Unknown*	1p32	Unclear/Late onset
PARK11	*GIGYF2*	2q36-q37	Dominant/Late onset
PARK12	Unknown	Xq21-q25	Unclear/Late onset
PARK13	*Omi/HTRA2*	2p13	Unclear/Late onset
PARK16	Unknown	1q32	Unclear/Unclear
***Loci* and genes associated with atypical parkinsonism**			
PARK14	*PLA2G6*	22q12-q13	Recessive/Early onset
PARK15	*FBX07*	22q12-q13	Recessive/Early onset

SNCA (chromosome 4q22.1), the gene encoding for the αSyn protein, was the first to be associated with familial PD [Marques *et al*, 2011]. A mutational mechanism in this gene involves the duplication [Chartier-Harlin *et al*, 2004] or triplication [Singleton *et al*, 2003] of the wild-type (WT) *SNCA* gene *locus* (PARK4 PD-associated *locus*). Furthermore, six missense mutations in this gene, causing the A30P [Kruger *et al*, 2001], E46K [Zarranz *et al*, 2004], A53T [Polymeropoulos *et al*, 1997] ("old mutations" – identified between 1997 and 2004 [Petrucci *et al*, 2016]) and H50Q [Appel-Cresswell *et al*, 2013], [Proukakis *et al*, 2013], G51D [Kiely *et al*, 2013] and A53E [Pasanen *et al*, 2014] ("new mutations" – identified between 2012 and 2014 [Petrucci *et al*, 2016]) amino acid substitutions of αSyn (PARK1 PD-associated *locus*), were identified. All these PD-related mutations are localized in the N-terminal membrane binding part of αSyn [Emanuele and Chieregatti, 2015] and were found to confer a

gain of cytotoxic functional effect, implicating upregulated expression levels and qualitative alterations of αSyn in PD onset and progression [Singleton *et al*, 2003], [Ross *et al*, 2008], [Cookson, 2005] (Figure 1.2)

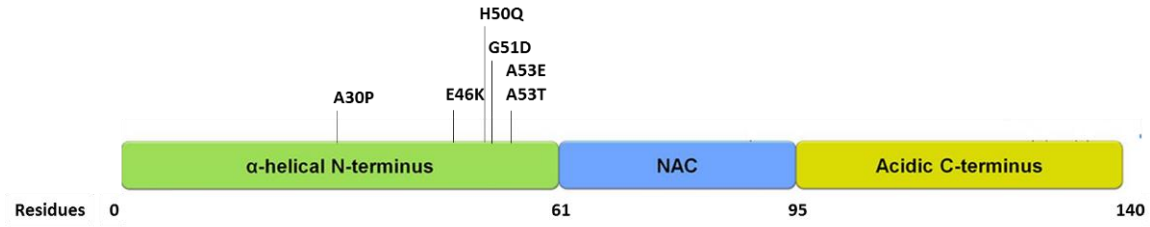

Figure 1.2. Schematic representation of αSyn protein and PD familial linked mutations. The six missense mutations identified to be linked to PD A30P, E46K, H50Q, G51D and A53T/E are localized in the N-terminal domain of the protein. Adapted from [Taymans and Baekelandt, 2014].

These αSyn point mutations are considered rare, being only reported in a few isolated cases of multigenerational PD families [Berg *et al*, 2005], while duplications and triplications of the gene are more prevalent [Puschmann *et al*, 2013] and the phenotype is more severe for patients carrying triplications of the gene, when compared with patients carrying duplications, suggesting that αSyn pathology induces a dose-dependent toxicity [Singleton *et al*, 2003], [Keyser *et al*, 2010], [Fuchs *et al*, 2007], [Ikeuchi *et al*, 2008], [Ibanez *et al*, 2009]. Regarding the most recent PD associated mutation of αSyn, the amino acid replacement alanine (A) to glutamic acid (E) on the amino acid position 53 of the polypeptide chain of this protein, this mutation was identified in a Finnish family in 2014 and it is pathologically and clinically characterized by an equally severe, early-onset phenotype, but slowly progressive parkinsonism [Pasanen *et al*, 2014], when compared to the other five familial-linked mutations (Table 1.2, ordered from the most recent to the oldest identified mutations).

Table 1.2. Major pathological and clinical features of the PD familial linked αSyn mutations and *SNCA* gene duplications and triplications. Adapted from [Fujioka *et al*, 2014] and [Petrucci *et al*, 2016].

αSyn Mutation	Year/ Country of Discovery	Number of Cases	Age of Onset (years)	Mean Disease Duration (years)	Clinical Phenotype
A53E	2014/ Finland	3	20 to 40	24	Early onset, slowly progressive; Severe spasticity, myoclonus and psychiatric disturbances; Cognitive impairment and autonomic dysfunction; Pyramidal signs; Mutation shares a common Finnish ancestral – Founder effect [Pasanen *et al*, 2017].
G51D	2013/ France	2	19 to 60	6	Early onset, rapidly progressive; Severe psychiatric disturbances, hallucinations and severe myoclonus; Cognitive impairment (not detected in early stages of the disease) and autonomic dysfunction; Severe pyramidal signs; Epilepsy.
H50Q	2013/ England and Canada	3	60, 56 and 71	5 and 12	Late onset, rapidly progressive; Psychiatric disturbances; Severe cognitive impairment; Mutation shares a common English ancestral – Founder effect.
E46K	2004/ Spain	5	53 to 67	-----	Late onset, very rapidly progressive; Psychiatric disturbances, hallucination, REM sleep behavior disorder; Cognitive impairment and autonomic dysfunction.
A30P	2001/ Germany	4	49 to 61	-----	Late onset, rapidly progressive (sustained response to L-dopa therapy); Mild dementia; Cognitive impairment.
A53T	1997/ Greece, Italy, United States, Sweden, Australia, Korea	70	35 to 59	4 to 12	Early onset, rapidly progressive; Psychiatric disturbances, dementia, dysautonomia, myoclonus, hallucinations; Autonomic dysfunction.

***SNCA* Copies**	2004/ France, Italy, Japan, Sweden, Korea **(Duplications)**	36	39 to 61	9 to 21	Early onset, rapidly progressive; Psychiatric disturbances dysautonomia, myoclonus, hallucinations; Cognitive impairment and autonomic dysfunction.
	2003/ Sweden, Japan **(Triplications)**	27	36 to 54	5 to 9	Early onset, very rapidly progressive; Severe psychiatric disturbances, dysautonomia, hallucinations, myoclonus; Severe cognitive impairment and autonomic dysfunction.

Functional and phenotypical characterization performed for the six missense mutations have been performed using *in vitro* and *in vivo* model systems. Regarding the oldest identified mutations (A30P, E46K and A53T), these three PD-linked *SNCA* mutations (A30P, E46K and A53T) accelerate αSyn oligomerization, but only two of these (E46K and A53T) enhance fibrillation *in vitro* and *in vivo* [Conway *et al*, 1998], [El-Agnaf *et al*, 1998b], [Conway *et al*, 2000]. Although the A30P mutation has been shown to result in enhanced αSyn fibrillation *in vivo*, as illustrated by an autopsy case of a patient with this mutation that had extensive LB pathology [Seidel *et al*, 2010], *in vitro* it exhibits reduced fibrillation compared to the WT protein and other mutants [Lashuel *et al*, 2013]. The three of them increase the toxicity of the protein in human cell lines [Outeiro *et al*, 2006] and, with the exception for A30P, in yeast [Lázaro *et al*, 2014]. Furthermore, they have an impact on several key cell mechanisms, such as the inhibition of proteasome activity [Bertoncini *et al*, 2005], [Jiang *et al*, 2010] and the mutants A30P and E46K show impairment of membrane and vesicles binding activity [Albuquerque *et al*, 2009], [Hofer *et al*, 2004], [Jensen *et al*, 1998], [Karpinar *et al*, 2009]. Concerning the group of the most recent identified linked mutations of αSyn, including the A53E mutation, the state-of -the-art of phenotypical and functional characterization, using both *in vitro* and *in vivo* approaches, is detailed in Table 1.3.

Table 1.3. Key points and state of the art of the phenotypical and functional characterization of the mutants A53E, G51D and H50Q of αSyn, when compared to WT protein, using different study systems.

αSyn Mutation	**Study System**	**Observations/Major Conclusions**
A53E	***Post-mortem* human brain analysis**	Inclusions with variable morphologies [Pasanen *et al*, 2014]; Mature inclusions up-phosphorylated at S129 [Pasanen *et al*, 2014].
	Mammalian cell lines	**Neuro2A cells:** Decreased propensity to aggregate into amyloid structures [Rutherford *et al*, 2015]; Formation of mature inclusions phosphorylated at S129 [Rutherford *et al*, 2015]; Increased cellular toxicity and dead under stress conditions (MPP^+), as well as mitochondrial impairment [Rutherford *et al*, 2015]. **HEK cells:**

		Different from WT protein in the dimerization/oligomerization process [Lázaro *et al*, 2016]; Similar inclusion formation when compared to WT [Lázaro *et al*, 2016]. **H4 cells:** Increased proteolytic activity of the proteasome [Lázaro *et al*, 2016]; Aggregation of A53E αSyn induces Golgi apparatus alterations [Lázaro *et al*, 2016].
	Biophysical/ Biochemical Characteri-zation	Accumulation of oligomers for a longer period of time [Ghosh *et al*, 2014]; Decreased formation of aggregates and amyloid structures [Ghosh *et al*, 2014]; Reduced membrane binding affinity (when compared to the WT protein and the A53T mutant) [Ghosh *et al*, 2014]; Similar structure of free and membrane-bound αSyn [Ghosh *et al*, 2014]; Slower fibril formation [Ghosh *et al*, 2014]; Formation of elongated amyloid fibrils morphologically similar to WT protein, but thinner [Rutherford *et al*, 2015]; Reduced αSyn amyloid formation [Lázaro *et al*, 2016].
G51D	***Post-mortem* human brain analysis**	αSyn inclusion formation [Kiely *et al*, 2013]; Up-phosphorylation at S129 [Kiely *et al*, 2013]; Partial co-localization with nuclear membrane markers [Fares *et al*, 2014].
	Transgenic mouse brain of α-Synucleino-pathies	**Primary neurons:** Enriched in the nuclear compartment [Fares *et al*, 2014]; Up-phosphorylation at S129 [Fares *et al*, 2014]; Increased αSyn-induced mitochondrial fragmentation [Fares *et al*, 2014]; Greater membrane-induced aggregation and enhanced toxicity [Ysselstein *et al*, 2015]. **Primary midbrain cells:** Decreased α-helical content in the presence of phospholipids [Ysselstein *et al*, 2015].
	Mammalian cell lines	**Neuro2A cells:** Decreased rate of amyloid formation [Rutherford *et al*, 2014]; Increased cellular toxicity under stress conditions (MPP^+) [Rutherford *et al*, 2014]; **SH-SY5Y cells:** Fibrils with increased toxicity [Lesage *et al*, 2013]; Increased activation of apoptosis related caspase-3 [Lesage *et al*, 2013]; Enriched in the nuclear compartment [Fares *et al*, 2014]; Up-phosphorylation at S129 [Fares *et al*, 2014]; Increased αSyn-induced mitochondrial fragmentation [Fares *et al*, 2014]; Greater membrane-induced aggregation and enhanced toxicity [Ysselstein *et al*, 2015]; Similar binding pattern to copper (Cu^{2+}) as the WT, with enhanced rate of fibril formation in the presence of Cu^{2+} [Ranjan *et al*, 2016]. **HEK cells:** Enhanced inclusion formation [Lázaro *et al*, 2014].
	Yeast	Impaired membrane association, forming few inclusions and non-toxic (similar results to A30P mutant) [Fares *et al*, 2014];

		Enhanced inclusion formation compared to WT protein expression [Lázaro *et al*, 2014].
	Biophysical/ Biochemical Characterization	Slower oligomerization rate [Lesage *et al*, 2013]; Decreased permeabilization of DOPG membranes [Stefanovic *et al*, 2015]; Similar fibrils and similar morphology of the mature inclusions [Rutherford *et al*, 2014]; Decreased kinetics of aggregation [Fares *et al*, 2014].
H50Q	***Post-mortem* human brain analysis**	Formation of αSyn inclusions [Appel-Cresswell *et al*, 2013], [Proukakis *et al*, 2013]; Up-phosphorylation at S129 [Appel-Cresswell *et al*, 2013], [Proukakis *et al*, 2013].
	Transgenic mouse brain of α-Synucleinopathies	**Primary neurons:** Increased mitochondrial fragmentation [Khalaf *et al*, 2014]; The presence of Cu^{2+} induces the formation of structurally different and less-damaging aggregates. These aggregates exhibit a stronger capacity to induce αSyn inclusion formation in recipient cells [Villar-Pique *et al*, 2016].
	Mammalian cell lines	**Neuro2A cells:** Increased rate of amyloid formation [Rutherford *et al*, 2014]. **SH- SY5Y cells:** Increased kinetics of aggregation [Ghosh *et al*, 2013], [Khalaf *et al*, 2014]; Similar early oligomer forming tendency [Ghosh *et al*, 2013]; Similar subcellular localization and ability to be phosphorylated by PLK2 and GRK6 (at S129) and by PLK3 (at S129) and CK1 (at S87) [Khalaf *et al*, 2014]; Increased secretion [Khalaf *et al*, 2014]; Increased toxicity and exacerbation of neuronal toxicity of extracellular αSyn [Khalaf *et al*, 2014]; Promotion of cellular toxicity under stress conditions (H_2O_2) [Rutherford *et al*, 2014]; Changes in the ratio between the concentrations of the WT and H50Q αSyn are closely related to the alteration of its aggregation behavior [Porcari *et al*, 2015]. **HEK cells:** The inclusion formation is similar in H50Q and WT αSyn [Lázaro *et al*, 2014]. **H4 cells:** Increased kinetics of aggregation [Ghosh *et al*, 2013]; Presence of Cu^{2+} does not alter the rate of fibril formation [Ranjan *et al*, 2016]. **BL21(DE3)-RIPL cells:** Increased kinetics of aggregation [Chi *et al*, 2014].
	Yeast	Inclusion formation is similar to WT protein [Lázaro *et al*, 2014].
	Biophysical/ Biochemical Characterization	Similar structure of free and membrane-bound αSyn monomeric and oligomeric states [Khalaf *et al*, 2014], and similar fibril formation [Rutherford *et al*, 2014]; Similar morphology of the mature inclusions [Rutherford *et al*, 2014]; Similar permeabilization capacity of DOPG membranes [Stefanovic *et al*, 2015].

1.3. αSyn

1.3.1. Biology, structure and physiological function of αSyn

αSyn is abundantly expressed in the human brain, especially in the neocortex, hippocampus, SN, thalamus and cerebellum [McLean *et al*, 2000a], [Yu *et al*, 2007], making up as much as 1% of the total protein content [Kim *et al*, 2014]. It is a 140 amino acid protein [Ueda *et al*, 1993] encoded by the *SNCA* gene (chr.4q22.1) in humans [Spillantini *et al*, 1995]. Regarding its cell localization, αSyn was initially described to be predominantly in the presynaptic terminals of neurons [Jakes *et al*, 1994]. However, it was also reported to be present in the nuclear envelope [Maroteaux *et al*, 1988], within the nucleus [Gonçalves and Outeiro, 2013], [McLean *et al*, 2000b], [Mori *et al*, 2002] in the cytosol (interacting with cytoplasmic proteins) [Goers *et al*, 2003], [Kontopoulos *et al*, 2006], [Specht *et al*, 2005] and in mitochondria-associated endoplasmic reticulum (ER) membranes (MAM) [Hayashi *et al*, 2009]. Furthermore, this protein is able to bind to membranes [Auluck *et al*, 2010], preferentially to high-curvature, detergent-resistant membranes enriched in cholesterol, sphingolipids, and acidic phospholipids [Jensen *et al*, 2011], [Middleton and Rhoades,2010]. αSyn belongs to the Synucleins protein family, that includes β- and γ-Synuclein [Lavedan, 1998] and its predominant form is the full-length protein [Venda *et al*, 2006], [Emamzadeh *et al*, 2016], although other spliced variants have been identified [Beyer, 2006].

Concerning its structure, αSyn has three distinct structural domains (Figure 1.2): 1) an amphipathic lipid-binding alpha-helix N-terminal region (residues 1 to 60) [Emamzadeh *et al*, 2016], which is a highly conserved region, a KTKEGV hexameric motif important in the formation of α-helix structures (and in reducing its propensity to form β-structures), crucial in modulating its interactions with membranes [Emamzadeh *et al*, 2016], [Sode *et al*, 2007] 2) a central hydrophobic region (residues 61 to 95) denominated as NAC (non-amyloid-β component), that is involved in fibril formation and in αSyn aggregation [Högen *et al*, 2012], and 3) a random coil, highly acidic, proline rich carboxyl-terminal tail (residues 96 to 140), C-terminal region [Emamzadeh *et al*, 2016], which has been implicated in regulating its nuclear localization and its interaction with metals, small molecules and proteins by being homologous with small heat shock proteins (HSPs) [Emamzadeh *et al*, 2016], [Kim *et al*, 2004]. αSyn is present as a natively unfolded, monomeric protein in the cytosol [Kim *et al*, 2014], forming a double α-helix structure, when interacting with phospholipids [Emamzadeh *et al*, 2016], [Ahn *et al*, 2002], suggesting that this protein might adopt different structures under specific stress induced conditions or upon interaction with other proteins, specific ligands, lipids and/or biological membranes, playing specific roles in different cell locations based on its dynamic structure [Lashuel *et al*, 2013].

The physiological function of αSyn is still elusive [Guardia-Laguarta *et al*, 2014]. However, based on its localization and interactions, the activity of this protein is thought to be related to neuroprotection, namely by suppressing apoptosis (through downregulation of PKCδ expression) [Jin *et al*, 2011] and by acting as an antioxidant (by reducing cytochrome c oxidase and directly inhibiting JNK) [Zhu *et al*, 2006], [Latchoumycandane *et al*, 2005], [Hashimoto *et al*, 2002], in the neuronal synaptic integrity, function and plasticity, through chaperone activity (SNARE complex assembly maintenance of structure in presynaptic membranes and release of neurotransmitters) [Burré *et al*, 2013], [Burré *et al*, 2014], [Choi *et al*, 2013], [Park *et al*, 2002], [Witt *et al*, 2013], [Chandra *et al*, 2005] as well as in neurotransmission (through the modulation of pre-synaptic size and synaptic vesicle pool organization) [Vargas K. *et al*, 2017] and regulation of dopamine biosynthesis and levels (by interacting with protein

phosphatase 2A and consequently inhibiting tyrosine hydroxylase (TH)) [Peng *et al*, 2005], [Yang *et al*, 2013b]. On the overall cell homeostasis, αSyn acts in the regulation of neuronal differentiation (Rab3a activity) [Ostrerova *et al*, 1999], [Fu *et al*, 2000], [Chen *et al*, 2013] and glucose levels (increasing glucose uptake by G-protein-coupled-receptor activation) [Geng *et al*, 2011], [Sharma *et al*, 2015], [Rodriguez-Araujo *et al*, 2015], [Rodriguez-Araujo *et al*, 2013], in the modulation of CaM activity (by converting it into an activator) [Martinez *et al*, 2003] and maintenance of PUFA levels (for synthesis of brain vital fatty acids through Acyl-CoA synthetase) [Ruipérez *et al*, 2010].

1.3.2. Pathophysiological role in PD

The pathophysiological role of αSyn arises from the aggregation of this protein within the cell, which can be triggered by a variety of factors [Xu *et al*, 2015]. αSyn toxicity occurs via different mechanisms and involves different intermediates [Xu *et al*, 2015]. The currently acceptable model for the aggregation of this protein in PD describes a starting event of monomeric αSyn misfolding, caused by a cellular failure to degrade this first specie, by the two major clearance pathways [Wales *et al*, 2013] the autophagy-lysosome pathway (ALP) [Cuervo *et al*, 2004], [Spencer *et al*, 2009], [Ebrahimi-Fakhari *et al*, 2011], [Poehler *et al*, 2014] or the ubiquitin-proteasome system (UPS) [Webb *et al*, 2003], [Ebrahimi-Fakhari *et al*, 2011], as further detailed below (Subtopic 1.5). The initial misfolded monomeric protein is then more prone to interact with other αSyn proteins due to alterations in its conformation/structure, which generates unstable dimers and oligomers [Wales *et al*, 2013]. Oligomers may associate with monomers and form a range of intermediary species, including insoluble amyloid fibrils, in a nucleation-dependent manner [Wales *et al*, 2013], [Wood *et al*, 1999]. The accumulation of amyloid fibrils leads to the formation of LBs, one of the primary hallmarks of Synucleinopathies (Figure 1.3) [Spillantini *et al*, 1997], [Lee and Trojanowski, 2006]. However, which of these species plays a major role on pathological conditions, as well as the precise mechanism for cellular toxicity and neurodegeneration are still elusive [Wales *et al*, 2013]. Numerous experiments have suggested that intermediates of αSyn, such as the oligomers and amyloid fibrils, are neurotoxic, while the ultimately mature fibrils formed are relatively less toxic [Sharon *et al*, 2003], [Chen *et al*, 2009].

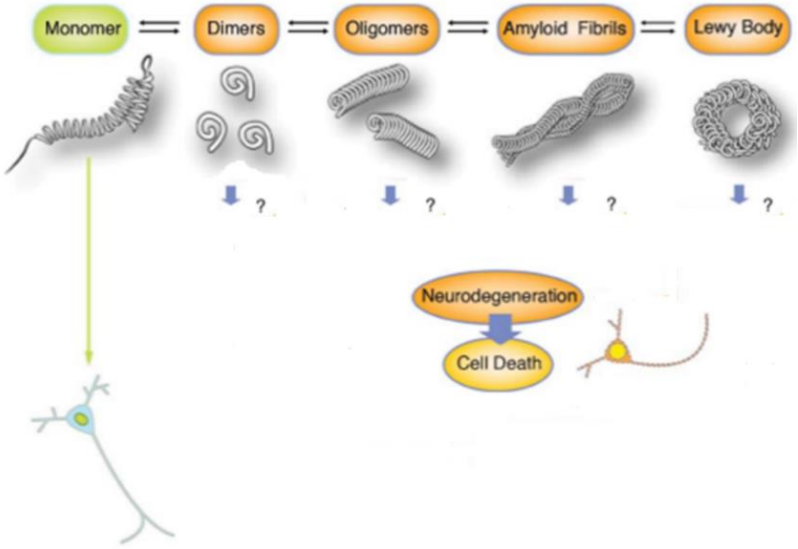

Figure 1.3. Schematic model of αSyn aggregation. Misfolded monomeric αSyn favors homo-interactions forming dimers and oligomers. These unstable species are able to associate with more monomers, forming amyloid fibrils in a nucleation-dependent manner and the accumulation of this last intermediary specie leads to formation of LBs. Nevertheless, which of these species is responsible for cellular toxicity that leads to cell death and neurodegeneration is still unknown. Adapted from [Wales *et al*, 2013].

LBs are mainly caused by a disequilibrium in αSyn protein metabolism [Kragh *et al*, 2012]. An imbalanced in homeostasis may cause a dysfunction on one or more degradation pathways or increased protein synthesis [Xu *et al*, 2015], [Kragh *et al*, 2012], which can result in abnormal levels of αSyn that might favor the formation and/or accumulation of oligomeric and fibrillary species, which represent toxicity to the cell and, consequently, neuronal death (Figure 1.4) [Lashuel *et al*, 2013].

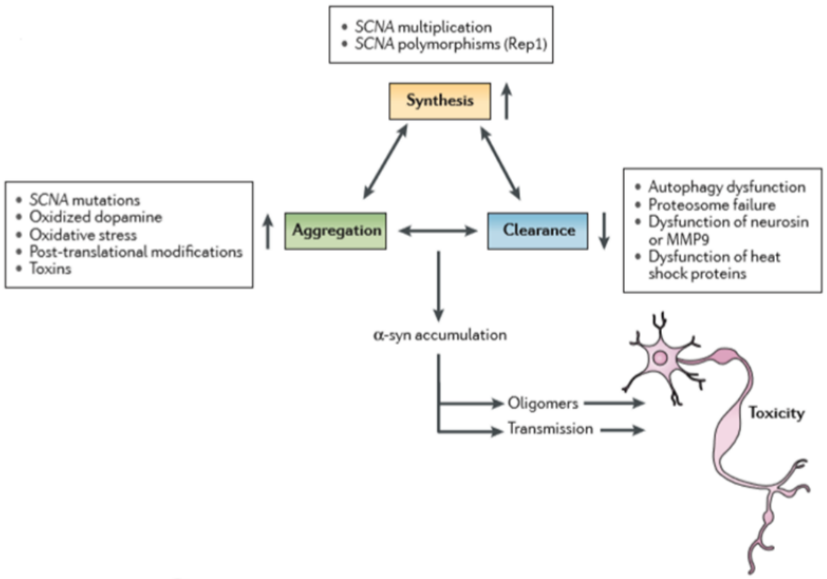

Figure 1.4. Schematic representation of the cellular events that control αSyn protein levels. Intracellular αSyn levels are tightly regulated by the balance between the rates of its synthesis, clearance and aggregation. Abnormalities increasing αSyn synthesis (*SNCA* multiplications and polymorphisms (such as Rep1)), a failure to degrade αSyn (due to an impairment of proteasome, proteases, autophagy and chaperones) or αSyn modifications that promote its aggregation (*SNCA* mutations, post-translational modifications, oxidative stress, toxins and interaction with oxidized dopamine) are responsible for αSyn accumulation, which can be transmitted to other neuronal cells, causing toxicity and leading to neurodegeneration [Lashuel *et al*, 2013].

Furthermore, it is postulated that αSyn oligomerization within specific cellular compartments may alter the distribution of functional forms of monomeric αSyn or result in monomer sequestration into non-functional oligomeric forms, thus resulting in partial loss of function of this protein [Colla *et al*, 2012]. There is an additional second possibility that the native or misfolded forms of the monomeric protein may contribute to αSyn toxicity and PD pathogenesis via aggregation-independent mechanisms [Lashuel *et al*, 2013]. Furthermore, post-translational modifications (PTMs), such as phosphorylation, are hypothesized to influence aggregation events [Wales *et al*, 2013], as further detailed in Subtopic 1.4.

Regarding the effect of the tridimensional structure of this protein, it is hypothesized that an interaction between the C-terminal domain and the NAC region of αSyn is essential to inhibit its aggregation [Emamzadeh *et al*, 2016]. Moreover, the tendency to form α-helix secondary structures, supposedly acquired upon interaction with its ligands [Lashuel *et al*, 2013], is inversely correlated with its aggregation tendency [Marsh *et al*, 2006].

This αSyn accumulation is a factor of toxicity for the overall cell homeostasis: at the nucleus level, αSyn is able to bind to DNA or transcription factors and promote transcription deregulation [Gupta *et al*, 2006], [Hegde *et al*, 2010], [Hegde *et al*, 2003], [Vasudevaraju *et al*, 2012]; at the cytoplasmic level, αSyn alters ER homeostasis, leading to an imbalance of intracellular calcium (Ca^{2+}) that will promote changes at mitochondrial level [Ryu *et al*, 2002], [Lindholm *et al*, 2002], [Lim *et al*, 2009], [Lee *et al*, 2010]. This protein is also able to affect mitochondria directly, by causing a Complex I dysfunction and alter mitochondrial dynamics by promoting mitochondrial fragmentation [Stichel *et al*, 2007], [Nakamura *et al*, 2011], [Kamp *et al*, 2010] as further detailed in Subtopic 1.5. Subsequently, an impairment at the mitochondrial level will promote even more cell and DNA damage [Padmaraju *et al*, 2011] by producing reactive oxygen species (ROS), causing oxidative stress and inducing apoptotic pathways [Doyle *et al*, 2011], through activation of caspases [Sugeno *et al*, 2008]. Furthermore, an increased content of ROS may lead to even more misfolded protein conformations, forming a positive feedback of cell degeneration [Wales *et al*, 2013]. αSyn protein may also be secreted into the extracellular space, which possibly leads to the disease transmission to other neurons, as already demonstrated by several *in vitro* and *in vivo* studies [Hansen *et al*, 2011], [Danzer *et al*, 2012], [Luk *et al*, 2012], [Desplats *et al*, 2009]. All these events, culminate in cell death and consequently neurodegeneration (schematically represented in Figure 1.5) [Wales *et al*, 2013].

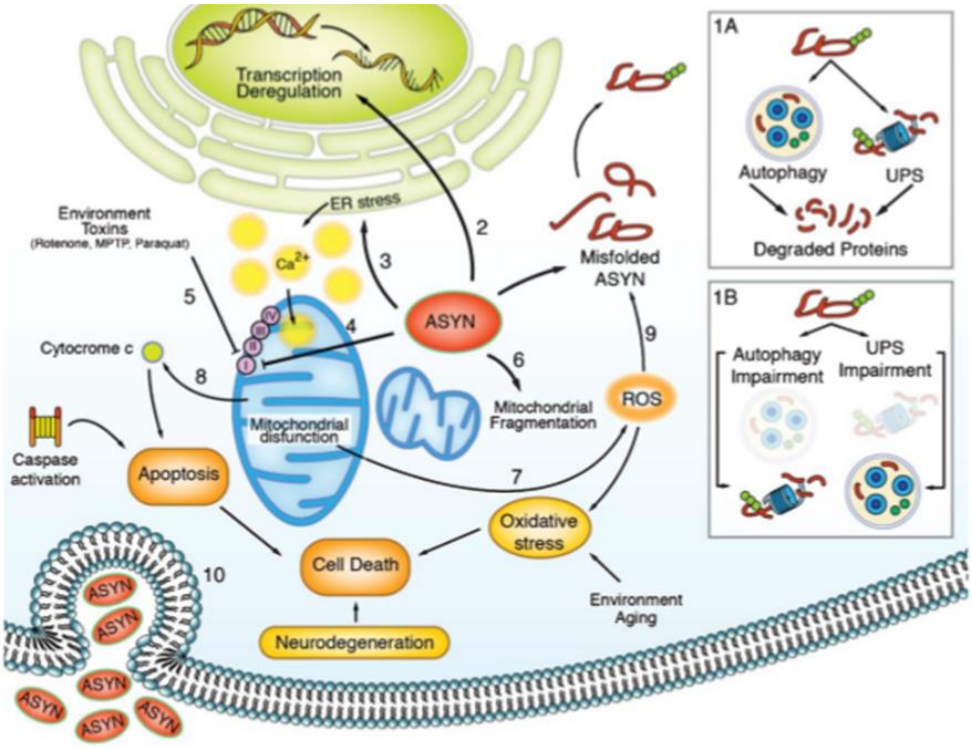

Figure 1.5. Schematic representation of the established αSyn pathological mechanisms in the cell. (1A) Autophagy and UPS are essential to degrade misfolded protein and maintain cell homeostasis; (1B) when aberrant αSyn accumulates due to a failure of these mechanisms, several organelles are affected, and αSyn will cause (2) transcription deregulation, (3) ER stress, (4) mitochondrial stress, that can also be exacerbated by (5) environmental toxins and (6) mitochondrial fragmentation, which will culminate in the (7) production of ROS and (8) apoptotic activation and, consequently (9) more misfolded proteins. All these events lead to cell death and consequently neurodegeneration [Wales *et al*, 2013].

1.4. PTMs of αSyn

αSyn is prone to several types of PTMs, namely the already identified: ubiquitination [Shimura *et al*, 2001], C-terminal truncation [Li *et al*, 2005] and phosphorylation, which are the major disease-associated modifications [Wales *et al*, 2013], but also SUMO modification (sumoylation) [Dorval and Fraser, 2006], N-terminal acetylation [Anderson *et al*, 2006], nitration on tyrosine residues [Giasson *et al*, 2000] and glycosylation [Dorval and Fraser, 2006]. These PTMs are able to alter the conformation and/or biological function of proteins as well as the impact of the protein on a number of pathological processes, such as protein folding and aggregation, LBs formation and neurotoxicity, thereby playing a critical role in PD [Tenreiro *et al*, 2014b].

1.4.1. Phosphorylation of αSyn

A total of four serine, four tyrosine and ten threonine residues are putative sites of phosphorylation in the αSyn sequence [Tenreiro *et al*, 2014b]. However, it is suggested that αSyn might be predominantly unphosphorylated under physiological conditions [Okochi *et al*, 2000], [Fujiwara *et al*, 2002]. For this reason, it was hypothesized that changes in αSyn phosphorylation could represent a response to biochemical events associated with PD pathogenesis [Tenreiro *et al*, 2014b]. Phosphorylation is the most common PTM of αSyn and occurs predominantly at serine residues 129 (S129) [Fujiwara *et al*, 2002] and, to a lesser extent, 87 (S87) [Paleologou *et al*, 2010] and at tyrosine residues 125, 133 and 136 (Y125, Y133 and Y136, respectively) [Okochi *et al*, 2000], [Nakamura *et al*, 2001]. Phosphorylation at the tyrosine residues have been inversely correlated with aggregation and S129 phosphorylation related toxicity, indicating a probable posttranslational cross-talk amongst several sites [Bill *et al*, 1989], however no correlation was established between increased levels of phosphorylation in these residues and the pathological condition [Chen *et al*, 2009], [Mahul-Mellier *et al*, 2014].

Except for the S87 residue, that it is localized in the NAC region of αSyn [Paleologou *et al*, 2010], these phosphorylation sites are all localized in the C-terminal of the protein and highly conserved across species [Oueslati *et al*, 2010] (Figure 1.6).

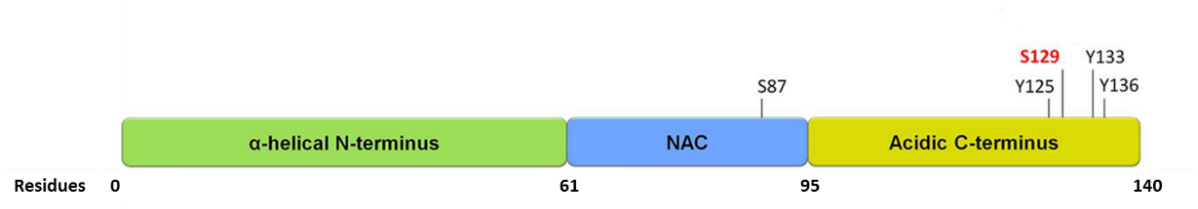

Figure 1.6. Schematic representation of αSyn protein and its phosphorylation sites. The two phosphorytable serines S87 and S129 are localized in the NAC and C-terminal domain of the protein, respectively, while the tyrosine residues Y125, Y133 and Y136 are localized in the C-terminal. S129 residue, the most common phosphorylated residue in LBs (90% of αSyn is phosphorylated, compared to the 4% under physiological conditions) is represented in red. Adapted from [Taymans and Baekelandt, 2014].

Phosphorylation can majorly affect protein conformation, function and fate in many different ways: phosphorylation may be required for proper protein folding, induce conformational changes that can result in lower or higher catalytic activity of the phosphorylated protein, may precede or function as a recognition signal for further modifications, such as ubiquitination, it is able to alter the subcellular

localization of the protein and it may modify protein-protein interactions [Salazar and Hofer, 2009]. In the case of neurodegenerative and protein misfolding diseases, phosphorylation has been shown to be involved in both protein aggregation and toxicity modulation [Tenreiro *et al*, 2014b].

Most attention has been devoted to the study of phosphorylation of αSyn [Tenreiro *et al*, 2014b], specially due to the fact that regarding the S129 protein residue, approximately 90% of αSyn is phosphorylated in LB lesions, *in vivo*, in contrast with only 4% of the soluble, cytosolic monomeric αSyn that is phosphorylated under physiological conditions [Anderson *et al*, 2006], [Fujiwara *et al*, 2002], [Saito *et al*, 2003], being this now considered a significant marker of these disorders [Anderson *et al*, 2006], [Fujiwara *et al*, 2002], [Okochi *et al*, 2000], [Takahashi *et al*, 2003]. However, the full functional relevance of phosphorylation, particularly at the S129 residue, in both physiological and pathological contexts is still elusive [Tenreiro *et al*, 2014b]. Initially, this up-regulation of phosphorylation suggested a close relationship between αSyn phosphorylation at S129 (pS129) and its aggregation, LBs generation and dopaminergic neurodegeneration [Fujiwara *et al*, 2002], but later reports ruled out the hypothesis that S129 phosphorylation leads to toxic effects in the cells or may accelerate LBs formation [Xu *et al*, 2015]. To further address this issue, several models were established to study the role of S129 phosphorylation on the context of PD, however, controversial results were obtained [Xu *et al*, 2015]. Below, it is detailed the most significant phenotypes obtained by mimicking or blocking phosphorylation at the αSyn residue S129 in different cellular models of PD (Table 1.4).

Table 1.4. Key points and state of the art of phenotypical and functional characterization of the effect of phosphorylation at the S129 residue of αSyn, using different study systems. Adapted from [Xu *et al*, 2015].

Study System	Observations/Major Conclusions
PD human brain analysis	S129 is up-phosphorylated in LB inclusions in the synaptic-enriched fractions of the frontal cortex in PD [Muntane *et al*, 2008]; S129 phosphorylation exacerbated PD progression [Zhou *et al*, 2011]; The aggregated phosphorylated αSyn may act as a substrate for kinases (CK2), which leads to pathological inclusion formation and proteasome dysfunction [Waxman and Giasson, 2008], [Waxman and Giasson, 2011].
Mammalian cell lines	**H4 cells:** Mimicking phosphorylation on S129 (S129D) or blocking it (S129A) does not have an effect on formation of inclusions, when compared to the WT protein [Lázaro *et al*, 2014]. **SH-SY5Y cells:** S129 phosphorylation enhances inclusion formation and it involves synphilin-1 and Parkin [Smith *et al*, 2005]; αSyn overexpression toxicity and S129 phosphorylation act together, inducing ER-Golgi trafficking defects and unfolded proteins responses (UPRs) [Sugeno *et al*, 2008]; Higher phosphorylated S129 levels enhanced toxicity, and inhibited proteasome function [Chau *et al*, 2009]; Pathological S129 phosphorylation controls mutant αSyn (A30P and A53T) membrane association [Visanji *et al*, 2011]; Tissue transglutaminase (tTG) phosphorylates S129, which induces αSyn aggregation and inclusion formation [Bi *et al*, 2011];

	αSyn (WT and A53T) S129 phosphorylation may precede cell degeneration in PD and correlates with ROS formation and mitochondrial dysfunction [Perfeito *et al*, 2014]; The aggregated phosphorylated αSyn may act as a substrate for kinases (CK2), which leads to pathological inclusion formation and proteasome dysfunction [Waxman and Giasson, 2008], [Waxman and Giasson, 2011]; Phosphorylation at S129 is neuroprotective by lowering the membrane binding affinity of αSyn [Kuwahara *et al*, 2012]. **3D5 cells:** αSyn phosphorylation is due to CK2 upregulation and lysosome proteases participate in truncated αSyn oligomer formation [Takahashi *et al*, 2007].
Squirrel and Monkey	**Dopaminergic neurons from the SN:** Toxic effect of phosphorylation at S129 is due to normal aging [McCormack *et al*, 2012].
Rodent	**Rodent brain:** Phosphorylation at S129 increases formation of insoluble αSyn aggregates and reduced cellular toxicity, by interaction of αSyn with the GTPase Rab8a [Yin *et al*, 2014].
	***Sprague Dawley* rat model:** Blocking phosphorylation at S129 (S129A) had a neuroprotective effect [Febbraro *et al*, 2013].
	Nigrostriatal system of recombinant adeno-associated virus of human αSyn expression injected rats: WT, mimicking and blocking phosphorylation at S129 (S129D and S129A, respectively) did not show any differences in αSyn aggregation and neurotoxicity [McFarland *et al*, 2009]. **Adeno-associated virus of human αSyn over-expression injected in the nigrostriatal tract:** Mimicking phosphorylation at S129 (S129D) attenuated αSyn-induced neurodegeneration [Gorbatyuk *et al*, 2008].
	Rat model: Phosphorylated S129 does not play a key role in cytotoxic pre-inclusion formation and aggregates accumulation [Azeredo da Silveira *et al*, 2009].
Mice	**Mouse brain:** PLK2 is responsible for αSyn activity and phosphorylation under physiological conditions [Bergeron *et al*, 2014]. **Transgenic mice brain of α-Synucleinopathies:** The aggregated phosphorylated αSyn may act as a substrate for kinases (CK2) which lead to pathological inclusion formation and proteasome dysfunction [Waxman and Giasson, 2008], [Waxman and Giasson, 2011]; S129 is up-phosphorylated in LB inclusions in the synaptic-enriched fractions of the frontal cortex [Muntane *et al*, 2008]; Pathological S129 phosphorylation controls mutant αSyn (A30P and A53T) membrane association [Visanji *et al*, 2011]; Phosphorylation at S129 does not have an obvious effect on αSyn function [Escobar *et al*, 2014].

	MN9D cells: S129D mutant lessens the neurotoxicity induced by the WT protein [Wu *et al*, 2011]; Phosphorylation at S129 may up-regulate TH levels and dopamine synthesis [Wu *et al*, 2011].
Yeast	αSyn toxicity is related to vesicular endocytosis [Zabrocki *et al*, 2008]; Phosphorylation can regulate αSyn toxicity and ER-Golgi trafficking, according to genetic modulation [Sancenon *et al*, 2012]; Phosphorylation can modulate αSyn cytotoxicity, aggregation, subcellular distribution and ER-Golgi trafficking and S129D can promote the clearance of protein inclusions [Tenreiro *et al*, 2014a].
D. melanogaster	Phosphorylation at S129 enhances neurotoxicity and inclusion formation [Chen and Feany, 2005].
C. elegans	**Transgenic worm model:** Phosphorylation at S129 is neuroprotective by lowering the membrane binding affinity of αSyn [Kuwahara *et al*, 2012].
E. coli	Phosphorylation at S129 has a protective effect against neurotoxic αSyn oligomers by preventing oligomer membrane binding [Nubling *et al*, 2014].
Biophysical/ Biochemical Characterization	Phosphorylation inhibits αSyn fibrillation process [Oueslati *et al*, 2010], [Paleologou *et al*, 2010], [Waxman and Giasson, 2011], [Beyer *et al*, 2013]. Fibrillated forms of αSyn become phosphorylated at S129 [Paleologou *et al*, 2010] [Waxman and Giasson, 2011]; Phosphorylation at S129 increases conformational flexibility of αSyn and suppresses its fibrillogenesis, but does not obstruct its membrane binding [Paleologou *et al*, 2008].

Up-regulated levels of phosphorylation at the S87 (pS87) residue were also connected to Synucleinopathies [Paleologou *et al*, 2010] and in recent years, it was revealed that phosphorylation at S87 may play a key role in αSyn modulation in the field of aggregation *in vivo* [Waxman and Giasson, 2008]. Unlike the other phosphorytable residues previously mentioned, S87 is localized in the NAC region, which was suggested to play a major part in protein aggregation and fibrillogenesis *in vitro* [Ueda *et al*, 1993], [El-Agnaf *et al*, 1998a,b], [Giasson *et al*, 2001].

The study of the phosphorylation at S87 is not as comprehensive and extensive as that at S129 site [Xu *et al*, 2015]. However, S87 is considered a secondary phosphorylation site [Okochi *et al*, 2000] and phosphorylation at S87 is unique for human αSyn, which made it crucial for studying and linking to neurodegenerative disorders [Xu *et al*, 2015]. Below, it is detailed the most significant phenotypes obtained by mimicking or blocking phosphorylation at the αSyn residue S87 in different cellular models of PD (Table 1.5).

Table 1.5. Key points and state of the art of phenotypical and functional characterization of the effect of phosphorylation at S87 residue of αSyn using different study systems.

Study System	Observation/Major Conclusions
PD *post-mortem* human brain analysis	S87 is up-phosphorylated in LBs [Paleologou *et al*, 2010].
Transgenic mice model of α-Synucleinopathies	S87 is up-phosphorylated in LBs [Paleologou *et al*, 2010].
Rat model of PD	S87 phosphorylation inhibits αSyn aggregation and protects against αSyn induced toxicity [Oueslati *et al*, 2012].
Mammalian cell lines	**SH-SY5Y cells:** Phosphorylation at S87 promotes inclusion formation and decreases cell viability [Kim *et al*, 2006]. **H19-7 cells:** Phosphorylation at S87 promotes inclusion formation and decreases cell viability [Kim *et al*, 2006].
Biophysical/Biochemical Characterization	Phosphorylation at S87 expands αSyn structure (increased flexibility) and blocks its fibrillation [Waxman and Giasson, 2008], [Paleologou *et al*, 2010]; Phosphorylation at S87 reduces αSyn binding to membranes [Paleologou *et al*, 2010].

Similar to what was observed in the studies regarding the S129 phosphorylation impact on αSyn aggregation and toxicity, for the study of the S87 phosphorylation, again, results obtained using different systems were contradicting [Tenreiro *et al*, 2014b].

Depending on the animal model and system used, the effect of phosphorylation on αSyn inclusion formation and toxicity has yielded to conflicting results, which may be due to the current state of the art to study this issue, both *in vitro* and *in vivo* [Tenreiro *et al*, 2014b]. These studies are based on two approaches: 1) mimicking or blocking this PTM by mutating specific serine or tyrosine residues to another phosphorylated or non-phosphorylated amino acid, respectively [Xu *et al*, 2015], as the widely employed S129D/E and S129A mimicking and blocking phospho-mutants, respectively [Leger *et al*, 1997] or by the 2) combined expression of αSyn with specific kinases involved in its phosphorylation, such as the casein kinase 2 (CK2) and the polo-like kinase 2 (PLK2) or specific phosphatases involved in its dephosphorylation, such as the protein phosphatase 2 (PP2A) (or kinases inhibitors) [Xu *et al*, 2015], [Tenreiro *et al*, 2014b]. Furthermore, S87 is one of the few residues and phosphorylation sites that distinguish the human αSyn sequence from that of mouse and rat αSyn [Xu *et al*, 2015], limiting the usage of these models to study αSyn phosphorylation. Regarding the phosphorylation at tyrosine residues, there are no mutants able to mimic the phosphorylated state of a tyrosine residue [Tenreiro *et al*, 2014b]. Moreover, biochemical and biophysical analysis of the phosphorylation-mimicking mutants S129E/D do not seem to fully reproduce the effect of phosphorylation on the structural and aggregation properties of αSyn *in vitro* [Xu *et al*, 2015] and regarding mimicking the phosphorylation at the S87, it was demonstrated that only CK1 was capable of reproducibly phosphorylate αSyn *in vivo* and *in vitro* [Waxman and Giasson, 2008], [Paleologou *et al*, 2010]. While several studies reported consistent results using in parallel genetic or pharmacological methods to alter αSyn phosphorylation status [Chen and Feany, 2005], [Smith *et al*, 2005], [Chen *et al*, 2009], other suggest that phospho-mutants may not fully recapitulate the real phosphorylation/unphosphorylation states of αSyn [Paleologou *et al*, 2008],

[Schreurs *et al*, 2014]. However, even considering these limitations, the use of αSyn phospho-mutants remain a unique and powerful mean to study phosphorylation [Tenreiro *et al*, 2014b]. Supporting this statement, the S129G and S129A mutations (that block αSyn phosphorylation), were both more toxic and resulted in increased inclusion formation compared to the WT protein in a yeast model, excluding that the observed phenotypes were due to specific structural consequences of S129A mutation on αSyn [Tenreiro *et al*, 2014a] and, in the same model organism, S129E aSyn exhibited the same phenotype of toxicity and inclusion formation as the WT protein, that is strongly phosphorylated at S129 by endogenous kinases [Tenreiro *et al*, 2014a]. As well, the S87E phospho-mimicking mutant has been widely used in *in vitro* biochemical studies [Waxman and Giasson, 2008], [Paleologou *et al*, 2010], mammalian single cell analysis and in animal models of PD (mice and rat model) [Paleologou *et al*, 2010], [Tenreiro *et al*, 2014b].

1.5. Cellular organelles and pathways cross-talk with αSyn in PD

The function of αSyn becomes more important during increased synaptic activity and aging, and could be a contributory factor in neurodegeneration [Kim *et al*, 2014]. To maintain the physiological function of this protein, the elimination of misfolded, aggregated and otherwise damaged forms of proteins is crucial [Lashuel *et al*, 2013], [Wales *et al*, 2013].

1.5.1. αSyn degradation systems: UPS and ALP

Protein degradation is a crucial process in intracellular homeostasis maintenance and it is ensured by two independent, but complementary, systems that work in symbioses: the UPS and the ALP, which are named according to the final destination of the protein to be degraded: the proteasome and the lysosome, respectively [Lopes da Fonseca *et al*, 2015].

Regarding αSyn degradation, monomeric species are degraded by both mechanisms, ALP and UPS [Cuervo *et al*, 2004], [Liu *et al*, 2003], that compensate each other upon one's failure [Yang *et al*, 2013a]. Nevertheless, the lysosome is the only one able to eliminate higher molecular species, as the case of αSyn oligomers and aggregates [Lee *et al*, 2004].

The importance of studying the UPS in neurodegenerative disorders, including PD, relies on its role as a critical regulator of protein homeostasis in eukaryotic cells, keeping the cellular environment free of misfolded, defective, and aggregation-prone proteins, whose accumulation are common hallmarks in neurodegenerative diseases [Ciechanover and Brundin, 2003]. A blockade of the UPS by the disease protein would result in global accumulation of proteasome substrates, which provides an explanation for the broad and diverse effects on cellular homeostasis in affected cells [Dantuma and Bott, 2014], [Mayer *et al*, 1989]. The idea that impaired clearance of misfolded proteins may be central to neurodegenerative diseases originates in part from the observation that approximately 90% of LBs contain ubiquitin, proteasome subunits, and other UPS components [Cummings *et al*, 1998]. Supporting this idea, it has been shown that the main constituent of LBs, αSyn, binds to proteasomes [Snyder *et al*, 2003] and inhibits UPS function both *in vitro* and *in vivo* [Stefanis *et al*, 2001], [Snyder *et al*, 2003], [Chen *et al*, 2006], while, αSyn expression levels of which can predispose individuals to PD [Singleton *et al*, 2003], can still be degraded by the proteasome [Bennett *et al*, 1999].

The UPS, which is the pivotal pathway for the clearance of short-lived, damaged and misfolded proteins in the cell nucleus and cytoplasm, occurs in two separate, consecutive steps: ubiquitylation and proteossomal degradation [Hershko and Ciechanover, 1998], [Kleiger and Mayor, 2014]. The first one, involves the presence of a ubiquitin activator, a conjugase, and a ligase catalyzes the covalent conjugation of the C-terminal of ubiquitin to an internal lysine of the substrate protein [Pickart, 2001], [Dantuma and Bott, 2014]. Multiple rounds of this event, that lead to the formation of a polyubiquitin chain, can function as a signal for degradation by the proteasome, a multi-protein complex consisting of a 20S core particle and 19S regulatory particles, at one or both ends [Bedford *et al*, 2010]. In the proteasome, the active sites responsible for the chymotrypsin-like, trypsin-like, and caspase-like activities are situated in the interior surface of the 20S core particle, shielding the proteolytic activity of this organelle [Bedford *et al*, 2010]. The second step of proteossomal degradation occurs by unfolding of the substrates by the proteasome and threading of this polypeptide chains through the inner channel, where they are cleaved into short peptides and released from the barrel [Bhattacharyya *et al*, 2014]. On

the cytoplasm, peptides are rapidly processed into amino acids by cellular aminopeptidases and recycled [Reits *et al*, 2003].

Nevertheless, the destiny of a given substrate protein may be different, depending on the type of ubiquitin assembly to which it is connected, since ubiquitylation is associated with several biological roles, additionally to proteasome degradation, as protein activity and localization, cell signaling, endocytosis or DNA repair [Dantuma and Bott, 2014], [Komander and Rape, 2012]. More recently, this ubiquitylation topology has been implicated in macroautophagy function [Kraft *et al*, 2010], highly interconnecting the UPS with other proteolytic and non-proteolytic cellular processes at multiple levels, whereby it controls many diverse functions in cells [Dantuma and Bott, 2014].

Autophagy is the process of decomposition and degradation of cellular components and organelles via the lysosomal compartment and it has two main biological functions: 1) the clearance of deleterious intracellular components and 2) the recycling of macromolecules from functional pre-existing organelles and proteins to guarantee proteome renewal [Mizushima and Klionsky, 2007].

Based on the cargo delivery method, autophagy is divided in three main types: chaperone-mediated autophagy (CMA), macroautophagy and microautophagy [Lopes da Fonseca *et al*, 2015]. Regarding these three types of autophagy mentioned, to date there is no evidence that microautophagy plays a role in αSyn degradation [Lopes da Fonseca *et al*, 2015]. CMA is a protein degradation mechanism linked to lysosome, based in the recognition of a specific amino acid sequence (KFERQ) motif that is found on approximately 30% of cytoplasmic proteins, including αSyn [Dice, 1990]. It is able to degrade monomers and dimers of αSyn, however not oligomers [Martinez-Vicente *et al*, 2008]. Additionally, protein misfolding, partial folding or PTMs, such as phosphorylation, can promote or inhibit the CMA pathway [Dice, 1990]. Mechanistically, CMA relies on the proper identification and binding of cytosolic heat shock chaperone 70 (cHsc-70) to the target substrate [Chiang *et al*, 1989], after this first step, this complex is directed to the lysosomal membrane, where it interacts with the lysosome-associated membrane protein type 2A (LAMP2A) [Eskelinen *et al*, 2005], [Cuervo and Dice, 1996] and at last targets the substrate to degradation, by the lysosome-associated Hsc70 (lHsc70) [Agarraberes *et al*, 1997]. LAMP2A down-regulation is the main cause of decreased CMA activity observed in ageing [Cuervo and Dice, 2000] and, together with Hsc70, it is down-regulated in the SN and amygdala of PD patients [Alvarez-Erviti *et al*, 2010]. Studies performed in cell culture models and lysosomes purified from liver cells already demonstrated that WT αSyn can be actively degraded by the CMA [Lopes da Fonseca *et al*, 2015]. However, some familial PD-linked mutations of αSyn (A30P and A53T) as well as αSyn phosphorylated at the S129 residue, impair CMA degradation since both αSyn familial mutants exhibit higher affinity to the LAMP2A receptor, blocking CMA at the LAMP2A level, which leads to a full impairment of the pathway [Cuervo *et al*, 2004]. When a failure of this system occurs, there is an activation of macroautophagy (or just called autophagy), which is the last resource of the cell to avoid protein aggregation, since it is a *content-blind* mechanism [Lopes da Fonseca *et al*, 2015]

Macroautophagy is the most well-known of the three autophagic mechanisms and relies on the formation of *de novo* double membrane-bound vesicles (autophagosomes) to sequester intracellular components, including whole organelles, towards the lysosome [Noda *et al*, 2002], [Kraft *et al*, 2012]. This membrane formation mainly relies on the autophagy related protein (Atg) 9, both in yeast and in humans [Reggiori *et al*, 2004], [Reggiori *et al*, 2005], [Orsi *et al*, 2012], [Young *et al*, 2006]. Macroautophagy is found constitutively active, but further activation via the mammalian target of rapamycin (mTOR) pathway [Cardenas *et al*, 1999] or the PI2kinase/beclin/vsp34 (mTOR-independent) pathway [Zeng *et al*, 2006] is possible. The autophagosome formation requires two ubiquitination steps highly regulated by Atg proteins [Thumm *et al*, 1994], [Tsukada and Ohsumi, 1994], [Klionsky, 2003]: Firstly, Atg12 is conjugated with Atg5 (which involves the participation of Atg7 and Atg10) [Mizushima

et al, 1998], [Tanida *et al*, 2001], then the Atg12-Atg5 complex is targeted to the autophagosome, with Atg16 [Mizushima *et al*, 1999], [Romanov *et al*, 2009]. The second ubiquitination step requires Atg8 (also known as LC3). LC3 is C-terminal cleaved by Atg4 to form LC3-I [Tanida *et al*, 2004], [Kabeya *et al*, 2000], which is conjugated to the lipid phosphatidylethanolamine (PE) by Atg7 and Atg3 to generate LC3-II [Tanida *et al*, 2001], [Tanida *et al*, 2002]. The Atg12-Atg5 complex originated from the first ubiquitination is necessary for the LC3 processing and localization at the autophagosome membrane [Otomo *et al*, 2013], [Fujita *et al*, 2008].

On the other hand, alternative players can be involved in macroautophagy, depending on the cargo being degraded. Namely, in the case of protein aggregates, the alternative is referred to as aggrephagy [Lopes da Fonseca *et al*, 2015].

Both in cell culture and in *in vivo*, WT or mutated αSyn can be degraded through macroautophagy [Spencer *et al*, 2009], [Tofaris *et al*, 2011], [Paxinou *et al*, 2001]. The blockade of this process generally leads to the accumulation of high molecular weight species of αSyn, although different macroautophagy inhibitors reveal distinct outcomes [Lee *et al*, 2004], [Vogiatzi *et al*, 2008]. Furthermore, in yeast, an organism lacking CMA, it was demonstrated that αSyn phosphorylation at S129 can modulate the protein degradation via macroautophagy and, ultimately, inclusion formation [Tenreiro *et al*, 2014a], [Lopes da Fonseca *et al*, 2015].

Macroautophagy is crucial for the lysosomal degradation of oligomeric and aggregated αSyn, since CMA is unable to handle large protein species [Martinez-Vicente *et al*, 2008], [Salvador *et al*, 2000]. Once inside the lysosome, αSyn is mainly degraded by Cathepsin D (CTSD) [Sevlever *et al*, 2008]. αSyn overexpression can inhibit macroautophagy via an interaction with Rab1a that culminates in a mislocalization of Atg9 [Winslow *et al*, 2010] and in cells overexpressing this protein, it was reported the presence of enlarged autophagosomes and lysosomes [Spencer *et al*, 2009]. Furthermore, an increase in mTor and decrease in Atg7 levels has been observed in both DLB patients and αSyn transgenic mice [Crews *et al*, 2010]. Additionally, αSyn aggregates are able to resist macroautophagy leading to a failure of the pathway and accumulation of autophagosomes [Tanik *et al*, 2013].

Furthermore, the mutations associated with familial forms of PD also seem to differentially affect this protein degradation pathway [Lopes da Fonseca *et al*, 2015]. In the E46K αSyn mutant, an impairment of autophagy was observed, via inactivation of the JNK1/Blc2 pathway [Yan *et al*, 2014], whereas the A53T mutation seems to promote increased mitophagy and the accumulation of autophagosomes due to an impaired degradation [Choubey *et al*, 2011]. It is now unquestionable that there is a strong interplay between αSyn and autophagy pathways, and that this may enable therapeutic interventions [Lopes da Fonseca *et al*, 2015].

Upon stress conditions, promoting disturbances of cellular proteostase, such as impairment of lysosomal and proteossomal function, and protein misfolding, there is an increase of αSyn release/secretion [Jang *et al*, 2010]. One important issue, yet unresolved, is the fate and/or the physiological role of the αSyn species that are present in the extracellular space [Lopes da Fonseca *et al*, 2015]. The clearance of extracellular αSyn species can be achieved through proteolysis by extracellular proteases or uptake by surrounding cells [Lopes da Fonseca *et al*, 2015]. However, the internalization of pathological forms of αSyn can seed the pathogenic conversion of soluble αSyn in the receiving cell, and this might be one of the fundamental steps for αSyn propagation and spreading of pathology [Costanzo and Zurzolo, 2013].

1.5.2. αSyn and mitochondria wellness

Mitochondria are free-floating organelles, found as clusters in the cytosol and capable of interacting physically with other subcellular organelles, thereby facilitating efficient rapid metabolism and signaling (e.g. interaction with the ER, forming MAMs) [Bose and Beal, 2016], [Cieri *et al*, 2016]. Structurally, mitochondria are the only entities within the cells surrounded by a double membrane and these two membranes differ in protein and lipid composition and in their functional roles [Cieri *et al*, 2016]. The outer membrane is porous and permeable to small solutes (up to 5 kDa), while the inner membrane is impermeable to ions and to most hydrophilic molecules and highly selective [Cieri *et al*, 2016]. This last one is enhanced by a process of membrane invagination that gives rise to the cristae, where the respiratory chain complexes and adenosine 5' triphosphate (ATP) synthases are localized [Cieri *et al*, 2016], as well as the mitochondrial DNA [Bose and Beal, 2016]. Each respiratory chain complex is composed of five protein multisubunits, that have as a final goal the production of ATP: I, III and IV (pump protons to generate an electrochemical gradient that maintain the membrane negative potential), II (couples the citric acid cycle to the electron transport chain) and V (ATP synthase protein) [Cieri *et al*, 2016].

Within the cell, mitochondria were regarded as the *powerhouse* of the cell for many years [Franco-Iborra *et al*, 2016], since its main biological function is to generate energy in the form ATP [Bose and Beal, 2016]. However, these organelles are involved in the metabolism of lipids and amino acids, in the storage of intermediate products of pyruvate oxidation and in the Krebs cycle, too [Bose and Beal, 2016]. Furthermore, they regulate Ca^{2+} homeostasis, and play a role in scavenging free radicals, in controlling programmed cell death and in maintaining the ALP pathway [Bose and Beal, 2016]. These are complex and dynamic organelles, undergoing constant morphological changes [Bose and Beal, 2016]. Mitochondrial shape and movements within the cells are regulated and have an impact on mitochondrial function, especially in the central nervous system, where mitochondrial trafficking is critical to provide strategic intracellular distribution, presumably according to local energy request [Cieri *et al*, 2016].

To guarantee the integrity of this variety of cell signaling pathways, the maintenance of a healthy mitochondrial network is fundamental and, for this reason, cells developed a sophisticated system of quality control to renew mitochondria, which is the fusion/fission process [Cieri *et al*, 2016], as well as to promote its turnover and selectively eliminate them when damaged via autophagy (in this case, called mitophagy) [Bose and Beal, 2016].

The renewal of mitochondria organelles controls its bioenergetic function, mitochondrial turnover, protects mitochondrial DNA [Franco-Iborra *et al*, 2016] and, by changing their size, shape and/or structure of their inner membrane, mitochondria form a complex reticulum with other organelles of the cell [Bose and Beal, 2016] that undergoes repetitive cycles of fission and fusion [Twig and Shirihai, 2011], determining the structure of the entire mitochondrial population [Bose and Beal, 2016].

Mitochondrial dynamics and maintenance of mitochondrial DNA play a pivotal role in mitochondrial health [Bose and Beal, 2016]. In neurons, maintaining a balance between fission and fusion is crucial for cell survival and synaptic function [Rappold *et al* 2014] and defects in these processes impact on mitochondrial function and lead to disordered cell function, which manifests as disease [Cieri *et al*, 2016]. It is now well established that mitochondrial dysfunction and oxidative stress play a major role in PD pathogenesis [Bose and Beal, 2016], as it was identified that in the SN, skeletal muscles and platelets of PD patients the activity of complex I is impaired [Beal, 2005], [Lin and Beal, 2006], [Chaturvedi and Beal, 2008] as well as evidence of oxidative damage was found [Dauer and

Przedborski, 2003]. These Complex I defects play a critical role in the loss of dopaminergic neurons [Perier *et al*, 2010], along with chronic production of ROS [Bose and Beal, 2016].

Furthermore, a considerable amount of genes associated with PD have a converging role on mitochondrial physiology [Cieri *et al*, 2016] and regarding the cross-talk between αSyn and mitochondrial homeostasis, it was already demonstrated that αSyn is able to bind to a translocase of the outer membrane (TOM20), inhibiting the import of proteins into the mitochondria, both *in vitro* and *in vivo* [Bose and Beal, 2016] and an abnormal αSyn-TOM20 interaction was also observed in the nigrostriatal dopaminergic neurons in *post-mortem* brains from PD patients [Di Maio *et al*, 2016].

Regarding the biological impact of αSyn on mitochondrial homeostasis, accumulation of WT αSyn in mitochondria of mice dopaminergic neurons also leads to reduced complex I activity and increased ROS production and this effect is further exacerbated in neurons expressing the A53T αSyn mutant [Devi *et al*, 2008], [Reeve *et al*, 2015]. Moreover, αSyn aggregation also results in reduced ATP levels and membrane potential and, again, mice carrying the A53T mutation display reduced activity of the complex IV, as well [Martin *et al*, 2006]. Overexpression of αSyn also results in increased mitochondrial fragmentation and this phenotype is worsened when αSyn contains the familial PD-linked mutations E46K and A53T [Nakamura *et al*, 2011], but it also occurs when the protein is knocked-down [Calì *et al*, 2012], [Guardia-Laguarta *et al* 2014], [Gui *et al*, 2012], [O'Donnell *et al* 2014]. Furthermore, WT αSyn overexpressing transgenic mice showed an increased number of deletions in their mitochondrial DNA [Bender *et al*, 2013] and mitochondrial DNA deletions were also found in individual dopaminergic neurons of PD patients [Bender *et al*, 2006], causing defects in the respiratory chain in the neurons of the SN [Kraytsberg *et al*,.2006]. Using the same αSyn overexpressing transgenic mice model organism approach, both the WT and mutant A53T protein promoted an up-regulation of mitophagy, resulting in massive mitochondrial degradation, bioenergetic deficits and neuronal death [Choubey *et al*, 2011], [Chinta *et al*, 2010].

Regarding the interaction of mitochondria with other cellular organelles, αSyn can also modulate this feature, namely when containing point mutations, αSyn can cause a reduction in the association of mitochondria with MAMs, which results in less apposition of the mitochondria with the ER [Guardia-Laguarta *et al* 2014]. In yeast cells, human αSyn triggers endonuclease G translocation between the mitochondria and nucleus, leading to DNA degradation mediated by endonuclease G [Büttner *et al* 2013].

1.6. Yeast as a model organism to study αSyn pathobiology

The unicellular yeast *Saccharomyces cerevisiae* (*S. cerevisiae*) is the most extensively studied eukaryotic organism, being the first to be fully sequenced (in 1996) [Goffeau *et al*, 1996] and having about 80% of the nearly 6000 proteins predicted to be encoded in the yeast genome characterized functionally [Suter *et al*, 2006], [Christie *et al*, 2009]. Additionally, high throughput data obtained from functional genomics approaches, such as transcriptomics, proteomics, metabolomics, interactomics (protein–protein interactions) and locasomics (protein subcellular localization), are well organized and permanently actualized in public databases [Tenreiro and Outeiro, 2010]. The powerful available genetic resources and the accumulated knowledge of the yeast cell, as well as the existence of several important conserved pathways between yeast and human were crucial factors in using yeast as a model organism to gain insights into many human diseases, including neurodegenerative diseases as PD [Tenreiro and Outeiro, 2010]. Namely, in the study of the fundamental molecular events involved in these pathologic processes [Gitler, 2008], such as in the understanding of transcriptional dysregulation [Hughes *et al*, 2001], mitochondrial quality control mechanisms [Braun, 2012], metabolism and biogenesis [Rinaldi *et al* 2010], apoptotic and necrotic cell death [Braun *et al*, 2010], protein folding and quality control systems, vesicular trafficking and secretion [Bonifacino and Glick, 2004].

Yeast features such as its short generation time, easy handling which is further simplified by its nonpathogenic nature, inexpensive culture conditions, and its amenability for genetic manipulation, make up the advantages of using this organism as a model [Tenreiro *et al*, 2013]. The principle to use yeast as a model organism to study human diseases relies on two approaches: 1) if the gene implicated in the human disease has a yeast homolog, it is possible to study its function directly, by performing experiments of genetic ablation or gene over-expression, 2) when the disease-associated gene does not have an obvious counterpart in yeast, the transgene can be heterologously expressed in yeast, and the resulting strains subjected to functional analyses [Tenreiro *et al*, 2013]. Furthermore, if the disease-associated gene function is already known, yeast models are useful to gain insights into the underlying molecular basis of the pathology of disease-associated mutations [Tenreiro *et al*, 2013]

In order to reproduce the features of αSyn accumulation that occurs in PD in yeast cells, the heterologous expression of αSyn complementary DNA (cDNA) in yeast cells (human *SNCA* gene sequence) is performed in selective-containing background WT yeast strains, through regulation of a house-keeping galactose-inducible promoter provided (*GAL1*) [Outeiro and Lindquist, 2003], [Tenreiro and Outeiro, 2010]. However, there are various yeast models based on the heterologous expression of αSyn, which present different phenotypes, depending on the expression system, since different expression systems leads to different levels of αSyn expression [Outeiro and Lindquist, 2003], [Willingham *et al*, 2003], [Cooper *et al*, 2006]. This feature has been explored according to the objectives of the studies [Menezes *et al*, 2015]. The use of multi-copy (or 2μ) plasmids revealed that yeast cells reduce the average plasmid copy number in order to reduce αSyn expression and toxicity [Outeiro and Lindquist, 2003]. To avoid this, an integrative approach based on the insertion of the αSyn coding sequence in the yeast genome enabled more stable expression, and the levels of toxicity could be manipulated by varying the number of copies of the αSyn cDNA inserted in the genome [Cooper *et al*, 2006], [Su *et al*, 2006].

PD features already characterized in other model organisms, such as rat primary mesencephalic cultures [Masliah *et al*, 2000], [Zhou *et al*, 2000], *D. melanogaster* [Feany and Bender, 2000] and *C. elegans* [Lakso *et al*, 2003], have been accurately recapitulated in yeast [Outeiro and Lindquist, 2003]. Namely, αSyn induced toxicity in a dose dependent manner, inhibiting cell growth and promoting cell

dysfunction and death when the protein is overexpressed in yeast cells [Outeiro and Lindquist, 2003]. Additionally, other PD features such as αSyn intracellular inclusions formation [Outeiro and Lindquist, 2003], oxidative stress [Flower *et al*, 2005], interaction with lipid rafts [Zabrocki *et al*, 2008], trafficking defects [Cooper *et al*, 2006], [Gitler *et al*, 2008], [Soper *et al*, 2008], [Su *et al*, 2010] and apoptosis [Flower *et al*, 2005] have been characterized in yeast.

To date, αSyn toxicity in yeast is known to involve several cellular pathways that were either 1) first described in yeast and then validated in higher eukaryotic models of PD or 2) identified in other systems and then successfully recapitulated in yeast [Tenreiro *et al*, 2013]. Amongst the different pathways involved in αSyn toxicity in yeast, induction of apoptosis, lipid droplet accumulation [Outeiro and Lindquist, 2003], mitochondrial dysfunction [Buttner *et al*, 2008], [Su *et al*, 2010], proteasome impairment [Outeiro and Lindquist, 2003], [Chen *et al* 2005], [Sharma *et al* 2006], oxidative stress [Sharma *et al* 2006], [Witt and Flower 2006], autophagy/mitophagy dysfunction [Petroi *et al* 2012], [Sampaio-Marques *et al* 2012], vesicle trafficking defects [Outeiro and Lindquist, 2003], [Soper *et al* 2008] and ER-Golgi trafficking impairment [Cooper *et al* 2006] were identified. Importantly, a recent study was performed, exploring the power of the budding yeast to gain insights regarding the protective or detrimental role of the phosphorylation at S129 residue in the context of PD pathology [Tenreiro *et al*, 2014a]. To achieve this purpose, [Tenreiro *et al*, 2014a] used integrative transformed yeast strains expressing human WT αSyn, as well as the phospho-mutants mimicking (S129D) or blocking (S129A) phosphorylation at S129 residue and results not only showed a protective effect of the phosphorylation at this residue, where the S129D mutant showed a rescue of cell toxicity, less inclusion formation and promotion of protein clearance through autophagy up-regulation, when compared with both the WT protein and with the non-phosphorytable mutant protein (S129A), but it also showed significant features, such as differences in the biochemical and morphological nature of inclusions formed (the S129A mutant showed bigger, more heterogeneous and insoluble inclusions as well as more oligomeric species, when compared to the inclusions formed by the WT and S129D mutant), the role of phosphorylation at S129 on αSyn dynamics (S129A formed more inclusions and sooner than the WT protein) and showed the modulation of non-phosphorytable αSyn toxicity by ER-Golgi trafficking enhancers, similarly to what was previously described for the WT protein [Tenreiro *et al*, 2014a]. This study introduced a novel link between αSyn phosphorylation, aggregation and cellular toxicity and showed that the phosphorylation state at S129 of this protein impact on the ability of cells to clear αSyn inclusions [Tenreiro *et al*, 2014a], one of the factors that is considered to exacerbate PD pathology [Cook and Petrucelli, 2012], [Xilouri *et al*, 2009] and therefore, autophagy playing a central role in this disease [Sampaio Marques *et al*, 2012], [Chu *et al*, 2011], [Winslow *et al*, 2010]. Hence, this simple but powerful yeast organism provided a contributing major step to create novel therapeutic approaches to synucleinopathies, through the modulation of its phosphorylation [Tenreiro *et al*, 2014a].

αSyn is also part of a diverse and highly conserved interaction network including proteins with diverse functions, namely kinases, phosphatases, deubiquitinating enzymes and metal transporters [Tenreiro and Outeiro, 2010]. This network was identified in genetic screens in yeast and was further validated in rat primary neuronal cultures and in nematode models [Gitler *et al*, 2009], [Yeger-Lotem *et al*, 2009]. This conserved network is evident in the observation that in yeast, αSyn is subjected to several PTMs observed in mammalian cells and in the brains of PD patients, namely phosphorylation at S129 [Anderson *et al*, 2006], [Zabrocki *et al*, 2008], [Chen *et al*, 2009]. Yeast may also be used for drug screens that resulted in the identification of several therapeutic candidates that rescue αSyn toxicity [Griffioen *et al*, 2006], [Fleming *et al*, 2008], [Su *et al*, 2010].

2. Objectives

αSyn inclusion formation is the hallmark of both sporadic and familial PD. PTMs of this protein, namely phosphorylation, are considered important factors in the process of αSyn fibrillation and in the modulation of its toxicity. Using as an established model of PD, the budding yeast *S. cerevisiae*, this project had two major purposes:

A) To phenotypically characterize the most recent PD familial linked mutation of αSyn, A53E.

The construction of a multi-copy yeast plasmid encoding for A53E αSyn was performed and a phenotypical characterization including cell viability, inclusion formation, protein expression and phosphorylation, solubility of aggregates and mitochondrial network was assessed.

B) To study the interplay between S87and S129 residues phosphorylation on αSyn induced toxicity.

A phenotypical characterization including cell viability, inclusion formation, protein expression, phosphorylation and clearance, and proteasome and autophagy function evaluation was performed, using integrative yeast strains encoding the αSyn phospho mutants that either block or mimic αSyn phosphorylation at those residues.

3. Materials and Methods

3.1. Molecular biology and genetics using *E. coli*

3.1.1. *E. coli* cell culture

E. coli competent cells were grown in selective solid Luria Broth (LB) (Sigma-Aldrich®, MI, USA) media containing the plasmid selection marker: Ampicillin (100 µg/ml) or Kanamycin (50 µg/ml) for 12 hours at 30°C (and 220 rpm for equivalent liquid media). Grown colonies were stored at 4°C for up to one month.

3.1.2. *E. coli* competent cells transformation

NZYStar® Competent Cells (nzytech® – genes & enzymes, Lisbon, Portugal) were thawed on ice and 1 µL (~100 ng) of plasmid DNA (or 10 µL of DNA, in case of reaction product) was added to 50 µl of *E.coli* competent cells, followed by incubation on ice for 30 minutes. Then, cells were heat-shocked for 40 seconds in a 42˚C water bath and placed on ice for 2 minutes. 900 µL of room temperature LB liquid media (Sigma-Aldrich®, MI, USA) without antibiotics was added to the reaction and cells were incubated at 37˚C and 220 rpm for 1 hour. After centrifuging for 1 minute at 5000 rpm and room temperature and removing 800 µL of media, cells were re-suspended in the remaining LB media and spread in LB agar plates containing the selection antibiotic (Ampicillin 100 µg/ml or kanamycin 50 µg/ml, depending on the plasmid selection marker). Plates were incubated overnight at 37˚C and stored at 4°C for up to one month.

3.1.3. *E. coli* plasmid DNA extraction and purification

For plasmid DNA extraction and purification from E.*coli* cells, a random colony of transformed cells was picked from the LB agar media containing the respective selection marker to 3 ml of equivalent liquid LB media and incubated overnight at 37˚C and 220 rpm for growth. Afterwards, bacterial cells were harvested by centrifugation (for 30 seconds, 11000 *g* and room temperature) and plasmid DNA was recovered and purified using NZYMiniprep™ Kit, according to the manufacturer's instructions (nzytech® – genes & enzymes, Lisbon, Portugal). Plasmid DNA was eluted in 52 or 32 µl of pre-heated (50˚C) milli-Q® (Millipore Merck®, MA, USA) water and samples were stored at -20˚C.

DNA concentrations and DNA sample quality evaluation were assessed using NanoDrop™ equipment and software, according to the manufacturer's instructions (ThermoFisher Scientific®, MA, USA).

3.1.4. Glycerol stocks construction for plasmid DNA storage

In order to perform a stable storage of plasmid DNA, 500 µl of *E.coli* cells transformed with the plasmid of interest and grown in LB liquid media (containing the correspondent antibiotic for selection), were added to 500 µl of Glycerol 50% (50% v/v) and cryopreserved at -80°C in 2 ml vials.

3.2. Gel electrophoresis

To perform DNA gel electrophoresis, an agarose (Agarose Ultrapure™, Invitrogen®, CA, USA) 1% gel was prepared using tris-acetate-EDTA (TAE) 1X Buffer (diluted from TAE 50X buffer stock, Sigma-Aldrich®, MI, USA). For DNA fragments visualization using UV light, GreenSafe® Midori DNA staining (Bulldog Bio®, NH, USA) was added (3 µl of dye per 100 ml gel) before gel solidification. For DNA fragment migration tracking, 6X DNA Loading Dye (ThermoFisher® Scientific, MA, USA) was added to each sample (to a final concentration of 1X). Resolving of the gel was performed using a constant voltage of 90 V for 30 minutes and the molecular weight of the DNA fragments determined by comparison with the DNA ladder GeneRuler 1 kb DNA Ladder 0.5 ng/µl (ThermoFisher® Scientific, MA, USA).

3.2.1. Purification of DNA fragments from an agarose gel

To recover and purify DNA fragments within the agarose gel, the portion of gel containing the desired fragment was cut and excised and purification of DNA was performed using the Wizard® SV Gel and PCR Clean-Up System Kit (DNA Purification by Centrifugation), according to the manufacturer's instructions (Promega®, WI, USA). DNA fragments were eluted in 30 µl of pre-heated (50˚C) milli-Q® (Millipore Merck®, MA, USA) water and samples were stored at -20˚C.

DNA concentrations and DNA sample quality evaluation were assessed using NanoDrop™ equipment and software, according to the manufacturer's instructions (ThermoFisher Scientific®, MA, USA).

3.3. Molecular biology and genetics using yeast S. *cerevisiae*

3.3.1.Yeast strains

The yeast strains used in this study are listed in *Annexes* section, Table 8.2.

The previously characterized yeast model of PD [Outeiro and Lindquist, 2003] was used in this study. The yeast strain W303.1A was transformed with the multi-copy yeast plasmid pRS426 containing

the *GAL1* inducible promoter and encoding the gene sequence for WT αSyn or A53E αSyn fused to a (enhanced) green fluorescent protein ((E)GFP) at the C- terminal, or with the empty plasmid, following the yeast transformation protocol detailed below (Subtopic 3.3.3).

Regarding the phospho-mutant yeast strains, VSY71 to VSY74 strains contain double genome insertions of *GAL1* prSNCA(WT, S129A or S129D)-GFP or of the empty vectors and were previously described [Sancenon *et al*, 2012], as for yeast strains SC_663 and SC_658, that contain double insertions of the *GAL1* prSNCA(S87E or S87E_S129D)-GFP, respectively. All transformed yeast strains were available at the *Cell and Molecular Neuroscience* laboratory (Chronic Diseases Research Center (CEDOC), NOVA Medical School (NMS) – New University of Lisbon (UNL), Lisbon, Portugal) and contain both the integrative yeast plasmids p304 GAL1pr-SNCA-GFP and p306 GAL1prSNCA-GFP, encoding for the respective αSyn mutation. These were integrated into W303.1A and W303.1B yeast strains, respectively, by linearization with *Eco*RI restriction enzyme [Tenreiro *et al*, 2014a]. The correct insertion of the integrative vectors was verified by performing a polymerase chain reaction (PCR) and the haploid strains were used to generate a diploid strain by mating. Diploids were selected in minimal media (SC) by uracil (URA) and tryptophan (TRP) prototrophy [Tenreiro *et al*, 2014a] and the identity of the yeast strains SC_658 and SC_663 was confirmed by PCR amplification of the *trp1* and *ura3* auxotrophic markers and by PCR amplification and confirmation by DNA sequencing of the *SNCA* gene, as described below (*Materials and Methods section*, Subtopic 3.11.).

The phospho-mutants yeast strains (VSY71 to VSY74, SC_658 and SC_663) were transformed with a centromeric plasmid encoding an unstable GFP protein (uGFP) protein for proteasome function evaluation or with a centromeric plasmid encoding the GFP-Atg8 protein for autophagy function evaluation, following the yeast transformation protocol described below (*Materials and Methods* section, Subtopic 3.3.3.).

Yeast strains were stored in glycerol stocks as previously described for *E. coli* cells and stored at -80°C for further use. For experimental manipulation, strains were thawed and cultivated in solid yeast extract peptone dextrose (YPD) or synthetic complete (SC) selective media (lacking the amino acids that complement the respective yeast auxotrophy), which were incubated at 30˚C until visible cell growth (approximately 48 hours), followed by storage at 4˚C up to one month.

3.3.2.Growth media and spotting assays

The composition of the medias used for growth of yeast cells is further detailed in, *Annexes* section, Table 8.3.

For αSyn expression induction experiments, yeast cells were pre-grown in 5 ml SC-Raffinose 1% or yeast extract peptone (YEP)-Raffinose 1% liquid media at 30˚C, with orbital agitation (220 rpm) for 24 hours (doubling time of approximately 3 hours). After 24 hours, optical density at 600 nm ($OD_{600\ nm}$) was measured and yeast cells were diluted to a standardized $OD_{600\ nm} = 0.6$ (1.5×10^6 cells/ ml) upon protein expression induction, in 5 ml SC-Raffinose 1% or YEP-Raffinose 1% liquid media and grown at 30˚C, with orbital agitation (220 rpm). At the time point calculated for yeast cells to reach an $OD_{600\ nm}$ of 0.6, cell cultures were centrifuged (4000 rpm, at 30˚C for 5 minutes) and cell pellet was then re-suspended in SC-Galactose 1% or YEP-Galactose 1% liquid media, respectively, and incubated at 30˚C, with orbital agitation (220 rpm) for 7 hours for protein expression induction.

For spotting assays, cell suspensions were adjusted to OD_{600nm} = 0.1 and used to prepare 1/3 serial dilutions that were applied as spots (4 µl) onto the surface of the YPD rich media used as control or SC-Galactose 1% (phospho-mutants αSyn assay) or SC-Galactose 0.5%/Raffinose 0.5% (A53E αSyn characterization assay) and incubated at 30˚C for 2–3 days.

For fluorescence microscopy and flow cytometry analysis, adenine was added to the growth media at a final concentration of 0.16 mg/ml to avoid background interactions by the red pigment production due to the presence of the *ade2* auxotrophic marker of the used yeast strains. Adenine supplementation did not alter growth phenotypes of the tested yeast strains.

For αSyn clearance experiments, the $OD_{600\ nm}$ of cell cultures was standardized to 0.6 upon protein expression induction, as previously described. After 7 hours of protein expression induction in 5 ml SC-Galactose 1% media, cell cultures were centrifuged (4000 rpm, 5 minutes and 30˚C) and washed with 5 ml of sterile distilled water twice. Following this washing step, cells were again centrifuged (4000 rpm, 5 minutes and 30˚C) and re-suspended in 5 ml of SC-Glucose 2% and incubated at 30˚C, with orbital agitation (220 rpm) for 13 hours, for protein expression repression.

3.3.3. Yeast cells transformation

Multi-copy (or 2µ) and centromeric yeast plasmids used in yeast strains transformations are detailed in *Annexes* section, Table 8.1.

Yeast cells transformation with centromeric or multi-copy plasmids was based on a protocol that aims to permeable yeast cellular membrane using lithium acetate (LiAc) and to induce its destabilization by tris-EDTA buffer (TE) and adding polyethylene glycol (PEG) 4000 50%, which allows and promotes plasmid DNA to enter the cell.

Prior to transformation, a single colony of each yeast strain to be transformed was picked from YPD solid media or SC media into 30 ml of YPD media and incubated at 30˚C and 200 rpm overnight (yeast pre-culture). After overnight incubation, the OD_{600nm} of the yeast pre-culture was measured and the culture diluted in 30 ml YPD fresh media to a final OD_{600nm}=0.6 upon yeast cells transformation (doubling time of approximately 90 minutes). At the time point calculated, cells were harvest by centrifugation (4000 rpm, 5 minutes and 4˚C), washed with 30 ml of sterile distilled water and re-suspended in 1 ml of sterile distilled water. Then, cells were centrifuged (17000 *g*, 30 seconds and 4˚C) and cell pellet was washed twice, each time with 300 µl of a solution containing 10% LiAc 1 M and pH=7.5 mixed with 10% TE buffer 10X (0.1 M Tris, 0.01 M EDTA, pH=7.5) and 80% sterile distilled water. Then, cell pellet was re-suspended in 300 µl of a solution containing 10% LiAc 1 M and pH=7.5 mixed with 10% TE buffer 10x (0.1 M Tris, 0.01 M EDTA, pH=7.5) and 80% PEG 4000 50%. For each transformation, 50 µl of cells were mixed with 1 µg of plasmid DNA, to which 10 µl of salmon sperm DNA (previously denatured for 10 minutes at 100˚C) were added. The mixture was homogenized by pipetting and incubated at 30˚C with orbital agitation of 220 rpm for 30 minutes. Subsequently, the transformation reaction was transferred to a 42˚C bath for 20 minutes and cells were washed with sterile distilled water two times and were re-suspended in 200 µl of sterile water, and plated onto appropriate selective SC-Glucose 2% solid media. The plates were incubated at 30˚C for 2-3 days and 3 of the transformant colonies obtained were picked to a new fresh equivalent solid media and incubated again at 30˚C for 2 days for biological replicates creation.

3.3.4. Yeast genomic DNA extraction

For yeast genomic DNA extraction, a portion of yeast culture was transferred from the respective SC-Glucose 2% selective solid media (previously thawed and grown as described above) to a bead-beater tube containing 250 µl of Buffer A1 (NZYMiniprep™, nzytech® – genes and enzymes, Lisbon, Portugal). To each sample, 100 µl of glass beads 425-600 µm (Sigma-Aldrich®, MI, USA), were added and the samples were submitted to three cycles of bead-beating for 30 seconds followed by 2 minutes on ice each. Following this, samples were centrifuged (11000 *g*, 30 seconds at room temperature) and the supernatant was transferred to a clean 1.5 ml *Eppendorf* tube to which 250 µl of Buffer A2 was added. Subsequently, genomic DNA was extracted and purified by following the NZYMiniprep™ (nzytech® – genes & enzymes, Lisbon, Portugal), according to the manufacturer's instructions. DNA was eluted in 52 µL of pre-warmed (52˚C) milli-Q® (Millipore Merck®, MA, USA) water and the samples stored at -20˚C.

DNA concentrations and DNA sample quality evaluation were assessed using NanoDrop™ equipment and software, according to the manufacturer's instructions (ThermoFisher Scientific®, MA, USA).

3.4. Construction of a yeast plasmid containing the αSyn familial linked PD-linked mutation A53E

3.4.1. Design of primers

In order to generate a multi-copy yeast construct encoding the mutant A53E αSyn, a Site-directed mutagenesis approach was performed using the WT αSyn coding gene sequence as a template.

Firstly, using the WT αSyn coding gene sequence, the position where the desired mutation ought to be introduced was determined, as illustrated below (Figure 3.1.).

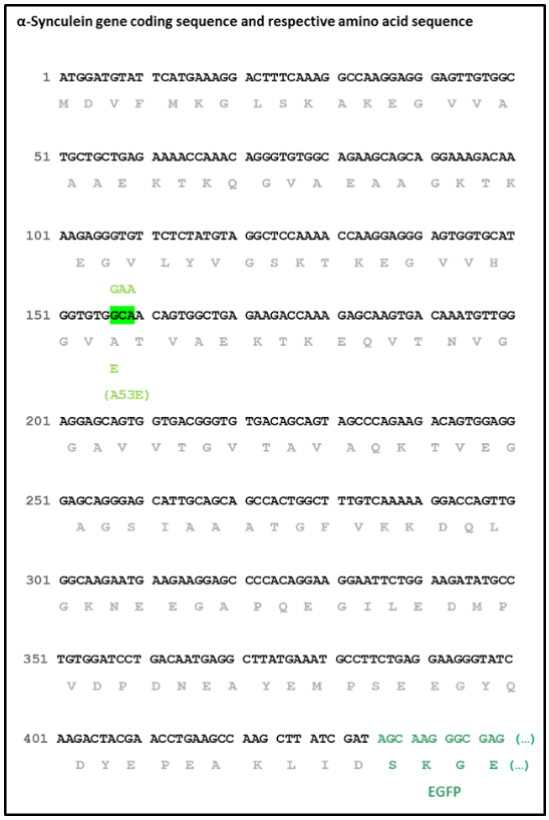

Figure 3.1. Schematic representation of the WT αSyn coding gene sequence (in black) fused to GFP (in green). The respective amino acid coded by each codon is represented (in gray). The familial mutation A53E (green highlighted codon) is represented and the expected codon and amino acid exchange (GCA codon is replaced for a GAA) for the mutation to occur is represented above the gene sequence [Pasanen *et al*, 2014].

Secondly, a pair of primers were designed to introduce the amino acid replacement A53E. These were optimized regarding the temperature of melting (T_m) and cytosine and guanine (CG) content, using *PrimerX* (Bioinformatics.org) bioinformatics tool (Table 3.1).

Table 3.1. Primers for the PCR of the site directed mutagenesis to obtain the mutant A53E αSyn. Primers created for the Site directed mutagenesis reaction to obtain the mutation of A53E αSyn (DNA sequence, percentage of CG content, temperature of melting and length). The introduction of the mutation is highlighted in bold within the primers sequence.

Primer Designation	DNA Sequence (5'→3')	CG Content (%)	Temperature of Melting (°C)	Length (bp)
A53E Forward	GTGCATGGTGTGG**A**AACAGTGGCTGAG	55.56	75.5	27
A53E Reverse	CTCAGCCACTGTT**T**CCACACCATGCAC	55.56	75.5	27

The alanine (A) to glutamic acid (E) amino acid change at codon 53 (A53E) of αSyn protein was achieved by mutating the nucleotide number 158 of the *SNCA* coding gene sequence from a cytosine (C) to an alanine (A) (c.158C>A), as highlighted in the DNA sequence of the primers designed (Table 3.1).

3.4.2.Site-directed mutagenesis reaction

The multicopy yeast plasmid p426*GAL* containing the WT αSyn fused to GFP coding gene sequence was used as a template for the Site-directed mutagenesis, performed using the QuickChange™ XL Site-Directed Mutagenesis Kit, according to the manufacturer's instructions (Agilent Technologies®, CA, USA). By using *Pfu* Ultra High-Fidelity DNA polymerase, the A53E mutation was introduced using the PCR conditions stated below (Table 3.2).

Table 3.2. PCR program used in the site directed mutagenesis reaction. It is detailed the number of cycles, temperature (˚C) and time (in minutes or seconds) used for each PCR segment.

PCR Segment	Number of Cycles	Temperature (°C)	Time
1	1	95	1 minute
2	18	95	50 seconds
		60	50 seconds
		68	8 minutes
3	1	68	10 minutes

Following PCR reaction, 1 µl of *Dpn*I endonuclease was added to the PCR reaction mix. This enzyme specifically recognizes the sequence 5´Gm6ATC-3', targeting methylated and hemimethylated DNA. Therefore, *Dpn*I only digests the plasmid DNA template (which is dam^+ methylated), leaving in solution the PCR synthesized DNA only. The sample was incubated overnight at 37°C for the digestion to occur and NZYStar® Competent *E.coli* cells (nzytech® – genes & enzymes, Lisbon, Portugal) were transformed and plasmid DNA extracted and purified, as previously described in subtopics 3.1.2. and 3.1.3. of *Materials and Methods* section, respectively. For confirmation of the mutation leading to the amino acid replacement A53E, DNA sequencing and full sequence alignment were performed (as described below), which confirmed the presence of the desired mutation (*Annexes* section, Figure 8.1).

3.4.3.DNA sequencing

In order to confirm the presence of the desired mutation and the identity of the clones generated, DNA sequencing was performed (Stabvida, Oeiras, Portugal). The primer used for DNA sequencing (Syn-seq-S), anneals with the beginning of the αSyn coding gene sequence within the yeast plasmid which allows the identification of mutations on the αSyn coding gene sequence (further detailed in Table 3.3). The presence of mutations was identified by full-sequence alignment using WT αSyn encoding gene sequence as template and *ClustalOmega* (European Molecular Biology Laboratory - European Bioinformatics Institute, England, UK) bioinformatics tool. All sequence alignments performed for confirmation of identity of clones are illustrated in *Annexes* section (Figures 8.1 and 8.2).

Table 3.3. Primer used for DNA sequencing of αSyn coding gene sequence. Details of the primer (DNA sequence, percentage of CG content, temperature of melting and length) used for the DNA sequencing of the αSyn coding gene sequence.

Primer Designation	DNA Sequence (5'→3')	CG Content (%)	Temperature of Melting (°C)	Length (bp)
Syn-seq-S	ATGGATGTATTCATGAAAGGACTTTC	34.61	65.9	26

3.5. Protein Extraction

3.5.1.Yeast protein extraction using the TCA-MURB approach

To perform yeast protein extraction, an equal amount of yeast cell correspondent to an OD_{600nm} of 1 (2.5×10^6 cells) were harvest by centrifugation, re-suspended on trichloroacetic acid (TCA) 10% and incubated on ice for 20 minutes. After a second centrifugation (15000 *g*, 3 minutes and room temperature), cells were washed two times with 800 µL of acetone (by centrifuging at 15000 *g*, 5 minutes and room temperature). Cell pellet was air dried for 1 hour and cell lysis was performed using MURB buffer (50 mM sodium phosphate, 25 mM MES, pH 7.0, 1% sodium dodecyl sulfate (SDS), 3 M urea, 0.5% β-mercaptoethanol) supplemented with 1 mM sodium azide, bromofenol blue and proteases and phosphatases inhibitors (Roche® diagnostics, Mannheim, Germany) and disrupted by glass beads (1/3 (v/v) (SigmaAldrich®, MA, USA) by 3 cycles of 30 seconds in the bead-beater, followed by 2 minutes on ice each. The samples were incubated at 70˚C for 10 minutes and membranes were removed by centrifugation at 10000 *g* for 1 minute and room temperature. The supernatant containing the proteins was collected and stored at -20˚C.

3.5.2. Yeast protein extraction for TritonX-100 soluble and insoluble protein fractions separation

To perform the TritonX-100 assay for soluble and insoluble protein fractions separation, an equal amount of yeast cell correspondent to an OD_{600nm} of 2.5 (4.2×10^6 cells) were harvest by centrifugation (3000 rpm, 4 minutes and 30˚C), re-suspended on distilled water and transferred to a bead-beater vial. Cells were again centrifuged and cell pellet was re-suspended in 100 µL of tris-buffered saline (TBS) 1X containing proteases and phosphatases inhibitors (Roche® diagnostics, Mannheim, Germany). Following this, yeast cells were lysed by glass beads (3 cycles of 30 seconds in the bead-beater, followed by 2 minutes on ice) and membranes were removed by centrifugation (700 g, 3 minutes and 4˚C). The supernatant was collected, sonicated for 5 seconds at 10 mA and stored at -20˚C. Protein concentration was determined using the bicinchoninic acid (BCA) protein assay reagent kit™ (ThermoFisher® Scientific, MA, USA), according to the manufacturer's instructions.

Soluble (TS) and insoluble (TI) TritonX-100 protein fractions were separated by collecting 200 µg of protein to a final volume of 120 µl of TBS 1X containing proteases and phosphatases inhibitors (Roche® diagnostics, Mannheim Germany). From the total volume of 120 µl, 20 µl were recovered and stored at -20˚C (correspondent to the total protein (TP)). To the remaining 100 µl sample, TritonX-100 detergent was added (1%) and after mixing by pipetting, samples were incubated on ice for 30 minutes, followed by centrifugation (15000 *g*, 1 hour and 4˚C). The supernatant was collected to a new 1.5 ml *eppendorf* tube (correspondent to the TS fraction) and stored at -20˚C. The pellet (TI fraction) was re-suspended in 40 µL of TBS 1X containing protease and phosphatase inhibitors and 2% SDS and it was sonicated for 5 seconds and 10 mA and stored at -20˚C.

Equal volumes of TI, TS and TP fractions (5 µl) were loaded into a sodium dodecyl sulfate polyacrylamide gel electrophoresis (SDS-PAGE) gel.

3.6. Western Blot analysis

3.6.1. Sample preparation

Samples from yeast protein extracted using the TCA-MURB protocol were thawed on ice, incubated at 70˚C for 5 minutes and centrifuged (10000 *g*, 1 minute and room temperature). Then, 5 µl of each sample was directly loaded into the gel.

Samples from TritonX-100 procedure were prepared by adding 2 µl of protein buffer sample (PBS) (4X, 1 M tris-HCl pH 6.8, β-mercaptoethanol, 20% SDS, glycerol 100%, bromophenol blue) to 5 µl of each protein sample. Then, samples were incubated at 70˚C for 5 minutes and the total sample volume was loaded in the gel.

3.6.2. Gel preparation

A 12% polyacrylamide gel was prepared by mixing 25% (v/v) of 1.5 M of Tris HCl (pH=8.8), 40% (v/v) of 30% acrylamide mix (Sigma-Aldrich®, MI, USA), 33% (v/v) of distilled water, 1% (v/v) of SDS 10%, 0.04% (v/v) tetramethylethylenediamine (TEMED) (Panreac AppliChem®, Darmstadt, Germany) and 1% (v/v) of 10% ammonium persulphate (APS) (Schleicher&Schuell GmbH® Biosciences, Dassel Germany) was added to initiate polymerization reaction. This solution was immediately transferred into a cast, overlaid with isopropanol and incubated for 30 minutes. Then, isopropanol was removed and a 5% stacking gel composed of 12.5 % (v/v) 1.5M Tris-HCl (pH 6.8), 17% of 30% Acrylamide mix (Sigma-Aldrich®, MI, USA), 68 % (v/v) distilled water, 1 % (v/v) of SDS 10%, 0.1% of TEMED (Panreac AppliChem®, Darmstadt, Germany) and 1 % (v/v) of 10% APS was prepared. The 5% stacking gel was immediately overlaid on the resolving gel and a gel comb was inserted. The gel was incubated at room temperature for at least 1 hour for polymerization to occur.

For proteasome function evaluation, a 15% polyacrylamide gel was prepared by mixing 25% (v/v) of 1.5 M of Tris HCl (pH 8.8), 50% (v/v) of 30% acrylamide mix (Sigma-Aldrich®, MI, USA), 23% (v/v) of distilled water, 1% (v/v) of SDS 10% and 0.04% (v/v) TEMED (Panreac AppliChem®, Darmstadt, Germany) and 1% (v/v) of 10% APS (Schleicher&Schuell GmbH® Biosciences, Dassel Germany) was added to initiate polymerization reaction. This solution was immediately transferred into a cast, overlaid with isopropanol and incubated for 30 minutes. Then, isopropanol was removed and a 5% stacking gel was added according to what was previously described.

3.6.3. SDS-PAGE and transference to a nitrocellulose membrane

Samples and loading protein ladder were loaded and ran in running buffer (250 mM tris base, 200 mM glycine, 1% SDS) at 80 V for 30 minutes and 120 V for 90 minutes. Protein migration was controlled by the migration of SDS molecular weight ruler used (PageRuler™ Prestained Protein Ladder, 10 to 180 kDa) (ThermoFisher® Scientific, MA, USA).

Proteins were transferred from the gel to a nitrocellulose membrane and the transference was carried out for 7 minutes and 25 V, using Trans-Blot Turbo™ System (Bio-Rad®, CA, USA) according to the manufacturer's instructions.

3.6.4. Immunostaining analysis

Following protein transference to a nitrocellulose membrane, membranes were blocked for 1 hour at room temperature with 5% bovine serum albumin (BSA) (or 5% skim milk powder) in TBS-Tween 1X (50 mM Tris, 150 mM NaCl, 0.05% Tween, pH=7,5).

Membranes were further incubated for 3 hours at room temperature (or overnight (ON) at 4°C) with the primary antibody, either mouse anti-Total αSyn at 1:2000 (BD® Biosciences, NJ, USA), mouse

anti-phosphorylated S129 αSyn (pS129) at 1:4000 (Wako®, NY, USA), mouse anti-GFP at 1:1000 (NeuroMab®, CA, USA) or mouse anti-phosphoglycerate kinase (PGK) at 1:2000 (Life Technologies®, NY, USA). Following incubation with the primary antibody, membranes were washed three times with TBS-Tween for 10 minutes each time and incubated with the secondary antibody anti-mouse horseradish peroxidase-conjugated (GE Healthcare®, England, UK) at 1:10000 (or 1:5000 for the primary antibody anti-PGK) prepared in 5% TBS-Tween.

Following incubation with the secondary antibody, membranes were washed three times (10 minutes each) with TBS-Tween and immune-detection was performed using an enzyme linked chemiluminescence (ECL) detection reagent, based on the horseradish peroxidase secondary antibody conjugate catalysis of luminol in alkaline conditions. Approximately, 1 to 2 ml of the luminol reagent and peroxide solution (Millipore Merck®, MA, USA) mixed 1:1, were applied to the membrane and the secondary antibody signal was detected by chemiluminescence using the Chemidoc Touch™ system (Bio-Rad®, CA, USA) according to the manufacturer's instructions.

3.6.5. Image editing and signal quantification

The band intensity of the different immunoblots signals was estimated using Image Lab™ software (Bio-Rad®, CA, USA) and normalized against the corresponding PGK signal. Namely, αSyn protein levels were determined by calculating the ratio between αSyn/PGK and normalized to the WT control assay (mean ± standard deviation (SD)); pS129-αSyn protein levels were determined by calculating the ratio between both values: (pS129-αSyn/PGK)/(αSyn/PGK) and normalized to the WT control assay (mean ± SD). Proteasome function evaluation was estimated by quantification of the ratio of uGFP signal to PGK signals (mean ± SD). Atg8 induction was inferred by observation of the fold increase of total GFP signal (GFP-Atg8 and free GFP signal/PGK) and autophagic flux was inferred by observing the vacuolar degradation of the Atg8 domain reporter (free GFP signal/PGK).

3.7. Fluorescence microscopy

Fluorescence microscopy analysis was performed using the Zeiss Axiovert 200M widefield fluorescence microscope (Carl Zeiss®, Munich, Germany) and equipped with a cooled charged-coupled device (CCD) camera (Roper Scientific® CoolSNAP™ HQ, Munich, Germany) to acquire images containing at least 400 cells per assay performed.

3.7.1. αSyn inclusion formation evaluation

For inclusion formation assessment by fluorescence microscopy, 1 ml of each yeast culture grown as described in *Materials and Methods* section, Subtopic 3.3.2. was centrifuged for 1 minute and

10000 *g* at room temperature and visualized under the microscope (120x total amplification). αSyn inclusions formation was evaluated by (E)GFP fluorescence and the percentage of cells with inclusions was determined by manually counting at least 400 cells per assay performed, being cell counting performed using Image J™ software (Tree Star®, OR, USA).

(E)GFP fluorescence was detected using the 488 nm laser line of an Argon (Ar) laser (25 mW nominal output) and a custom wavelength detection window set to 493–556 nm.

3.7.2. Cellular mitochondrial network and nuclei localization evaluation

For simultaneous evaluation of mitochondrial network integrity and nuclei localization, an OD_{600nm} correspondent to 1 was recovered from each yeast culture grown as described in *Materials and Methods* section, Subtopic 3.3.2. After harvesting the respective volume of culture, cells were centrifuged for 1 minute and 10000 *g* at room temperature and cell pellet was re-suspended in 1 ml of phosphate-buffered saline solution (PBS 1X) (0.137 M NaCl, 0.05 M NaH_2PO_4, pH=7.4) (ThermoFisher® Scientific, MA, USA). Following this washing step, 10 µl of MitoTracker Deep Red stock solution (10 µM) (ThermoFisher® Scientific, MA, USA), for assessment of mitochondrial network integrity, was added to each sample and cells were incubated at 30˚C and 220 rpm for 1 hour and in the dark. After a 45 minutes incubation, 1 µl of Hoechst 33342 stock solution (10 mg/ml) (Invitrogen®, CA, USA) dye was added to the sample for assessment of nuclei localization, and incubation was carried for the remaining time. Before visualizing cells on the microscope (120X total amplification), samples were washed twice with 1.5 ml PBS 1X followed by centrifugation (1 minute, 10000 *g* and at room temperature).

MitoTracker Deep Red fluorescence was detected using the 644 nm laser line of an Ar laser (25 mW nominal output) and a wavelength detection set to 665 nm, whereas Hoechst 33342 fluorescence was detected using the 350 nm laser line of an Ar laser (25 mW nominal output) and a wavelength detection set to 493–556 nm.

3.8. Flow cytometry

3.8.1. Cell viability evaluation

Yeast cell membrane integrity was evaluated with PI staining using a Fluorescence-Activated Cell Sorting (FACS) Canto II (BD® Biosciences, San Jose, CA). An $OD_{600\ nm}$ of 1 of yeast cells was harvested and re-suspended in 1 ml PBS 1X. Yeast cells were incubated with 5 µl of propidium iodide (PI) 0.1 mg/ml (Sigma-Aldrich®, MI, USA) for 15 min at 30˚C and 220 rpm in the dark. As a positive control, cells boiled for 10 minutes previously to PI addition were used. After washing once with PBS 1X, cells were re-suspended in 2 ml PBS 1X and analyzed using the FL-2 channel for PI fluorescence detection and a minimum of 5000 events were collected for each experiment. Simultaneously,

fluorescence intensity of αSyn-GFP was measured using a 488 nm laser for excitation and a 502 LP mirror in conjunction with a 530/30 BP filter for detection (BD® Biosciences, San Jose, CA).

3.8.2. Cellular mitochondrial network integrity evaluation

For mitochondrial network assessment, an $OD_{600\ nm}$ of 1 of yeast cells was harvested and re-suspended in 1 ml PBS 1X. Yeast cells were incubated with 10 µl of MitoTracker Deep Red dye 10 µM for 1 hour at 30˚C and 220 rpm in the dark. After washing once with PBS 1X pH=7.4 (ThermoFisher® Scientific, MA, USA), cells were re-suspended in 2 ml PBS 1X and MitoTracker fluorescence was analyzed by excitation at 579 nm and emission at 599 nm, simultaneously with (E)GFP fluorescence.

For flow cytometry data, analysis was performed using FlowJo™ software (Tree Star®, OR, USA). Results were expressed as median fluorescence intensity (MFI) of a molecule.

3.9. Confirmation of the identity of integrative transformed yeast strains

Previously to the use in functional studies, genomic DNA from the phospho-mutant yeast strains SC_658 and SC_663 was extracted and purified (as described previously) and a PCR approach for both the amplification of the *trp1* and *ura3* auxotrophic markers and for amplification of the αSyn coding gene sequence was performed.

The phospho-mutants yeast strains SC_658 and SC_663 used in this study were transformed with both a plasmid that complement the *ura3* auxotrophy (pRS306) and the *trp1* auxotrophy (pRS304) followed by the αSyn-GFP protein coding gene insert, similarly to the phospho-mutants VSY71 to VSY74, as schematically represented in the figure below (Figure 3.2).

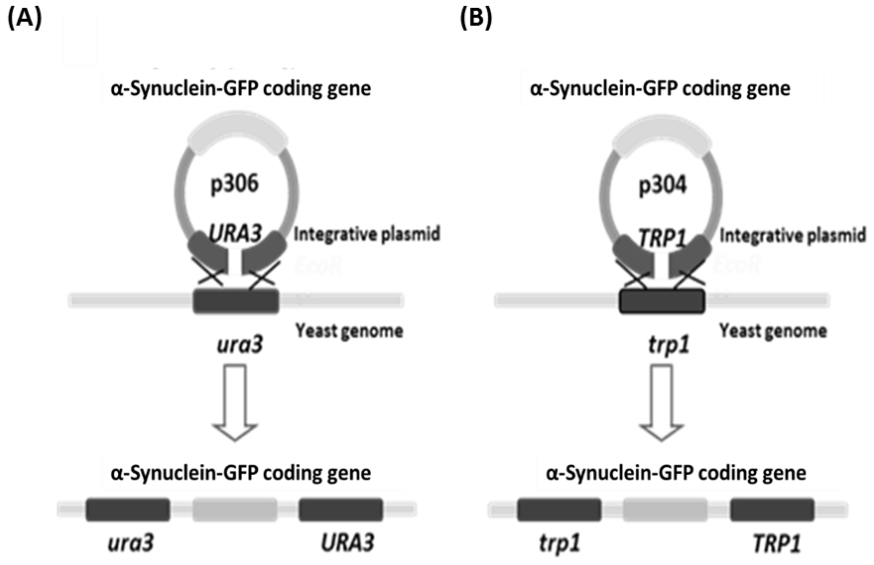

Figure 3.2. Schematic representation of yeast genomic integration of integrative plasmids that contain the protein coding gene of interest. In order to occur homologous recombination, plasmids containing the αSyn coding gene are previously

linearized with restriction enzymes that have their restriction sites in the middle of the gene that complement (URA3 *or* TRP1) the yeast auxotrophy mark (*ura3* or *trp1*). (A) p306 integrative plasmid containing the αSyn coding gene is incorporated within the yeast genome (lacking or with a mutated form of the gene that produces the amino acid uracil – *ura3*); (B) p304 integrative plasmid containing the αSyn coding gene is incorporated within the yeast genome (lacking or with a mutated form of the gene that produces the amino acid tryptophan – *trp1*). With these insertions, transformed yeast cells produce the αSyn protein and are selected by their ability to grow in YPD media lacking (A) uracil, (B) tryptophan or both (in the case of double transformed yeast strains).

Firstly, one PCR reaction was performed in order to amplify the αSyn-GFP protein encoding gene insert contained in the yeast genome, for DNA sequencing (PCR program detailed in Table 3.5), using the set of primers Syn-seq-S and GFP-Internal-R (further detailed in Table 3.4).

Table 3.4. Primers used for amplification of αSyn coding gene sequence by PCR. It is detailed the DNA sequence, percentage of CG content, melting temperature (˚C) and length (bp) of the primers forward (Syn-seq-S) and reverse (GFP-Internal-R).

Primer Designation	DNA Sequence (5'→3')	CG Content (%)	Temperature of Melting (°C)	Length (bp)
Syn-seq-S (P15)	ATGGATGTATTCATGAAAGGACTTTC	34.61	65.9	26
GFP-Internal-R (P99)	GAACTTCAGGGTCAGCTTGC	55.00	65.3	20

The primers presented above were chosen to amplify the αSyn protein coding gene insert and part of the GFP coding gene sequences, as schematically represented below (Figure 3.3), originating a fragment of approximately 700 bp (0.7 Kb).

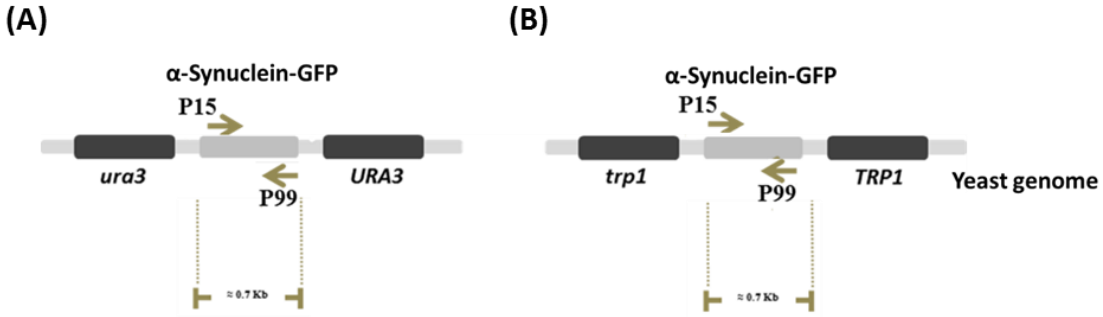

Figure 3.3. Schematic representation of the sites of hybridization of the set of primers P15/P99 within the yeast genome transformed with the integrative plasmids (A) p306 (URA3 mark) or (B) p304 (TRP1 mark). For both integrative plasmids, this set of primers was used to amplify the fragment correspondent to the αSyn coding gene sequence (approximately 0.5 Kb) and part of its linked GFP coding sequence (approximately 0.2 Kb), since P99 is a primer that hybridizes with an internal sequence of the GFP coding gene, originating a fragment weighting around 0.7 Kb in both cases.

To amplify the DNA fragment encoding for the αSyn-GFP protein of both yeast strains, it was chosen the polymerase DreamTaq™, preparing the reaction mixture according to the manufacturer's

instructions (ThermoFisher® Scientific, MA, USA) and using the PCR program further detailed (Table 3.5).

Table 3.5. PCR program for auxotrophies presence confirmation and αSyn coding gene sequence amplification. PCR program used in the amplification of the αSyn coding gene sequence within the genomic DNA of the yeast strains SC_658 and SC_663 and for the amplification of the auxotrophic markers *ura3* and *trp1*.

PCR Segment	Number of Cycles	Temperature (°C)	Time
1	1	95	5 minutes
2	30	95	30 seconds
		55	30 seconds
		72	2 minutes
3	1	72	10 minutes

The occurrence and molecular weight of the PCR product was visualized by gel electrophoresis, as illustrated below (Figure 3.4).

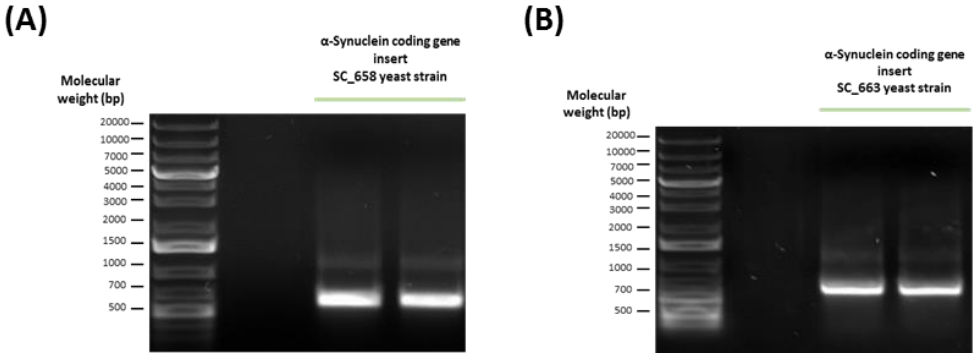

Figure 3.4. Amplification of the αSyn coding gene sequence. Gel electrophoresis (1% Agarose and GreenSafe™ Midori stain) pattern obtained for the PCR product for amplification of the αSyn coding gene sequence within the yeast strains (A) SC_658 and (B) SC_663. A band at approximately 700 bp (0.7 Kb) is visualized for both the samples tested.

Both yeast strains (SC_658 and SC_663) contain the αSyn-GFP coding gene sequence within its genome (Figure 3.4, band at approximately 700 bp), therefore the DNA fragments were excised from the gel and purified (as previously described in Subtopic 3.2.1 of *Materials and Methods* section), and DNA was sequenced (Stabvida, Oeiras, Portugal), using primer *GFP-Internal-R* (P99), that anneals with the GFP coding gene sequence fused to αSyn coding gene. For confirmation of the presence of the phospho-mutations S87E and S129D for the yeast strain SC_658 and S87E for the yeast strain SC_663 (*Annexes* section, Figure 8.2), the DNA sequence obtained from sequencing was reverse-complemented, using *Reverse Complement* bioinformatics tool (Bioinformatics.org) and submitted to a full sequence alignment using *ClustalOmega* bioinformatics tool, as previously described.

Secondly, in order to check that the yeast strains SC_658 and SC_663 contain a double insertion of the αSyn coding gene sequence (are transformed with both plasmids pRS304 and pRS306), it was performed a PCR for the amplification of the yeast strain genomic auxotrophic markers *ura3* and *trp1*

(schematically represented in Figure 3.5), maintaining the experimental conditions described for the amplification of the αSyn-GFP coding gene sequence described above, but using the set of primers Down_*ura3*_AS/Forward_VI_S and Down_*trp1*_AS/Forward_VI_S (further detailed in Table 3.6) that amplify the *ura3* and *trp1* auxotrophic markers, respectively.

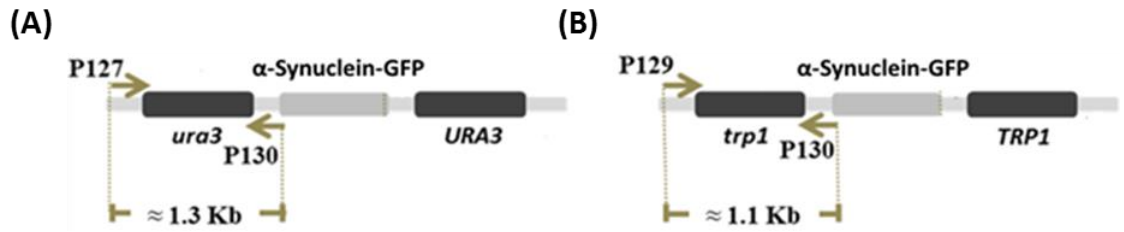

Figure 3.5. Schematic representation of the sites of hybridization of the set of primers within the yeast genome. The yeast strains are transformed with the integrative plasmids p306 (URA*3* mark) or p304 (TRP1 mark) and therefore containing the *ura3* and *trp1* auxotrophic markers, respectively. (A) The set of primers P127/P130 was used to amplify the fragment correspondent to the auxotrophy *ura3*, weighting approximately 1.3 Kb. (B) The set of primers P129/P130 was used to amplify the fragment correspondent to the auxotrophy *trp1*, weighting approximately 1.1 Kb.

Table 3.6. Primers used for the amplification of the yeast genomic auxotrophic markers. Details of the primers, namely DNA sequence, percentage of CG content, melting temperature (˚C) and length (bp) used for the amplification of *ura3* and *trp1* auxotrophic markers within the yeast genomes of the yeast strains SC_658 and SC_663.

Primer Designation	DNA Sequence (5'→3')	CG Content (%)	Temperature of Melting (°C)	Length (bp)
Down_*ura3*_AS (P127)	CTTTGGAGTTCAATGCGTCCATC	47.83	67.8	23
Down_*trp1*_AS (P129)	CCCTGCGATGTATATTTTCCTG	45.45	64.3	22
Forward_VI_S (P130)	GTGATGACGGTGAAAACCTCTG	50.00	66.3	22

The occurrence and molecular weight of the PCR product was visualized by gel electrophoresis, as illustrated below (Figure 3.6).

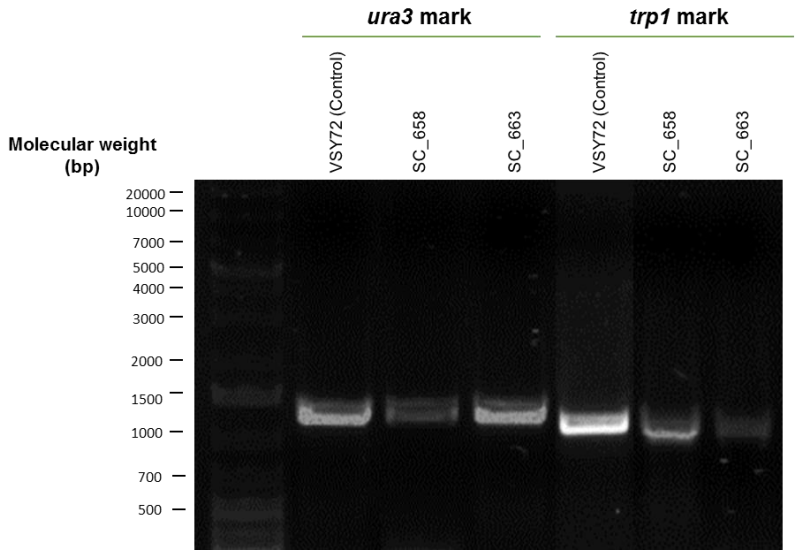

Figure 3.6. Amplification of the auxotrophic markers *ura3* and *trp1*. Gel electrophoresis (1% Agarose and GreenSafe^{TM} Midori stain) pattern obtained for the PCR product of the genomic DNA auxotrophic mark insert amplification from the yeast strain VSY72 (positive control for the *ura3* and *trp1* markers) and the yeast strains to be confirmed, SC_658 and SC_663. The fragment amplified for each assay was supposed to have a molecular weight of 1300 bp and 1100 bp for the auxotrophic markers *ura3* and *trp1*, respectively. It occurred an amplification at approximately 1300 bp for the two yeast strains containing the *ura3* mark and an amplification at approximately 1100 bp for the yeast strains containing the *trp1* mark.

Both yeast strains (SC_658 and SC_663) contain both the *trp1* and *ura3* auxotrophic markers within its genome (Figure 3.6., band at approximately 1.1 Kb and 1.3 Kb, respectively) and were able to grow in medias lacking the amino acids TRP (-TRP), URA (-URA) or both (-TRP-URA) (Figure 3.7), therefore are transformed with the plasmids that complement both auxotrophies and the identity of the yeast strains SC_658 and SC_663 was confirmed.

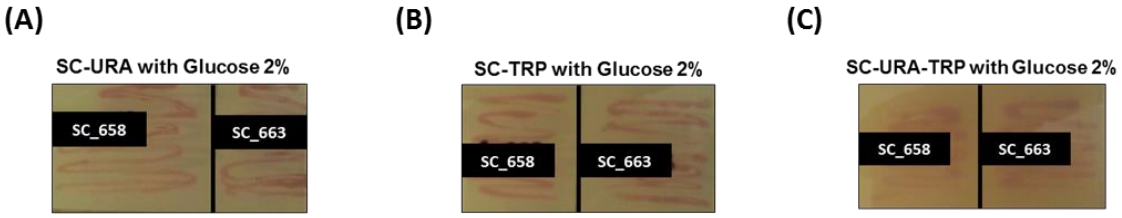

Figure 3.7. Evaluation of yeast growth in SC media. Growth of the yeast strains SC_658 and SC_663 on different minimum selective SC solid media with Glucose 2% (after 48 hours incubation at 30˚C). Both yeast strains SC_658 and SC_663 show growth in SC media lacking the amino acid uracil (A), the amino acid tryptophan (B) or both (C).

3.10. Data representation and statistical analysis

For statistical evaluation of data, Graphpad® PRISM 6 (GraphPad Software®, CA, USA) software was used. Values presented represent the mean ± SD of at least three independent experiments. To compare the results obtained between different samples, One-Way ANOVA analysis followed by Bonferroni's Multiple Correction Test correction was performed, for which significance was considered

for p-values (p) inferior to 0.05 ($p < 0.05$), where * corresponds to $p < 0.05$, ** corresponds to $p < 0.01$ and *** corresponds to $p < 0.001$.

4. Results

4.1. Molecular insights into the effect of the αSyn familial PD-linked mutation A53E

To phenotypically characterize the most recent αSyn PD-linked mutation, it was performed the construction of a yeast plasmid expressing the A53E αSyn mutant protein, by site directed mutagenesis reaction approach. To perform the site-directed mutagenesis, the mutation to be introduced ought to be determined: as stated in the literature, the A53E αSyn protein encoding gene is characterized by a mutation on the nucleotide number 158, where the DNA base pair C is replaced by an A (c.158C>A) of the *SNCA* gene of the patient [Pasanen *et al*, 2014]. This mutation leads to an amino acid replacement of an A to an E at the position 53 of the polypeptide chain of αSyn, due to the changing in the codon 53 from GCA to GAA. In order to obtain the desired mutation, a set of primers were designed using the *PrimerX* bioinformatics tool (*Materials and Methods* section, Table 3.1) and a multi-copy yeast plasmid (p426GAL) encoding the gene sequence for WT αSyn protein was used as a template (illustration of the amino acid replacement in *Materials and Methods* section**,** Figure 3.1). Toward the confirmation of the presence of the desired αSyn PD linked mutation, DNA sequencing was performed, followed by full sequence alignment with WT αSyn coding gene sequence (results illustrated in *Annexes* section, Figure 8.1).

4.1.1. Phenotypic characterization of the αSyn familial PD-linked mutation A53E in Yeast

To perform a phenotypic characterization of the most recent identified PD familial linked mutation of αSyn, the A53E amino acid replacement, evaluation of the toxicity, subcellular localization, intrinsic phosphorylation and mitochondrial network integrity were carried, using the WT αSyn protein as control.

To achieve this purpose, the already characterized [Outeiro and Lindquist, 2003] yeast models of PD were used. In particular, W303.1A yeast strain was transformed with the respective multi-copy plasmid containing the gene coding for WT αSyn (from further on termed the WT assay) and with the A53E αSyn (from further on, termed the A53E assay), in both cases linked to the reporter GFP protein coding gene sequence. Protein expression modulation was achieved through the control of the promoter *GAL1* that was induced when Galactose 1% (or Galactose and Raffinose in several proportions) was the media carbon source and consequently, αSyn expression was induced. When the media carbon source was switched to Glucose 2% or Raffinose 1%, the *GAL1* promotor was repressed and consequently αSyn expression was repressed (Figure 4.1).

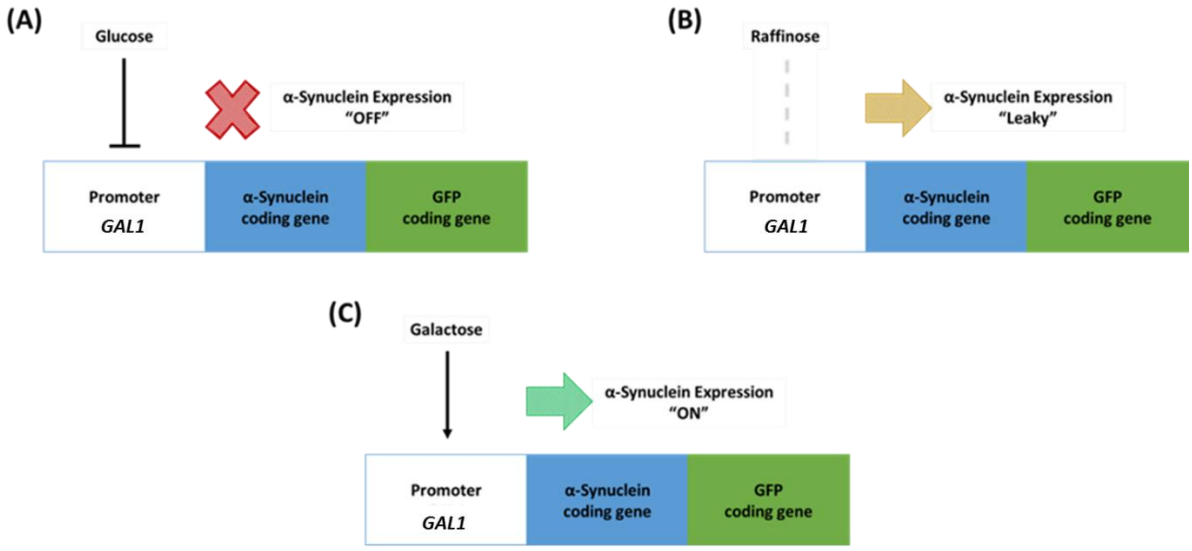

Figure 4.1. Schematic representation illustrating αSyn expression modulation in yeast cells by activity control of the *GAL1* promoter. (A) When glucose is the media carbon source, the expression of the *GAL1* promoter is completely inhibited and consequently αSyn protein fused to GFP will not be expressed in the cell. (B) When raffinose is the media carbon source, *GAL1* promoter is not being either repressed or induced, therefore αSyn protein fused to GFP is expressed at very low levels (therefore, represented with a spaced and lighter arrow) ("leaky" expression) in the cell. (C) When galactose is the media carbon source, *GAL1* promoter is induced and consequently αSyn protein fused to GFP will be expressed in the cell.

4.1.2. A53E effect on αSyn toxicity and inclusion formation

There is a correlation between cytotoxicity and subcellular distribution of αSyn-GFP in yeast cells [Outeiro and Lindquist, 2003], [Gitler *et al*, 2008], [Zabrocki *et al*, 2008]. As stated previously, αSyn associates with the plasma membrane and subsequently, upon increased accumulation of the protein, fluorescent inclusions appear adjacent to the plasma membrane, becoming cytoplasmic inclusions at a final stage [Outeiro and Lindquist, 2003]. To evaluate the mutant A53E αSyn propensity for inclusion formation and the toxicity of its expression to yeast cells, the percentage of cells displaying inclusions was determined by fluorescence microscopy ((E)GFP fluorescence) at the time point of 7 hours following protein expression induction. This time point was chosen based on what was previously described for phenotypic characterization of αSyn expression in yeast cells by [Tenreiro *et al*, 2014a] (Figure 4.2).

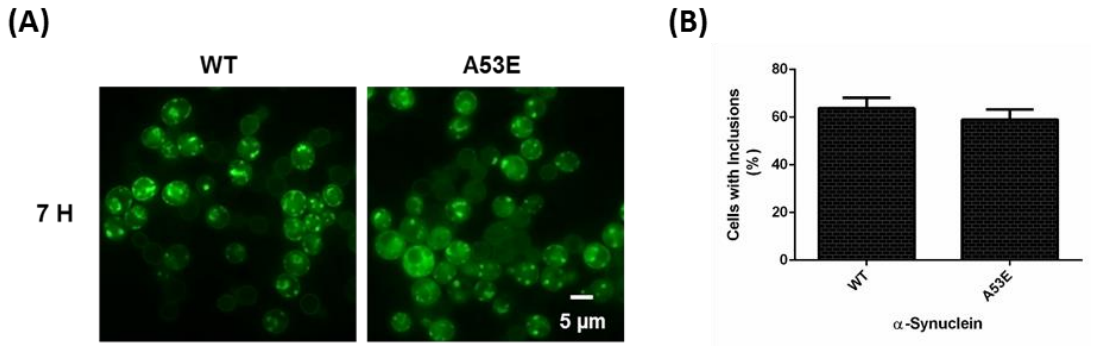

Figure 4.2. Inclusion formation evaluation for the A53E αSyn mutant expression in yeast cells. (A) Intracellular localization of the WT or A53E αSyn-GFP and (B) respective percentage of yeast cells containing αSyn-GFP inclusions, assessed by fluorescence microscopy after 7 hours of αSyn-GFP expression induction. A representative result is shown from at least three independent experiments. Values represent the mean ± SD and statistical analysis were performed by One-Way ANOVA with Bonferroni's multiple comparison test.

From the results illustrated in the figures above (Figure 4.2), it is inferable that the percentage of cells with inclusions in yeast cells expressing the mutant A53E protein was similar to the WT, prone to decrease, although not statistically significant (63.67±4.49% for WT αSyn and 58.98±4.24% for A53E αSyn).

In the meantime, spotting assays were performed in order to qualitatively characterize A53E αSyn expression toxicity to yeast cells. Yeast cells expressing the empty vector (control Empty), the WT αSyn or the A53E αSyn protein were incubated in Galactose selective solid media for 72 hours and the toxicity induced from the expression of the A53E αSyn mutant was compared to the one produced by the WT αSyn protein expression (Figure 4.3).

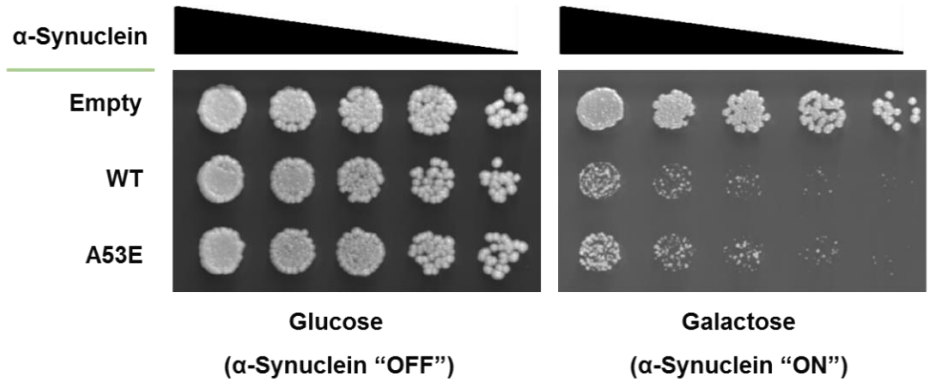

Figure 4.3. Spotting assay of the indicated yeast cells (Empty, WT and A53E). Cell suspensions were adjusted to the same OD_{600nm}, serially diluted and spotted onto the surface of the solid media containing either glucose (control) or galactose (induced αSyn expression) as carbon source. A representative result is shown from at least three independent experiments.

The spotting assays results illustrated above (Figure 4.3) show that both expression of mutant A53E and the WT αSyn were toxic for yeast cells, since these ones presented less growth compared to the empty control. However, qualitatively evaluating, the toxicity induced by the expression of WT and the A53E mutant proteins were similar to one another. Therefore, in the attempt to distinguish the toxicity induced by the A53E mutant from the WT protein expression and to quantitatively evaluate

toxicity, flow cytometry analysis was performed after 7 hours of protein expression induction, on which staining of cells with PI was executed, indicating the relative quantity of cells that have their membrane compromised (the cell lost viability). Hence, a population of cells presenting fluorescence for both PI and GFP, were cells expressing αSyn that were not viable, whereas cells only positive for the GFP but not the PI, were viable cells expressing αSyn (Figure 4.4).

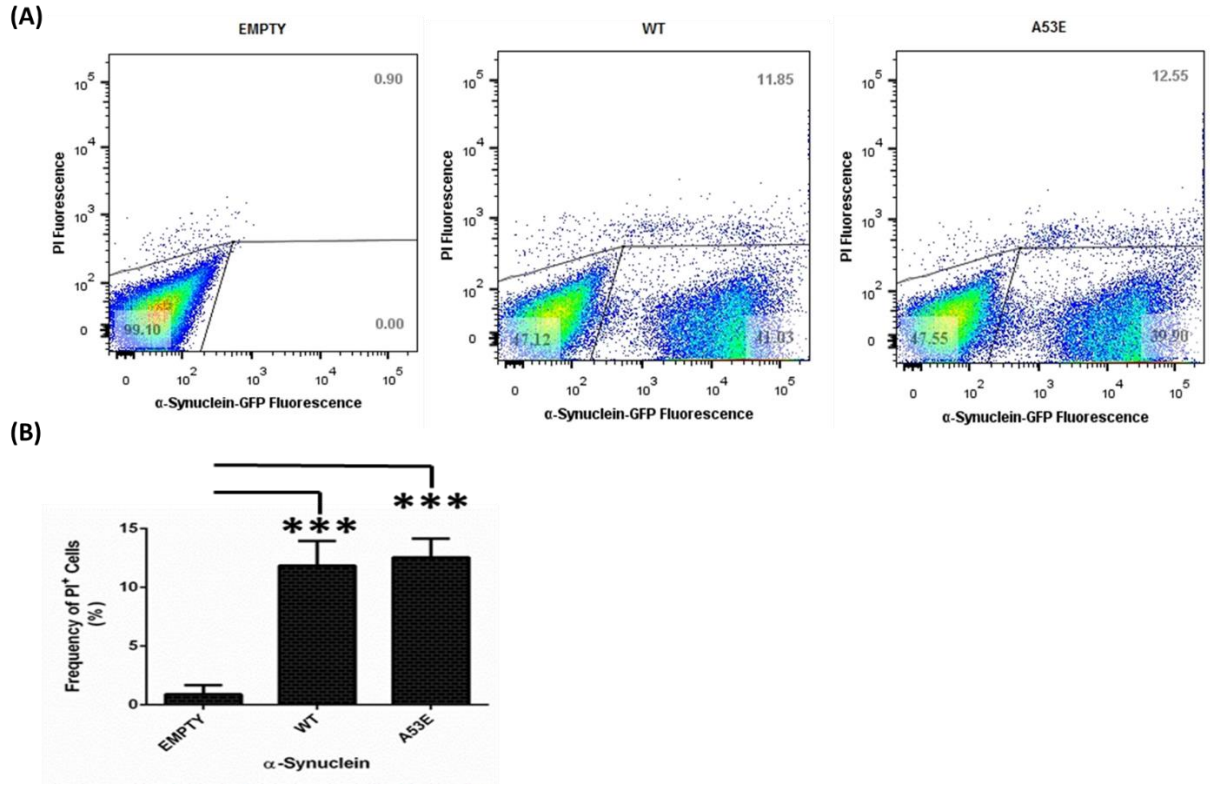

Figure 4.4. Toxicity assessment of the A53E αSyn mutant expression for yeast cells. (A) Illustration of αSyn-GFP fluorescence *versus* PI fluorescence after 7 hours of αSyn expression induction assessed by flow cytometry analysis in the indicated yeast cells Empty, WT and A53E and (B) Frequency of PI positive cells, in the indicated yeast cells Empty, WT and A53E. A representative result is shown from at least three independent experiments. Values represent the mean ± SD and statistical analysis were performed by One-Way ANOVA with Bonferroni's multiple comparison test (where *** represents a significance of $p<0.001$).

Both the expression of the WT or the A53E mutant αSyn significantly induced cell death (approximately 10% more), when compared to the Empty control, measured by the increase in PI^+ population (0.90±0.77%, 11.85±2.11% and 12.55±1.60% of PI^+ positive cells for the Empty, WT and A53E assay, respectively) and consequently, both forms of αSyn expression were toxic for yeast cells. Nevertheless, there was no statistical difference between the expression of the WT or the mutant A53E αSyn protein in induced cell toxicity, which was in key with the results obtained for the qualitatively analysis performed for toxicity (spotting assays in Figure 4.3). To validate these results, GFP MFI and PI MFI were assessed for the expression of both WT and mutant A53E αSyn and no differences were found (*Annexes* section, Figure 8.3). Furthermore, to assess if the A53E mutation had an effect on the expression levels of αSyn by yeast cells, it was also assessed the percentage of cells expressing GFP (GFP^+ cells), which were similar between the two assays (WT and A53E) (*Annexes* section, Figure 8.3).

4.1.3. A53E effect on αSyn protein levels and S129 phosphorylation levels

Total αSyn and αSyn pS129 protein levels were evaluated for the WT and the A53E assays in order to search for alterations introduced by the mutation A53E. Yeast cells were grown as in the previous assays and after 7 hours of protein expression induction, protein quantity correspondent to an $OD_{600\ nm}$ of 1 was extracted and purified from yeast cells, using the MURB-TCA protocol. The levels of total αSyn and pS129 were assessed by SDS-PAGE followed by Western Blot (Figure 4.5).

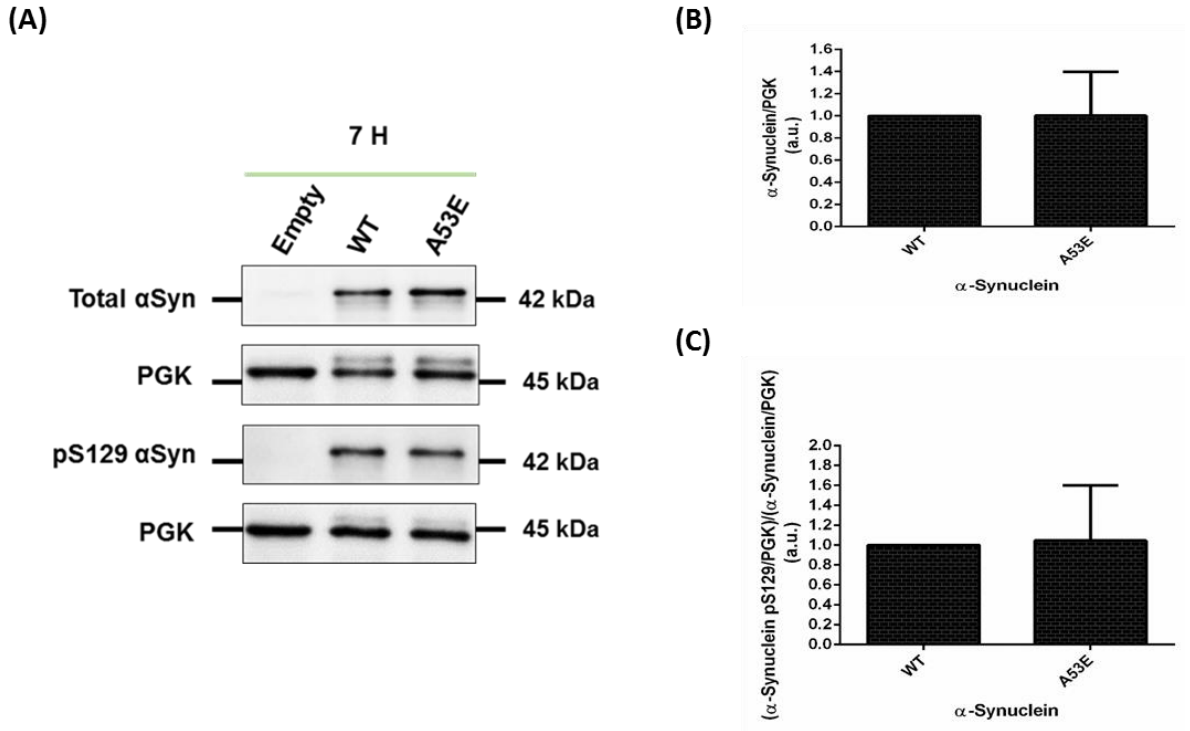

Figure 4.5. Effect of the A53E mutation on total and phosphorylated at S129 αSyn protein levels. (A) WT and A53E αSyn-GFP expression and pS129 levels in yeast cells assessed by Western Blot analysis of total protein extracts, 7 hours after αSyn-GFP expression induction. (B) and (C) Densitometric analysis of the immunodetection of αSyn-GFP relative to the intensity obtained for PGK, used as loading control, presented in arbitrary units (a.u.), for both (B) total αSyn and (C) pS129 residue αSyn. Results shown are from one representative experiment from at least three independent experiments. Values represent the mean ± SD and statistical analysis were performed by One-Way ANOVA with Bonferroni's multiple comparison test.

It was observed that the introduction of the A53E mutation had no effect on αSyn protein levels (Figure 4.5 A and B) (1.00±0.00 a.u. and 1.00±0.40 a.u. for WT and A53E assays, respectively). Concerning alterations in the phosphorylation at S129 of αSyn, it was observed that the PD linked mutation A53E was similarly phosphorylated at S129 when compared to the WT protein, with no statistically significant differences between them (Figure 4.5. A and C) (1.00±0.00 a.u. and 1.05±0.56 a.u. for WT and A53E assays, respectively).

4.1.4. A53E effect on protein solubility

With the aim to distinguish between soluble and insoluble protein fractions of the mutant A53E αSyn and, consequently acquire more insights regarding the oligomerization degree induced by the amino acid replacement A53E, Triton-X 100 detergent protein solubility evaluation assay was applied (further detailed in *Materials and Methods* section). After 7 hours of protein expression induction, extraction of yeast total protein was performed. Protein samples were quantified by the BCA method and submitted to the Triton-X 100 solubility evaluation, followed by TP, TS and TI protein fractions loading onto the gel and SDS-PAGE and Western Blot, using PGK as a control for TI fraction purity (Figures 4.6).

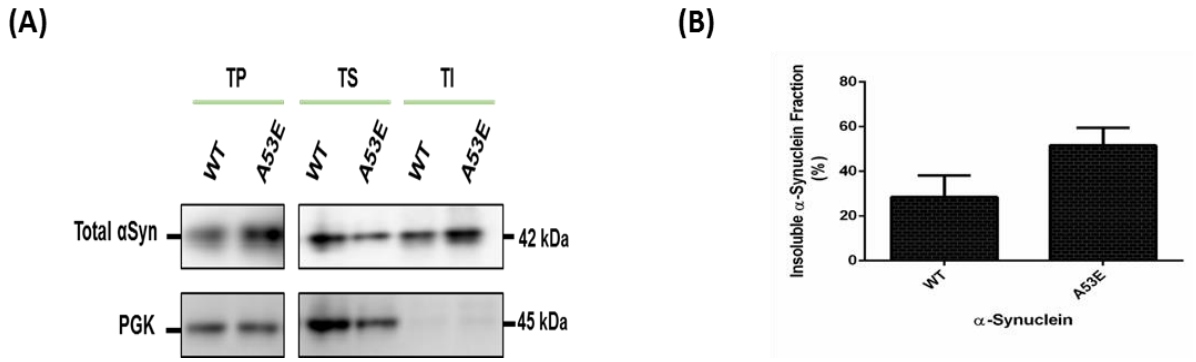

Figure 4.6. Evaluation of A53E mutation on αSyn solubility. (A) Triton-X soluble (TS) and Triton-X insoluble (TI) fractions of WT or A53E αSyn assessed by Western Blot analysis. (B) Determination by densitometric analysis of the percentage of TI αSyn, 7 hours after protein expression induction. PGK was used as an internal control for the experiment. A representative result is shown from at least three independent experiments. Values represent the mean ± SD and statistical analysis were performed by One-Way ANOVA with Bonferroni's multiple comparison test.

Upon evaluation of Triton-X 100 αSyn solubility, the A53E mutant had a slight increase in TI fraction, when compared to the WT αSyn expressing cells (51.55±7.96% compared to 29.89±9.61%, respectively), showing a tendency of the A53E mutant to form more oligomeric species, although this difference was not statistically significant (Figure 4.6 B).

4.1.5. A53E effect on mitochondrial network integrity

Several theories have been suggested for the pathogenesis of PD, of which mitochondrial dysfunction plays a pivotal role in both sporadic and familial forms of the disease. Amongst them, changes in dynamics of the mitochondria such as fusion or fission and changes in size and morphology of this organelle are implicated [Bose and Beal, 2016]. Furthermore, expression of both WT and the PD familial linked mutation A53T αSyn already have been linked to mitochondrial function impairment and fragmentation [Choubey *et al*, 2011], [Chinta *et al*, 2010] and regarding the mutant protein A53E, this one was shown to enhance toxicity in cells experiencing mitochondrial stress [Rutherford *et al*, 2015] Therefore, emerged the attempt to evaluate mitochondrial network integrity in yeast cells expressing

A53E αSyn. To achieve this purpose, mitochondria of yeast cells were stained with MitoTracker Deep Red dye. Moreover, yeast cells were stained with Hoechst 33342 fluorescent dye to determine nuclei localization within the cell and αSyn expression was evaluated through GFP fluorescence (Figure 4.7).

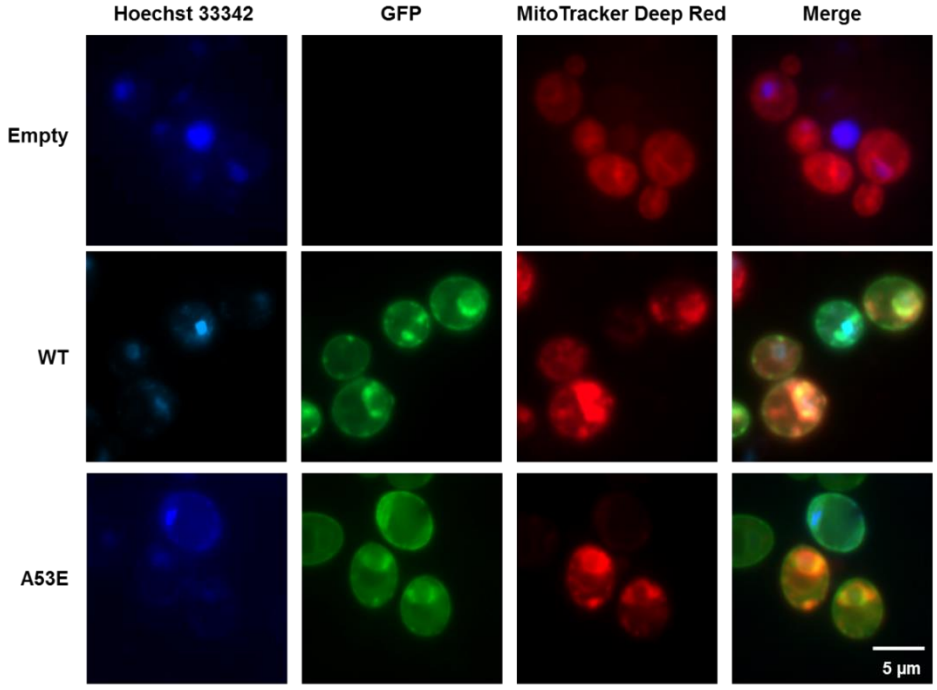

Figure 4.7. Intracellular localization of the WT or A53E αSyn-GFP and mitochondrial network assessment by MitoTracker Deep Red staining. Nuclei was stained with Hoechst 33342 dye. Results shown are from one representative experiment from at least three independent experiments.

The results illustrated in Figure 4.7 show a tendency for a *clustering* of mitochondria, upon 7 hours expression, for both WT and A53E αSyn expressing cells when compared to the Empty control. However, in order to quantitatively check for alterations on the mitochondrial membrane potential, flow cytometry analysis was performed (Figure 4.8).

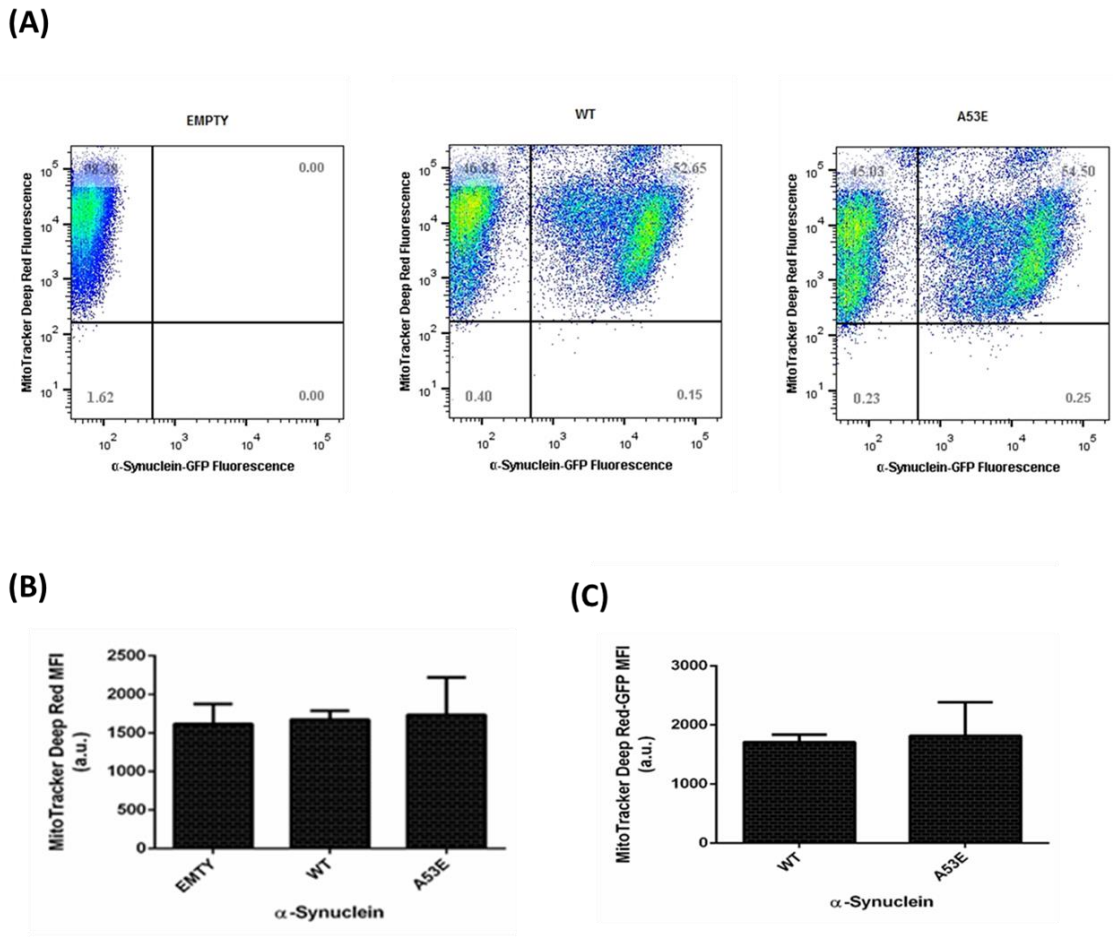

Figure 4.8. Evaluation of the effect of the A53E mutation on mitochondrial network integrity. (A) Illustration of αSyn-GFP fluorescence *versus* MitoTracker Deep Red fluorescence after 7 hours of αSyn expression induction, assessed by flow cytometry analysis in the indicated yeast cells Empty, WT and A53E.(B) MitoTracker Deep Red MFI, in the indicated yeast cells Empty, WT and A53E and (C) MitoTracker Deep Red-GFP MFI, in the indicated yeast cells WT and A53E. Results shown are from one representative experiment from at least three independent experiments Values represent the mean ± SD and statistical analysis were performed by One-Way ANOVA with Bonferroni's multiple comparison test.

The statistical analysis states no differences between MitoTracker Deep Red MFI marked cells (mitochondrial localization and membrane potential) between the cells expressing αSyn WT or A53E and the Empty vector (1674±112, 1736±487 and 1618±257 a.u., respectively). Equally, MitoTracker Deep Red-GFP MFI was similar between cells expressing WT and A53E αSyn (1711±123 and 1815±568 a.u., respectively). Taken together, this result indicates that the expression of both αSyn WT or A53E mutant had no effect on mitochondrial membrane potential within yeast cells expressing αSyn or not, on the tested experimental conditions (Figure 4.8).

Overall, the characterization of the PD familial linked mutation A53E in yeast showed that no relevant phenotypic differences emerge in the presence of this mutation, when compared to the WT protein expression, in this model organism and in the tested conditions, being both αSyn proteins equally toxic for yeast cells.

4.2. αSyn phosphorylation role on PD – The interplay between S87 and S129 phosphorylation

In order to study the effect of phosphorylation at the key residues S87 and S129 and the phosphorylation interplay between them in αSyn aggregation and toxicity, a group of W303.1A yeast strains carrying two copies of the human *SNCA* cDNA integrated in the genome (already available in the host group) were selected for phenotypic characterization. In particular, these yeast strains contained the integrative plasmids coding for αSyn where: a) phosphorylation on the S129 is blocked or mimicked (S129A and S129D assays, respectively), b) phosphorylation on S87 residue is mimicked (S87E assay) and c) phosphorylation on both S87 and S129 residues is mimicked (S87E_S129D assay) (further detailed in *Annexes* section, Table 8.2). The phenotypic characterization of the expression of these αSyn phospho-mutations were compared to the integrative expression of the WT protein (WT assay) on further studies. The phospho-mutants selected express the αSyn protein fused to GFP and protein expression regulation is achieved under a galactose inducible promoter (*GAL1*), as previously described [Outeiro and Lindquist, 2003].

4.2.1. S87 and S129 phospho-mutations effect on αSyn toxicity and inclusion formation

To qualitatively characterize the toxicity induced by the expression of each αSyn phospho-mutation for the cells, spotting assays were performed (Figure 4.9).

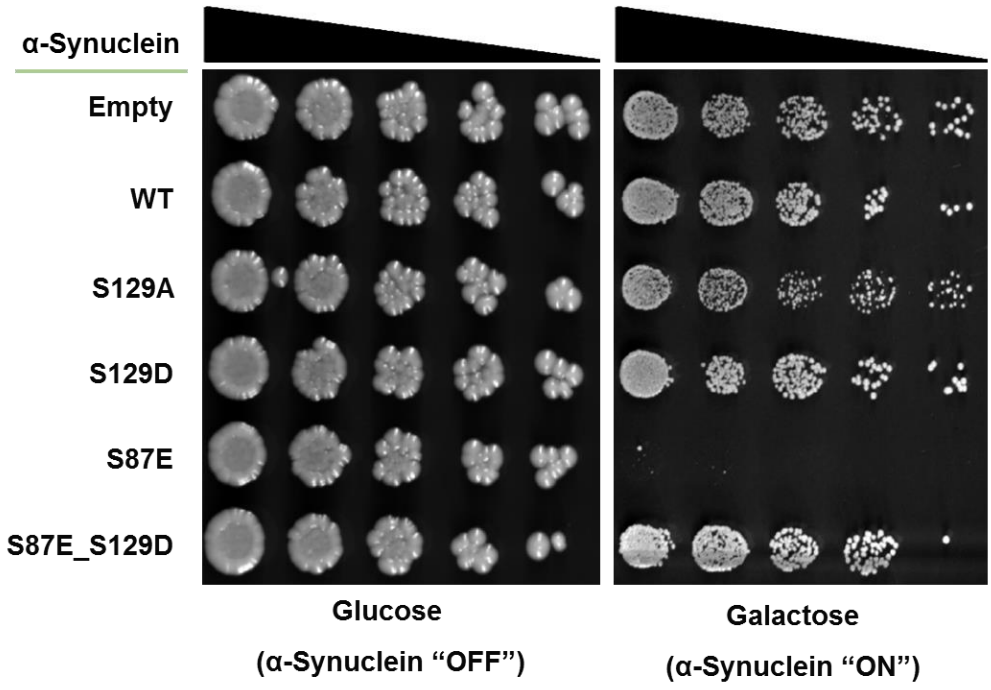

Figure 4.9. Spotting assay of the indicated yeast cells containing two copies of the indicated αSyn forms (Empty, WT, S129A, S129D, S87E and S87E_S129D) integrated on the genome. Cell suspensions were adjusted to the same OD_{600nm}, serially diluted and spotted onto the surface of the solid media containing either glucose (control) or galactose (induced αSyn expression) as carbon source. A representative result is shown from at least three independent experiments.

After 72 hours of αSyn expression induction (galactose media) it was possible to notice a more toxic phenotype when the phosphorylation at the residue S87 of the αSyn protein (S87E assay) was mimicked, characterized by the almost total absent yeast growth, when compared to the other phospho-mutants (S129A and S129D) and WT αSyn expressing cells. Under these conditions, the effect amongst the expression of the S129A, S129D and WT protein was more homogeneous (with a slight less toxicity when S129D αSyn was expressed). Interestingly, when the mutation S87E was coupled with the mutation that mimics the phosphorylation on the S129 residue (S87E_S129D assay), the protective effect of the S129D mutation overlapped the toxic effect induced by the presence of the S87E mutation and yeast cells carrying the double mutation S87E_S129D had even an increased growth when compared to the WT protein expression (WT assay), having a growth similar to the Empty control.

In order to confirm the results obtained by the spotting assays and to quantify the toxicity induced by each phospho-mutation, αSyn expression induced toxicity was assessed by flow cytometry analysis by staining the cells with PI (as previously described) (Figure 4.10).

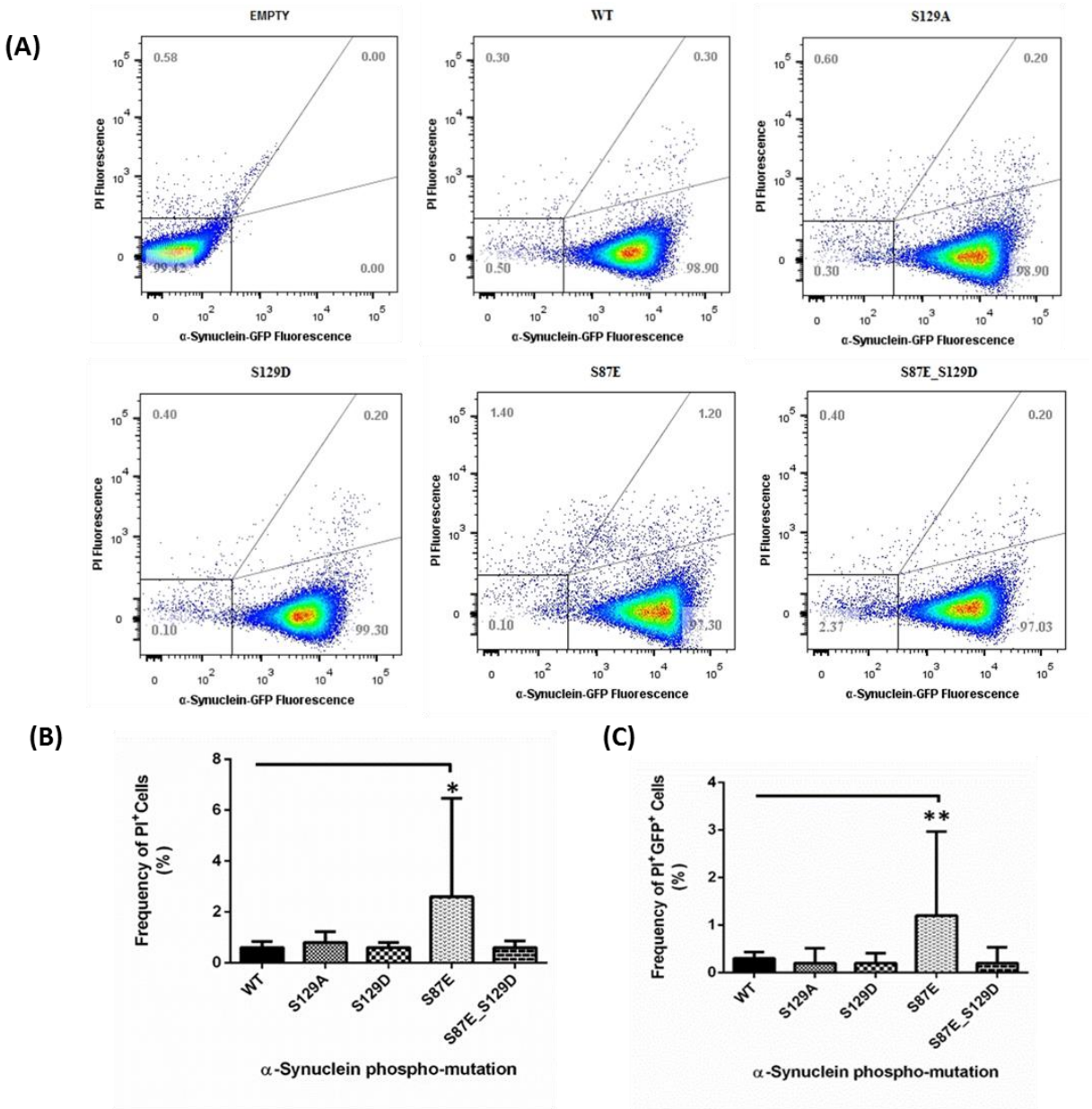

Figure 4.10. Toxicity assessment of the αSyn phospho-mutations expression for yeast cells. (A) Illustration of αSyn-GFP fluorescence *versus* PI fluorescence after 7 hours of αSyn expression induction, assessed by FACS analysis in the indicated yeast cells Empty, WT, S129A, S129D, S87E and S87E_S129D. (B) Frequency of PI positive cells, in the indicated yeast phospho-mutants and (C) Frequency of PI positive cells, expressing αSyn-GFP (PI^+GFP^+) in the indicated yeast phospho. Results shown are from one representative experiment from at least three independent experiments. Values represent the mean ± SD and statistical analysis were performed by One-Way ANOVA with Bonferroni's multiple comparison test (where * represents a significance of $p<0.05$ and ** represents a significance of $p<0.01$).

In key with what was observed for the spotting assays, flow cytometry analysis showed that upon expression of the mutant S87E αSyn, the frequency of cells with a compromised plasma membrane was almost two times higher than when cells express the WT protein (1.20±1.77% for S87E and 0.30±0.13% for WT regarding the frequency of PI^+GFP^+ cells and 2.60±3.86% for S87E and 0.60±0.24% for WT regarding the frequency of PI^+ cells). Furthermore, when the S87E was coupled to the S129D mutation, the protective effect induced by S129D mutation prevailed and the frequency of compromised cells was lower than when the WT protein was expressed in yeast cells (0.20±0.34% of frequency of PI^+GFP^+ cells and 0.60±0.26% of frequency of PI^+ cells). Regarding the mutants mimicking

and blocking phosphorylation at the S129 residue (S129D and S129A, respectively), αSyn toxicity was similar between them and similar to the WT protein expression, under the experimental conditions tested (0.20±0.31% and 0.20±0.22% of frequency of PI^+GFP^+ cells and 0.80±0.43% and 0.6±0.20% regarding the frequency of PI^+ cells, for the S129A and S129D phospho-mutants, respectively). The percentage of cells expressing αSyn was assessed as a control for αSyn expression homogeneity for the phospho-mutants and it was similar amongst all phospho-mutants, with no statistical significant differences (*Annexes* section, Figure 8.4).

To evaluate if the toxic effect induced by the presence of the S87E mutant αSyn was translated to an increased number of cells with αSyn inclusions, inclusion formation was assessed by fluorescence microscopy ((E)GFP fluorescence) at two time points: after 7 hours of protein expression induction and after 24 hours of protein expression induction (Figure 4.11).

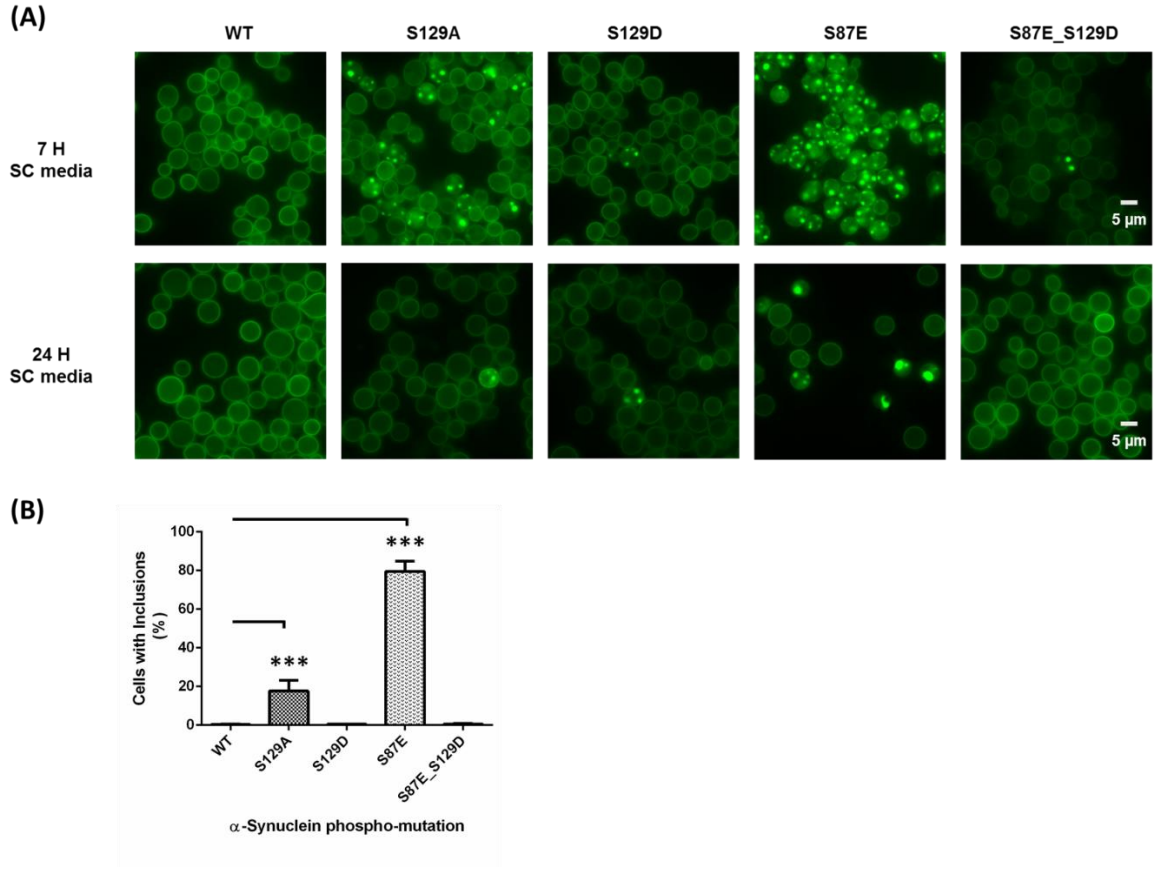

Figure 4.11. Inclusion formation evaluation for the αSyn phospho-mutants expression in yeast cells in SC media. (A) Intracellular localization of the WT and phospho-mutants S129A, S129D, S87E and S129D_S87E αSyn-GFP at the indicated time points of 7 hours and 24 hours in SC media. (B) Percentage of yeast cells containing αSyn-GFP inclusions, assessed by fluorescence microscopy at the indicated time point of 7 hours after αSyn-GFP expression induction Results shown are from one representative experiment from at least three independent experiments. Values represent the mean ± SD and statistical analysis were performed by One-Way ANOVA with Bonferroni's multiple comparison test (where *** represents a significance of $p<0.001$).

After 7 hours of αSyn expression induction in SC media, it was possible to notice a more predominant phenotype when the phosphorylation at the residue S87 of the αSyn protein was mimicked (S87E assay), characterized by a dramatically increased number of inclusions formed within yeast cells, (compared to the WT, S129A or S129D αSyn expressing cells), with the percentage of cells with inclusions of 0.30±0.22%, 17.59±5.52%, 0.46±0.08% and 79.55±5.28% for the WT, S129A, S129D and

S87E assays, respectively. On the other hand, when the mutation S87E was coupled with the mutation that mimicked the phosphorylation on S129 residue, the S129D mutation (S87E_S129D assay), the percentage of cells with inclusions decreased to 0.58±0.20%, which was an additional evidence of the overlapping protective effect of the S129D mutation over the toxic effect induced by the S87E mutation. The percentage of cells expressing αSyn was similar for the six yeast strains analyzed, as previously mentioned (and illustrated in *Annexes* section, Figure 8.4).

Conversely, when inclusion formation assessment was performed after 24 hours of protein expression induction, it was possible to observe that all six assays showed less inclusions, particularly the S87E assay, where most of the yeast cells had died. This may have occurred due to two possible reasons: the first one, the expression of the αSyn protein for this amount of time, particularly the S87E mutant, may be toxic for the cells, therefore, cells that were able to survive were cells that developed mechanisms of coping with protein inclusion formation (and as a result do not have αSyn inclusions anymore); the second one, after 24 hours of protein expression induction, yeast cell cultures may be entering the decline or death phase of growth. To shed a light on this issue and evaluate the impact of the mutant S87E αSyn expression on other cellular organelles, proteasome function evaluation and autophagic flux/autophagy induction evaluation were assessed, as further explored on Subtopic 4.2.4.

To better distinguish the overall phenotype for inclusion formation induced by each phospho-mutant and, since it was previously described that the S129A αSyn mutant expression formed more heterogeneous and larger inclusions within yeast cells [Tenreiro *et al*, 2014a], it was hypothesized that the expression of the S87E αSyn mutant might also form inclusions with these particular characteristics, as it is likewise characterized by an increase percentage of cells with inclusions. To address this question, protein expression of the integrative phospho-mutants was induced for 7 hours in enriched growth culture media YEP and inclusion formation assessed by GFP fluorescence (Figure 4.12).

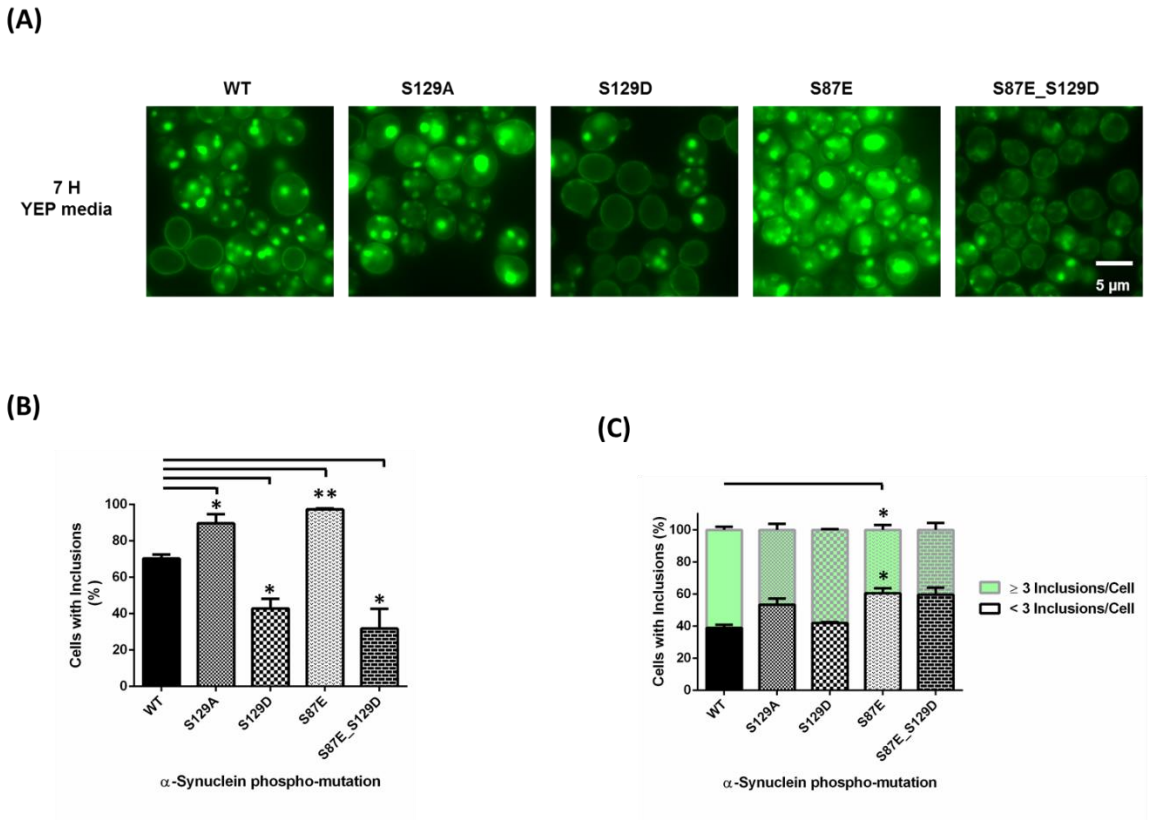

Figure 4.12. Inclusion formation evaluation for the αSyn phospho-mutants expression in yeast cells in YEP media. (A) Intracellular localization of the WT and phospho-mutants S129A, S129D, S87E and S129D_S87E αSyn-GFP at the indicated time point of 7 hours in YEP media. (B) Percentage of yeast cells containing αSyn-GFP inclusions, assessed by fluorescence microscopy at the indicated time point of 7 hours after αSyn-GFP expression induction and (C) Percentage of cells presenting less than 3 inclusions, or 3 or more inclusions per cell Results shown are from one representative experiment from at least three independent experiments. Values represent the mean ± SD and statistical analysis were performed by One-Way ANOVA with Bonferroni's multiple comparison test (where * represents a significance of $p<0.05$ and ** represents a significance of $p<0.01$).

As a first observation, after 7 hours αSyn expression induction in YEP media (Figure 4.12), it was possible to observe that the inclusion formation for each mutation followed a similar tendency as the assays performed in SC media (Figure 4.11): the S129D mutant showed a significant reduced amount of percentage of cells with inclusions than the WT protein, exhibiting the protective effect of this mutation on αSyn induced toxicity and inclusion formation (42.85±5.39% as opposed to 70.33±2.16% for the WT protein), whereas blocking phosphorylation on S129 residue (S129A mutant) increased inclusion formation (89.63±4.99%), as expected and previously described by [Tenreiro *et al*, 2014a]. Furthermore, S87E αSyn mutant significantly increased αSyn inclusion formation when compared to the WT protein expression (97.32±0.58%) and once more when coupled with S129D (S87E_S129D mutant), the phenotype for inclusion formation became similar to the one obtained for the protective S129D mutation (31.81±10.82% of cells with inclusions).

Secondly, in key to what was observed for the expression of the S129A αSyn by [Tenreiro *et al*, 2014a], the S87E mutant displayed an increased number of percentage of cells with fewer number of inclusions, nonetheless larger and more heterogeneous when compared to the WT protein (60.46±3.12% of cells with less than three inclusions as opposed to 38.94±2.02% for the WT protein expression), while for the S129A and S129D mutants the phenotype obtained was accordingly to what was previously described (53.42±3.73% and 41.95±0.55% of cells with less than three inclusions per cell, respectively). Strikingly, when the S87E mutation was coupled to the protective αSyn mutation S129D (S87E_S129D),

it was observed that within the cells containing inclusions, these ones display a similar phenotype of larger and fewer inclusions alike to the S87E mutant (59.61±4.33%).

4.2.2. S87 and S129 phospho-mutations effect on αSyn protein levels and S129 phosphorylation levels

To further check that the differences observed for toxicity and inclusion formation were due to the presence of the phospho-mutations *per se* and not different levels of αSyn-GFP protein in the yeast strains tested, protein was extracted after 7 hours of protein expression induction and Western Blot analysis was performed. Whereas the levels of total αSyn were similar amongst the six phospho-mutants, additionally, in order to study the phosphorylation state of the residue S129 amongst the group of phospho-mutants, a Western Blot with a second antibody that specifically recognizes pS129 αSyn was performed and the ratio of phosphorylated:total αSyn was determined (Figure 4.13).

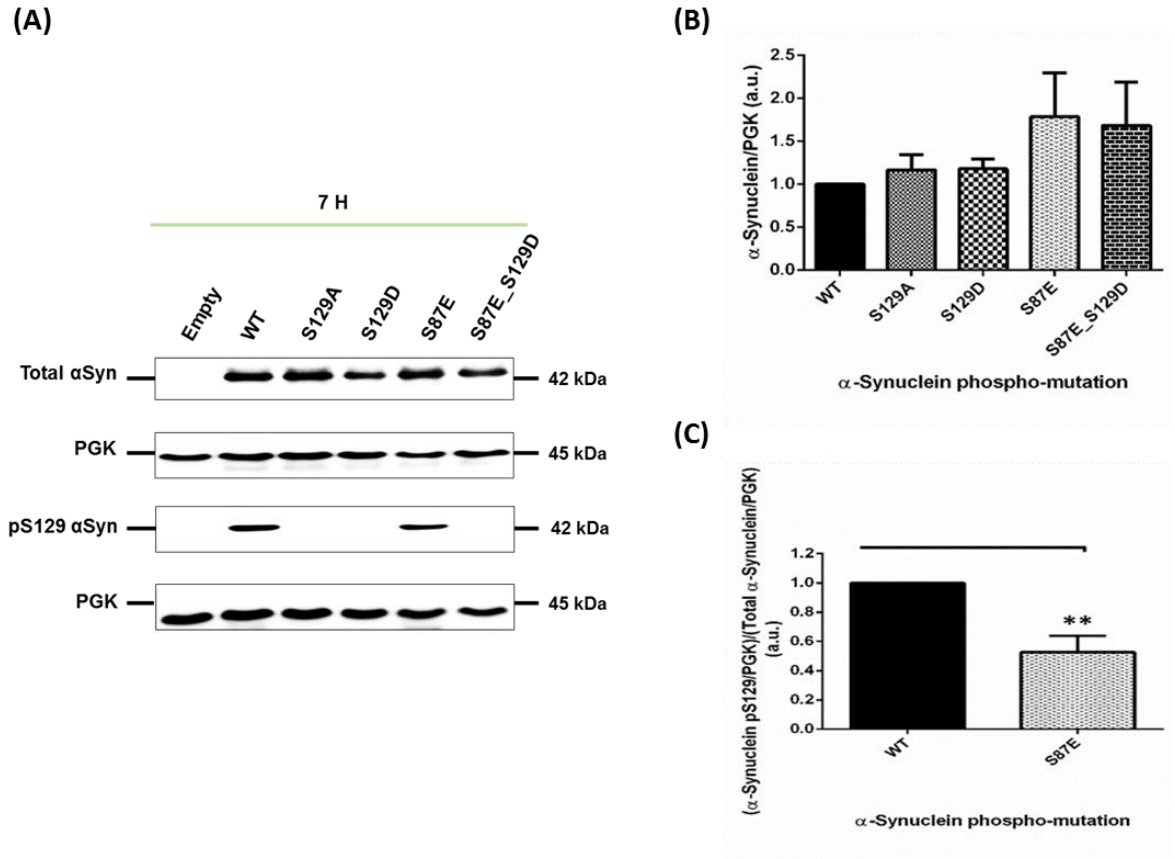

Figure 4.13. Effect of the phospho-mutations on total and phosphorylated at S129 αSyn protein levels. (A) WT, S129A, S129D, S87E and S87E_S129D αSyn-GFP expression and pS129 levels in yeast cells assessed by Western Blot analysis of total protein extracts, 7 hours after αSyn-GFP expression induction. (B) and (C) Densitometric analysis of the immunodetection of αSyn -GFP relative to the intensity obtained for PGK, used as loading control, presented in arbitrary units (a.u.), for both (B) total αSyn and (C) pS129 αSyn. Results shown are from one representative experiment from at least three independent experiments. Values represent the mean ± SD and statistical analysis were performed by One-Way ANOVA with Bonferroni's multiple comparison test (where ** represents a significance of $p<0.01$).

Regarding pS129 αSyn levels, the phosphorylation at residue S129 was significantly decreased (to almost half) on the S87E αSyn mutant when compared to the WT assay (0.53±0.11 a.u. of pS129 for the S87E phospho-mutant), supporting the presumably protective effect of S129 phosphorylation. Only the WT and the S87E phospho-mutant assays show phosphorylation of αSyn at the residue S129, as expected (Figure 4.13 A).

4.2.3. S87 and S129 phospho-mutations effect on αSyn protein clearance

To test if the differences observed for the phenotypes of inclusion formation and toxicity for the different phospho-mutant yeast strains were due to differences in protein clearance, the six phospho-mutant yeast strains were incubated in galactose 1% media for 7 hours to induce the expression of αSyn-GFP in yeast cells. After 7 hours of protein expression induction, protein was recovered (0 hours of clearance) and at this time point, expression of αSyn-GFP was ceased by switching the media carbon source to glucose 2% and consequently repressing *GAL1* promoter. At the time point of 13 hours from the carbon source switching to glucose to repress αSyn expression (13 hours of clearance), protein was recovered (schematically represented in Figure 4.14 B).

In order to quantify total and pS129 αSyn levels, a Western Blot analysis was performed. Total levels of αSyn were observed to decrease for the overall phospho-mutants when compared to protein levels after 7 hours of protein expression induction (0 hours of clearance), as expected **(**Figure 4.14 A and C**)**. More specifically, for the WT, S129D or S129A phospho-mutant proteins, the total levels of protein had a mild significant decrease 13 hours after protein expression was repressed when compared to the protein levels 7 hours after protein expression induction (zero hours of clearance) (from 1.00±0.00 to 0.67±0.06, from 1.01±0.03 to 0.64±0.07 and from 1.11±0.14 to 0.57±0.06 for the WT, S129A mutant and S129D mutant, respectively), under the experimental conditions tested. Interestingly, the mutant that showed to induce less toxicity and formed less inclusions, the S87E_S129D phospho-mutant, also showed more easiness in clearing αSyn protein, presenting the most significant αSyn levels decrease (from 1.01±0.07 to 0.36±0.07 a.u.). Even when compared to the WT protein levels at 13 hours of clearance, the S87E_S129D phospho-mutant has significant decreased levels of αSyn (0.36±0.07 a.u. and 0.67±0.06 a.u. for the S87E_S129D and WT assays, respectively). Finally, the S87E mutant showed the least significant protein clearance (from 1.23±0.22 a.u. to 0.68±0.15 a.u.) (Figure 4.14 C), which was expected, since the high number of inclusions formed and the toxic effect of this mutation was expected to be translated in a less significant protein clearance. This difference in protein clearance was not due to differences in phosphorylation on the S129 residue, as in both time points the phosphorylation on this residue is unaltered (Figure 4.14 A). As a control, differences in total levels of αSyn after 7 hours of protein expression induction were assessed for the six phospho-mutants, but no statistical significant differences were detected.

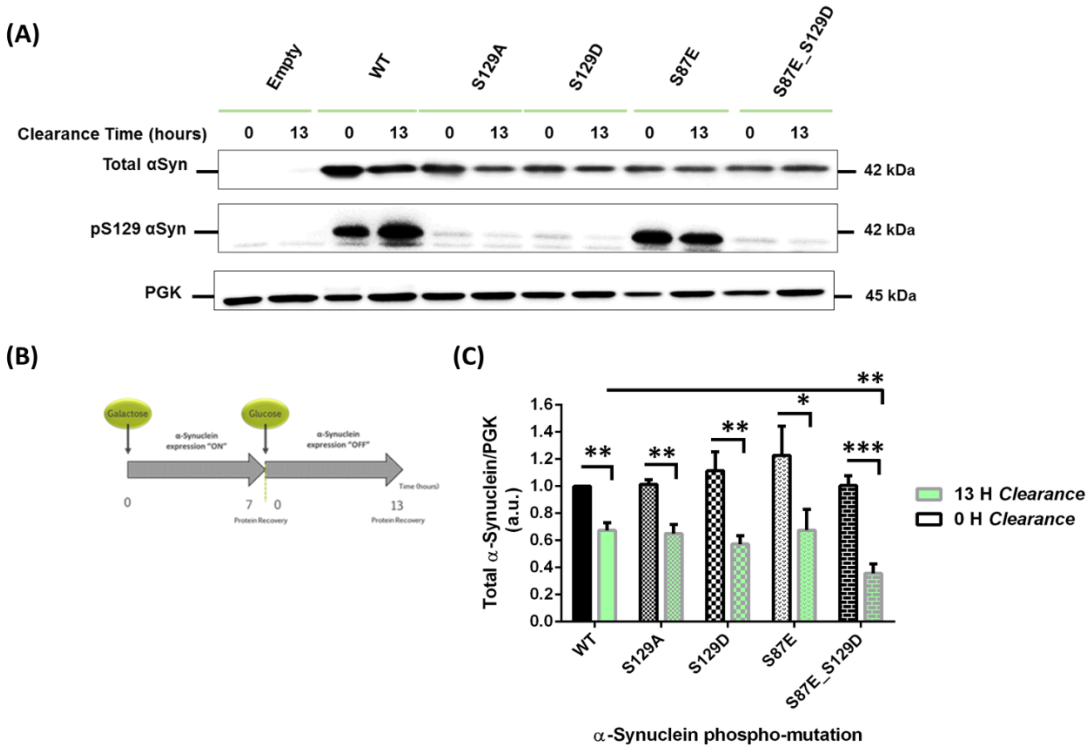

Figure 4.14. Effect of the phospho-mutations on total and phosphorylated at S129 αSyn protein levels during protein clearance. (A) WT, S129A, S129D, S87E and S87E_S129D αSyn-GFP and pS129 protein levels residue in yeast cells assessed by Western Blot analysis of total protein extracts at the time points of αSyn -GFP clearance of 0 and 13 hours. (B) Schematic representation of the experimental procedure followed to evaluate αSyn clearance in the phospho-mutants under study. After 7 hours of protein expression induction in Galactose media, protein was recovered. After this time point, the media carbon source was replaced to Glucose (the time point of 7 hours of αSyn expression induction and the time point of 0 hours of clearance are the same). After 13 hours in glucose SC media, protein was again recovered. (C) Densitometric analysis of the immunodetection of αSyn relative to the intensity obtained for PGK, used as loading control, presented in arbitrary units (a.u.) Results shown are from one representative experiment from at least three independent experiments. Values represent the mean ± SD and statistical analysis were performed by One-Way ANOVA with Bonferroni's multiple comparison test (where * represents a significance of $p<0.05$, ** represents a significance of $p<0.01$ and *** represents a significance of $p<0.001$).

4.2.4. S87 and S129 phospho-mutations effect on cell degradation systems: UPS function evaluation and ALP activity assessment

To further explore the effect of the phospho-mutations on the link amongst toxicity, inclusion formation and clearance of protein, it was explored their impact on the cell degradation systems, namely on the proteasome and autophagy functions.

Firstly, to evaluate proteasome function, the six phospho-mutants under study were transformed with a centromeric yeast plasmid coding the uGFP protein reporter. This reporter substrate is an established model for monitoring protein degradation by the proteasome. The theoretical basis for this assay relies on the fact that this modified fluorescent protein is fused to degradation signals that target the fusion protein for constitutive turnover via the proteasome [Neefjes and Dantuma, 2004]. Therefore, the levels of uGFP reporter inversely correlate with proteasome activity [Dantuma *et al*, 2000], [Bence *et al*, 2001] and accumulation of reporter protein relative to baseline levels is typically interpreted as reduced proteasome function, although, reporter protein levels may be affected by changes in expression [Bowman *et al*, 2005], [Tokui *et al*, 2009] or protein synthesis, to which they are very sensitive as a

consequence of their short half-life [Li *et al*, 1998]. However, these reporter substrates are important tools for studying proteasome functionality in cell and mouse models of neurodegenerative diseases [Dantuma and Bott, 2014] and, accordingly, it has already been demonstrated a reduced proteasome function, evaluated using uGFP, in yeast cells expressing WT αSyn [Outeiro and Lindquist, 2003].

Thus, when protein levels are assessed by Western Blot using an antibody that specifically recognizes GFP, a signal at approximately 27 kDa is expected to be seen, correspondent to uGFP within the cell cytoplasm that was not degraded by the proteasome, and the intensity of this band will be directly proportional to the degree of proteasome function impairment.

In order to evaluate impact of the several phospho-mutants of αSyn on proteasome function over time, total protein was extracted at two time points: after 7 hours and 24 hours of protein expression induction, which was followed by SDS-PAGE and Western Blot with a specific antibody that recognizes GFP protein (Figure 4.15).

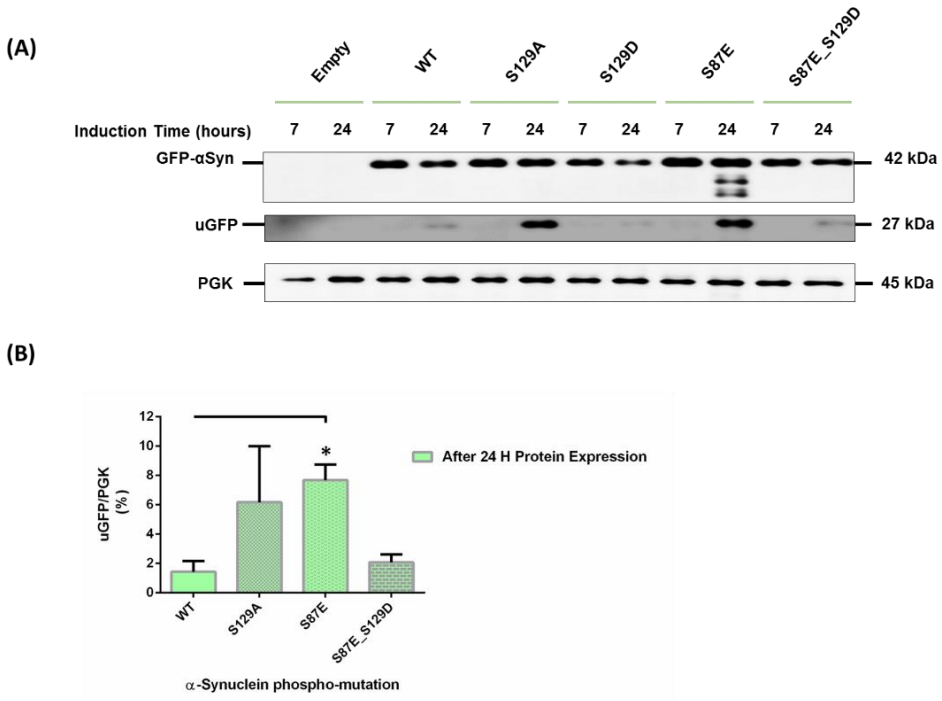

Figure 4.15. Effect of the phospho-mutations on uGFP levels, for proteasome function evaluation. (A) WT, S129A, S129D, S87E and S87E_S129D αSyn -GFP protein levels and uGFP protein levels assessed by Western Blot analysis of total protein extracts at the time points of αSyn -GFP expression induction of 7 hours and 24 hours. (B) Densitometric analysis of the immunodetection of uGFP relative to the intensity obtained for PGK, used as loading control, presented in percentage (%) at the time-point of αSyn expression induction of 24 hours. Results shown are from one representative experiment from at least three independent experiments. Values represent the mean ± SD and statistical analysis were performed by One-Way ANOVA with Bonferroni's multiple comparison test (where * represents a significance of $p<0.05$).

After 7 hours of protein expression induction, the proteasome is active in all phospho-mutants since no signal is visible for uGFP at the expected protein size (27 kDa). However, after 24 hours of protein expression induction, the mutant S129A showed an impairment of proteasome function and this impairment was also evident for the mutant S87E (6.17±3.83% and 7.68±1.05% of uGFP, respectively, when normalized to the loading PGK). This impairment was significantly increased for the S87E mutant when compared to the WT (1.43±0.72% of uGFP) assay at the same time point and when compared to its homologous after 7 hours of protein expression (no signal for uGFP) (Figure 4.15). Furthermore, the S87E mutant showed two additional signals below the mark for S87E αSyn-GFP, which might indicate

the presence of intermediary degraded αSyn fused to GFP species (Figure 4.15 A). This intermediary GFP signal was only observed for this mutant in particular. On the other hand, when the S87E mutation was coupled to the S129D mutation (S87E_S129D mutant), proteasome is functional both after 7 hours and 24 hours of protein expression induction, with a slight decrease of proteasome function on the latter timepoint (2.08±0.54% of uGFP). Likewise, it is possible to see that under the experimental conditions tested, the expression of the WT and S129D mutant proteins do not cause an impairment of the proteasome function after 7 hours of protein expression induction, however the expression of the WT protein cause a slight impairment of the proteasome when protein expression is induced for 24 hours (1.43±0.72% of uGFP). The absence of uGFP signal for the S129D mutant is evidence of the similar behavior to the WT protein, as described previously by [Tenreiro *et al*, 2014a] (Figure 4.15 A and B).

The results observed for proteasome function evaluation were not due to significant alterations in αSyn expression levels between the phospho-mutants at the timepoints tested (*Annexes* section, Figure 8.5).

Afterwards, in order to assess the contribution of autophagy to the clearance of αSyn protein in the six phospho-mutants, evaluation of *ATG8* induction and autophagic flux was performed. To achieve this purpose, the GFP-Atg8 processing assay was performed [Klionsky *et al*, 2012], [Shintani and Klionsky, 2004] phospho-mutant yeast strains were transformed with a yeast centromeric plasmid expressing GFP-Atg8 fusion protein under the regulation of the *ATG8* natural promoter, a similar approach as used by [Tenreiro *et al*, 2014a]. On one hand, *ATG8* induction is measured by quantifying the increase of total GFP signal (GFP-Atg8 and free GFP signal) normalized to the loading control (PGK), reflecting autophagy induction. On the other hand, autophagic flux is quantified by measuring the vacuolar degradation of the Atg8 domain of the reporter (ratio of free GFP to total GFP signal) [Klionsky *et al*, 2012], [Shintani and Klionsky, 2004]. Both quantifications performed by Western Blot analysis using a GFP-specific antibody and PGK-specific antibody for the loading control.

In yeast, the Atg8 protein is a ubiquitin-like protein, being an autophagy and cytoplasm-to-vacuole targeting essential factor [Harding *et al*, 1995], [Lang *et al*, 1998], [Scott *et al*, 1996]. Therefore, this protein will be upregulated in stress conditions, when autophagic cargo recruitment and autophagosome biogenesis are crucial [Huang *et al*, 2000]. As a consequence of autophagy upregulation, the GFP-Atg8 coding plasmid will be expressed and a signal at approximately 40 kDa is visualized by Western Blot analysis, whereas GFP-Atg8 targeting to the vacuole is characterized by GFP cleavage (and a signal at 27 kDa is visualized) [Klionsky *et al*, 2012], [Shintani and Klionsky, 2004] (Figure 4.16).

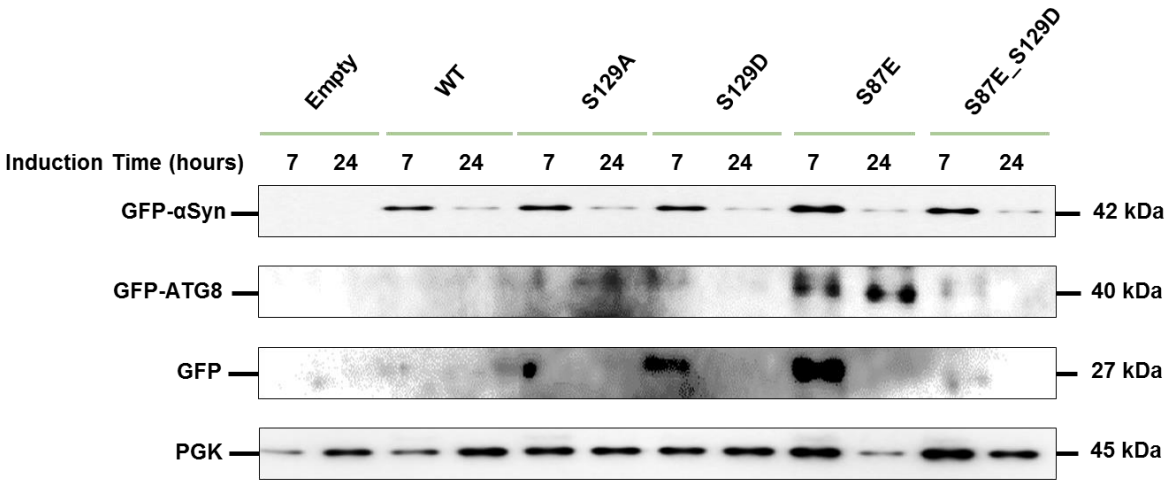

Figure 4.16. Effect of the phospho-mutations on Atg8 levels, for autophagy function evaluation. Autophagy evaluated by GFP-Atg8 processing assay in yeast cells expressing GFP-Atg8 under the regulation of the endogenous promoter alone (control Empty) or together with either WT, S129A, S129D, S87E or S87E_S129D αSyn, at the indicated time points of protein expression induction of 7 hours and 24 hours, assessed by Western Blot, using anti-GFP antibody. Results shown are from one experiment with three biological replicates.

From the results illustrated in the figure above (Figure 4.16) it was possible to visualize a signal at approximately 42 kDa, 7 hours after protein expression induction for all phospho-mutants which was correspondent to the αSyn protein fused to GFP. However, for all mutants this signal loses intensity after 24 hours of protein expression induction, which might be due to the following possible reasons: the overexpression of the Atg8 protein helps in αSyn clearance by upregulating autophagy and as a consequence, αSyn total levels are decreased (and signal intensity also decreases) or, as observed by fluorescence microscopy, yeast cells do not display inclusion formation after 24 hours of protein expression induction and, therefore, no signal appears. By comparing this first result from the autophagy assay to the proteasome assay (as in the last one, anti-GFP antibody was also used), one may infer that the latter hypothesis is unlikely since this decrease in GFP-αSyn signal was not observed when proteasome function was assessed. Therefore, autophagy upregulation might help cells coping with increasing αSyn levels and inclusion formation.

Regarding the autophagy induction and flux, the results obtained using the *ATG8* processing assay indicate that after 7 hours of αSyn expression induction, the mutation S87E resulted in higher levels of autophagy induction and flux, followed by the mutations S129A and S129D. After 24 hours of αSyn expression induction, only the cells expressing the S87E αSyn show autophagy induction (Figure 4.16), although not translated in an increasing of autophagy flux.

Although qualitatively evaluating this pattern is maintained throughout the three biological replicates tested, only one experiment was performed, which does not allow to quantitatively evaluate with an appropriate error range and validate the results obtained.

4.2.5. Confirmation of the phenotype of S87E αSyn

In summary, S87E αSyn phospho-mutant showed the highest toxicity when compared to the WT protein and the phospho-mutants S129A, S129D and S87E_S129D, being the last one the one that

presented less toxicity and a protective effect compared to the WT protein expression. To assure that the phenotype obtained was in fact due to the amino acid replacement S87E and to validate the functional characterization performed, three experimental approaches were chosen.

First a phenotypic study was performed comparing W303.1A yeast strains transformed with the equivalent multi-copy yeast vectors encoding the WT αSyn or S87E αSyn proteins (further detailed in *Annexes* section, Table 8.1).

Similarly, to what was observed for the integrative transformed phospho-mutants, spotting assays performed with these yeast strains confirmed that the expression of the S87E αSyn mutant was toxic for yeast cells and qualitatively evaluating, more toxic than the WT protein (Figure 4.17).

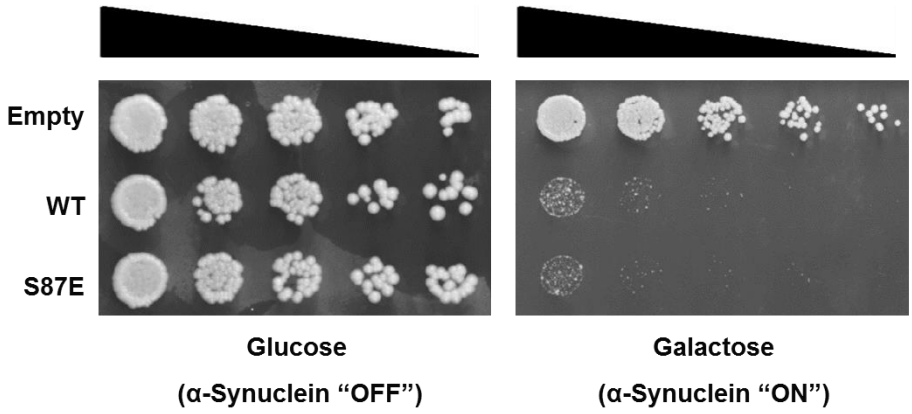

Figure 4.17. Spotting assay of the yeast cells expressing either the WT or the S87E αSyn from a multi-copy plasmid. Cell suspensions were adjusted to the same OD_{600nm}, serially diluted and spotted onto the surface of the solid media containing either glucose (control) or galactose (induced αSyn expression) as carbon source. Results shown are from one representative experiment from at least three independent experiments.

Furthermore, fluorescence microscopy performed after 7 hours of protein expression induction, showed a higher percentage of cells with inclusions when the multi-copy yeast plasmid encoding the S87E mutant αSyn is expressed, compared to the expression of the WT protein (Figure 4.18).

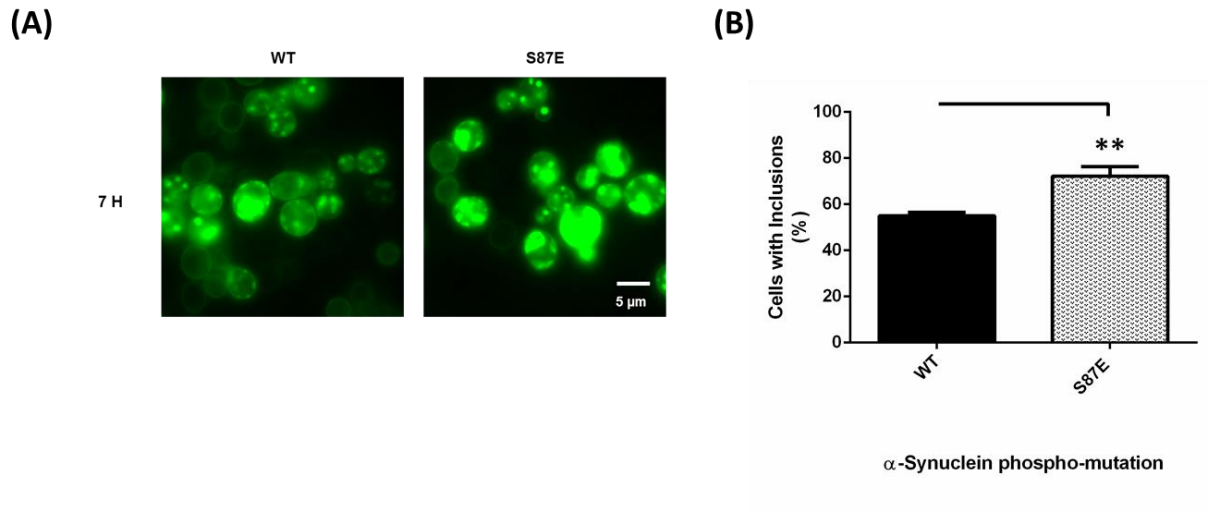

Figure 4.18. Inclusion formation evaluation for the S87E αSyn mutant expression in yeast cells harboring a multi-copy plasmid. (A) Intracellular localization of the WT or S87E αSyn-GFP and respective (B) percentage of yeast cells containing αSyn-GFP inclusions, assessed by fluorescence microscopy at the indicated time point of 7 hours after αSyn-GFP expression induction Results shown are from one representative experiment from at least three independent experiments. Values represent the mean ± SD and statistical analysis were performed by One-Way ANOVA with Bonferroni's multiple comparison test (where ** represents a significance of $p<0.01$).

As a control, the effects observed were not due to differences in protein expression levels. Moreover, S87E αSyn mutant and WT αSyn encoded by the multi-copy yeast plasmids are similarly phosphorylated on the residue S129 when compared to its integrative homologous, with the mutant S87E αSyn presenting 0.69±0.21 a.u. of phosphorylated αSyn at S129 compared to the WT protein. (Figure 4.19).

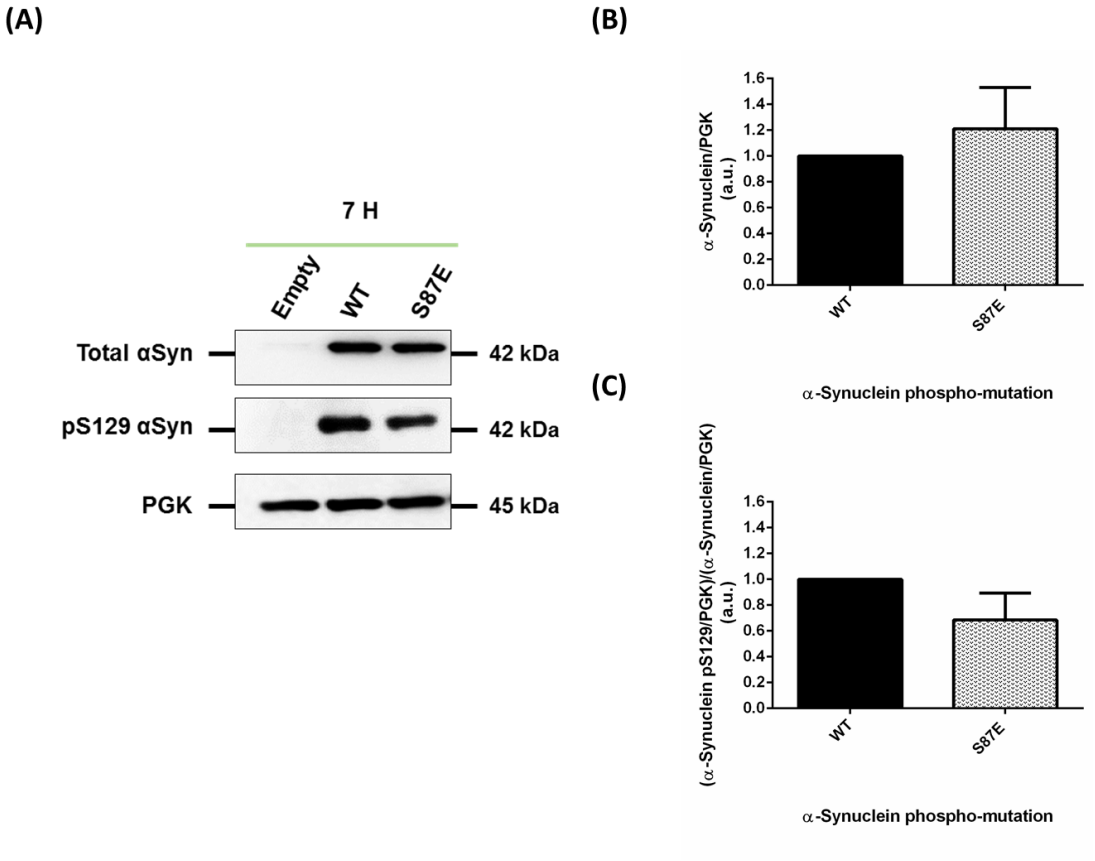

Figure 4.19. Effect of the S87E mutation on total and phosphorylated at S129 αSyn protein levels. (A) WT and S87E αSyn-GFP expression and pS129 levels in yeast cells assessed by Western Blot analysis of total protein extracts, 7 hours after αSyn-GFP expression induction. (B) Densitometric analysis of the immunodetection of αSyn-GFP relative to the intensity obtained for PGK, used as loading control, presented in arbitrary units (a.u.), for (B) total αSyn and (C) pS129. Results shown are from one representative experiment from at least three independent experiments. Values represent the mean ± SD and statistical analysis were performed by One-Way ANOVA with Bonferroni's multiple comparison test.

Another approach used to validate the results above was to evaluate if the observations were reproducible in another yeast strain. Namely, one yeast strain, the SC665, containing the two integrative plasmids coding for the S87E αSyn, which was obtained from the same crossing and sporulation as the one used in the studies performed above (the SC663) was selected and phenotypically characterized.

Maintaining the experimental conditions previously described for the functional characterization of the integrative phospho-mutants, both yeast strains SC663 and SC665 were induced for protein expression for 7 hours following fluorescence microscopy (Figure 4.20). The homologous yeast strains SC663 and SC665 have a similar phenotype for the percentage of cells with inclusions (87.21±1.30% and 81.82±4.86%, respectively).

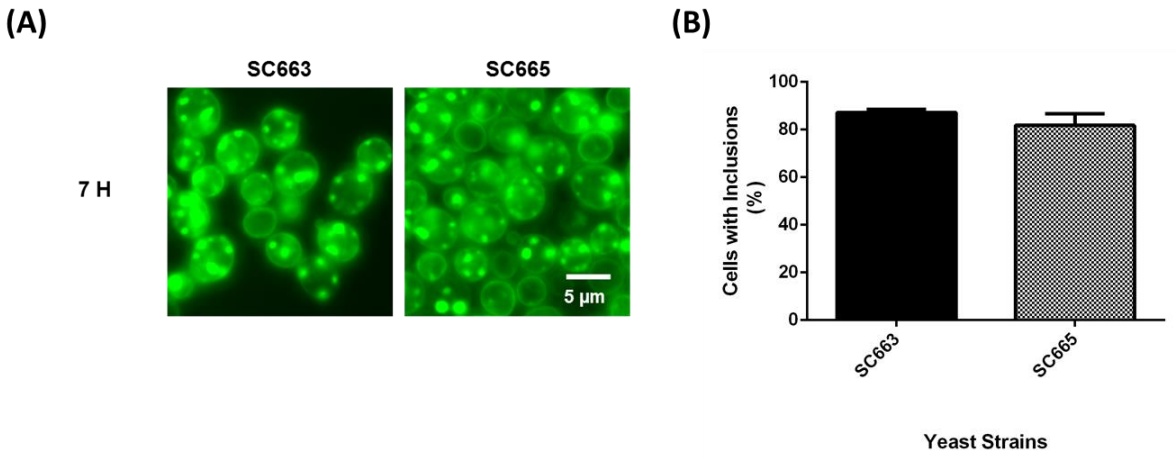

Figure 4.20. Inclusion formation evaluation for the S87E αSyn mutant expression in yeast cells. (A) Intracellular localization of the S87E αSyn-GFP protein on the homologous yeast strains SC663 and SC665 and respective (B) percentage of yeast cells containing αSyn-GFP inclusions, assessed by fluorescence microscopy at the indicated time point of 7 hours after αSyn-GFP expression induction. Results shown are from one representative experiment from at least three independent experiments. Values represent the mean ± SD and statistical analysis were performed by One-Way ANOVA with Bonferroni's multiple comparison test.

In order to confirm the identity of the coding gene sequence of S87E αSyn, yeast genomic DNA was extracted and a PCR reaction was performed in order to amplify the desired DNA fragment, which was purified after gel electrophoresis (*Materials and Methods* section, Figure 3.5). Toward the confirmation of the presence of the desired αSyn mutation, DNA sequencing was performed (*Stabvida*, S.A., Oeiras, Portugal) followed by full sequence alignment (*ClustalOmega* bioinformatics tool) with WT αSyn coding gene sequence (*Annexes* section, Figure 8.2).

In order to confirm the presence of a double genomic insertion for the yeast strain tested, yeast genomic DNA was extracted and a PCR reaction was performed to amplify the desired DNA fragments correspondent to the *ura3* and *trp1* auxotrophic marks (*Materials and Methods* section, Figure 3.7) and upon gel electrophoresis it was possible to visualize both amplified DNA fragments correspondent to the auxotrophic marks and on the expected molecular weight (*Materials and Methods* section, Figure 3.4). Therefore, by following these approaches, the identity of the yeast strain containing the most prominent phenotype was confirmed.

5. Discussion

αSyn has been the center of focus in understanding the etiology of a group of overlapping neurodegenerative disorders, including PD, which are pathologically characterized by the progressive cytoplasmic accumulation [Kim *et al*, 2014], in a nucleation dependent manner, of this protein [Wood *et al*, 1999]. Furthermore, in PD there is a strong dichotomy between the rare early onset familial form of PD and a more common age and environment-related sporadic form, since αSyn is a common link between both forms [Marques *et al*, 2011], [Lopes da Fonseca *et al*, 2015]. For this reason, the understanding of the molecular mechanisms underpinning the genetic forms of the disease has already provided insights into the pathogenesis of the sporadic forms as well [Fujioka *et al*, 2014]. Whereas familial PD is characterized by duplications [Chartier-Harlin *et al*, 2004] and triplications [Singleton *et al*, 2003] of the *SNCA* gene, leading to αSyn overexpression and disruption of cell homeostasis, as well as six missense genetic mutations that lead to the αSyn amino acid substitutions A30P [Kruger *et al*, 2001], E46K [Zarranz *et al*, 2004], H50Q [Appel-Cresswell *et al*, 2013], [Proukakis *et al*, 2013], G51D [Kiely *et al*, 2013], A53T [Polymeropoulos *et al*, 1997] and A53E [Pasanen *et al*, 2014], both types of PD show up-phosphorylated levels at S129 residue in LB inclusions, as well as at S87, suggesting a critical role of PTMs, and more importantly phosphorylation, in αSyn aggregation, LB formation and neurotoxicity [Tenreiro *et al*, 2014b]. Currently, the shift of αSyn physiological function to its pathological condition, as well as the cellular mechanisms by which it induces toxicity, are still elusive [Wales *et al*, 2013], which it is a backwards key point in the development of new and curative therapeutic strategies to this disease.

Using the yeast *S. cerevisiae* as a model organism to study αSyn aggregation and pathobiology, similar to what occurs in the brains of PD patients, the present study aimed at tackled the two forms of PD etiology: the rarer familial PD, by phenotypically characterize the most-recently identified and, therefore, less investigated, αSyn mutation A53E, and the more common sporadic PD, by the study of the phosphorylation interplay between the two major up-phosphorylated residues of αSyn in LBs, the S87 and S129 [Fujiwara *et al*, 2002], [Paleologou *et al*, 2010].

To investigate the phenotype characterized by the expression of the most-recent familial PD linked mutation of αSyn, the experimental approach used was based on transforming wild-type yeast cells with multi-copy yeast plasmids expressing human αSyn A53E mutation or WT fused to GFP and under the regulation of an inducible promoter *GAL1*. Comparable to the WT αSyn, the A53E mutant protein is phosphorylated at S129. This is in key with the identification of up-phosphorylated levels at S129 in *post-mortem* human brain analysis [Pasanen *et al*, 2014] and in *in vivo* studies of mouse brain analysis and additionally, in three cellular models, Neuro2A [Rutherford *et al*, 2014], HEK and H4 [Lázaro *et al*, 2016]. Furthermore, accumulation of αSyn phosphorylated at S129 is detected in both *post-mortem* human brain analysis and functional studies where other PD-familial linked mutations and WT αSyn are expressed [Anderson *et al*, 2006], [Fujiwara *et al*, 2002], [Saito *et al*, 2003], [Kiely *et al*, 2013], [Appel-Cresswell *et al*, 2013], [Proukakis *et al*, 2013]. However, whether the phosphorylation at S129 has a protective or detrimental role remains elusive, both for familial and sporadic PD [Tenreiro *et al*, 2014b]. Concerning the tendency for inclusion formation induced by the A53E mutant expression, since the replacement of the amino acid A at position 53 by an E residue introduces an additional negative charge in the protein, it was expected that the intrinsic aggregation propensity of αSyn would be reduced, as it was already demonstrated *in vitro* that the A53E mutation had a decreased propensity to aggregate into amyloid structures, showing slower fibril formation [Ghosh *et al*, 2014]. However, it was observed that, inclusion formation in yeast cells expressing the mutant A53E protein was similar to the WT protein. These results are in key with the inclusion formation pattern detected for HEK cells expressing A53E αSyn [Lázaro *et al*, 2016], but opposing to Neuro2A cells, where A53E αSyn showed decreased propensity to aggregate into amyloid structures, when compared to the WT protein expression [Rutherford *et al*, 2015]. These differences may be due to the fact that in a cellular context, the behavior

of a protein is not only due to its intrinsic properties, but also depends on different interactions due to a crowed environment and the action of various protein quality control mechanisms. To further address the nature of the inclusions formed by the WT and A53E αSyn mutant, TritonX solubility was assessed and, although no statistical differences in solubility were detected due to presence of the mutation, the A53E showed a tendency to be more insoluble when compared to the WT protein. *In vitro* assays previously performed report a reduced membrane binding affinity of the A53E mutant, when compared to the WT protein and the also PD-linked mutation of αSyn, the A53T mutant [Ghosh *et al*, 2014]. However, in the context of the detergent used in this assay, more insoluble may also mean that it forms more oligomers, whereas more soluble meaning that it forms smaller oligomers or majorly monomers. If this last hypothesis is the case, the results are in accordance to *in vitro* studies that report an accumulation of αSyn oligomers for a longer period of time [Ghosh *et al*, 2014] when in the presence of the A53E mutation, compared to the WT protein. However, a study performed in a living human cellular model showed that the A53E mutant decreases αSyn oligomerization [Lázaro *et al*, 2016]. Further studies regarding the nature of the species as well as the aggregation process of the A53E mutant αSyn protein ought to be carried in the future.

Regarding toxicity, the expression of WT and A53E αSyn are equally toxic to yeast cells, which follows the trend observed in previous studies performed for this mutant using other cellular models [Ghosh *et al*, 2014], [Rutherford *et al*, 2015]. To further address specific mechanisms leading to cell toxicity, induced by the presence of the A53E mutation, mitochondrial network integrity was evaluated. Previous studies report that both WT and A53T mutant αSyn have been shown to cause mitochondrial function impairment and up-regulate mitophagy, leading to cell homeostasis disruption and neuronal death in mice models of PD [Choubey *et al*, 2011], [Chinta *et al*, 2010]. Furthermore, *in vitro* studies showed that A53E αSyn increased cellular toxicity and dead under stress conditions and mitochondrial impairment [Rutherford *et al*, 2015]. As opposed to what was expected, in yeast cells the expression of both WT and A53E αSyn do not show any impact on mitochondrial network dynamics. Although the fluorescence assay approach shows a *clustering* of mitochondria co-localized with αSyn in yeast cells, both for WT and A53E, however, the flow cytometry analysis evaluation stated no differences in the mitochondrial membrane potential in cells expressing αSyn or not. Accordingly, the conclusions regarding the effect of the A53E αSyn expression in mitochondrial network integrity are weak and further optimizations of the experimental protocol would be necessary.

Overall, the A53E αSyn shows no significant differences regarding general cell toxicity, inclusion formation and nature of the inclusions formed in yeast cells and these results are in accordance with what was previously described in other functional studies performed using different cellular models [Ghosh *et al*, 2014], [Rutherford *et al*, 2015], suggesting that the early-onset PD phenotype that characterizes the A53E mutation of αSyn might be caused by other specific cellular mechanisms that eventually are not conserved in yeast, or likely differences in the initial steps of the aggregation process (dimerization/oligomerization) of αSyn, and not the later steps that culminate with the formation of the mature inclusions, since there is the hypothesis that different familial PD αSyn linked mutations lead to cell toxicity through different mechanisms.

Concerning the study of the interplay between the S87 and S129 phosphorylation residues and its impact on αSyn toxicity, these were carried by using integrative transformed yeast strains with the *SNCA* human gene encoding the WT αSyn, the single-mutants encoding for the protein mimicking and blocking the phosphorylation at S129, S129D αSyn and S129A αSyn, respectively, as well as mimicking phosphorylation on the S87 residue, S87E αSyn and the double mutant encoding the protein mimicking phosphorylation in both residues, S87E_S129D αSyn, under the regulation of the inducible promotor *GAL1*.

Upon assessment of αSyn toxicity of the group of phospho-mutants, it was observed that when phosphorylation at the S87 residue was mimicked, the phenotype was characterized by the almost total absence of yeast growth in spotting assays and an increase in PI^+ cells, when compared to the other phospho-mutants (S129A and S129D) and WT αSyn expressing cells, which suggested that the S87E mutation exacerbates the toxicity induced by αSyn expression. Surprisingly, when the mutation S87E was coupled with the mutation that mimics the phosphorylation on the S129 residue, yeast cells had an increased growth when compared to the WT protein expression, even similar to the empty control and accordingly, the population of PI^+ cells decreased to marginal numbers. Furthermore, the effect observed for the toxicity accompanied the percentage of cells with inclusions: whereas the S87E single-mutant showed a dramatically increased percentage of cells with inclusions (of almost 80% in SC media and 100% in YEP media), compared to the WT, S129A or S129D αSyn expressing cells, when this mutation was coupled to the S129D mutation, the percentage of cells presenting inclusions decreased to almost zero in SC media (and 30% in YEP media). This data suggests that phosphorylation on the residue S87 increases the toxicity and tendency for inclusion formation of αSyn protein. However, when coupled to the phosphorylation on S129, the protective effect previously described for this mutation, using a similar yeast model [Tenreiro *et al*, 2014a], prevails over the toxic effect of the S87 phosphorylation and one may even suggest that, when coupled with the phosphorylation at the S129 residue, the phosphorylation at the S87 plays a synergic protective effect. Supporting this hypothesis, the quantification of αSyn phosphorylated at S129 showed that the mutant S87E alone has significant less phosphorylated S129 αSyn, when compared to the WT protein.

Nevertheless, when comparing to the state of the art regarding the S87 phosphorylation effect on αSyn toxicity and inclusion formation, studies performed using a mouse model of PD showed that, although LB inclusions show up-phosphorylation at the S87 residue (as also detected in *post-mortem* human brain analysis) [Paleologou *et al*, 2010], S87 phosphorylation inhibits αSyn aggregation and protects against its induced toxicity and, as well, *in vitro* studies showed that phosphorylation at this residue expands αSyn structure (conferring flexibility), blocking its fibrillation and ability to bind to membranes [Paleologou *et al*, 2010], [Oueslati *et al*, 2012], [Kim *et al*, 2006], [Waxman and Giasson, 2008]. One explanation for the this antagonism regarding the phosphorylation at S87 amongst yeast, mice models and *in vitro* assays may rely on the limitations of each model used: on one hand, *in vitro* assays do not recapitulate the crowded environment and multiple interactions that exists within a cell and, on the other hand, S87 is one of the few positions that is distinguishable between the human and mice or rat αSyn, which limits the usage of these models in the study of the role of phosphorylation in neurodegenerative diseases [Xu *et al*, 2015]. Furthermore, S87 is only phosphorytable in humans [Xu *et al*, 2015], which is an evidence of its role in PD pathology. To further check if the toxic effect observed in yeast cells expressing the S87E mutant was due to the presence of that specific mutation of αSyn (namely if this mutant mimics the behavior of WT protein) several assays were performed: first, the yeast strain ability to grow in medias correspondent to the yeast autotrophies was carried and in fact, the yeast strain encoding S87E αSyn was able to grow in medias lacking the amino acid URA, TRP or both, which is an evidence that the yeast strain was transformed with both plasmids and that the expression of αSyn was stable; this was supported by the PCR amplification of both yeast genomic auxotrophic marks (*ura3* and *trp1*). Furthermore, DNA sequencing of the αSyn coding gene sequence was performed, which confirmed the presence of the amino acid substitution S87E and confirmed other positions, such as the S129, and, lastly, similarly the expression of a multi-copy yeast plasmid encoding S87E αSyn showed toxicity to yeast cells and increased inclusion formation when compared to the expression of the WT protein. The less severe phenotype using multi-copy yeast plasmids was expected, since the cells are able to control and better regulate αSyn expression levels, especially when this is being toxic, on the contrary to genomic insertions of αSyn coding gene insert. This suggests that the S87E αSyn mutant

might constitute a valid approach for the assessment of the cellular responses involved in the accumulation of this protein.

Since in yeast it was previously observed that blocking the phosphorylation on the S129 residue increased toxicity and inclusion formation, although forming fewer but bigger and more heterogeneous inclusions per cell [Tenreiro *et al*, 2014a], the group of phospho-mutants were grown in enriched media to better distinguish the nature of the inclusions formed and the toxicity observed when growth in poor selective media in the presence of each phospho-mutation. The S129A showed an identical phenotype to what was previously described [Tenreiro *et al*, 2014a] and additionally, the S87E mutant showed the same phenotype of nature of the inclusions formed as described for the S129A mutant. Interestingly, for the double-mutant S87E_S129D, within the cells with inclusions, the same phenotype displayed by the S87E and S129A single-mutants was observed. From this point of view, results suggest that the number and/or size of inclusions formed per cell is not a major factor in αSyn induced toxicity.

In PD, proteostase is the major key point in the development of the pathology, therefore a balance between the rates of αSyn synthesis, aggregation and clearance is pivotal [Kragh *et al*, 2012] and a dysfunction in one of these factors could favor the accumulation and/or formation of protein oligomers and inclusions that ultimately lead to cytotoxicity [Lashuel *et al*, 2013]. To address if the inclusion formation detected for the S87E mutant was due to an impairment of protein degradation, protein levels were assessed after protein synthesis repression. In fact, the S87E showed less easiness to clear protein when compared to the WT and interestingly, when the phosphorylation on S87 was coupled to the phosphorylation on S129, protein is more easily cleared when compared to the WT and even to the S129D mutant proteins. The double mutant S87E_S129D did not show a high percentage of cells with inclusions, therefore it was expected that monomers of αSyn would be more easily degraded than protein inclusions, since as previously described, on the contrary to high molecular weight inclusions, monomeric αSyn can be degraded through several quality control mechanisms (UPS and ALP) or even be refolded by the activity of chaperones, avoiding the tendency to aggregate [Lashuel *et al*, 2013]. Furthermore, the double mutant S87E_S129D higher ability to clear αSyn protein compared to the single mutant S129D, already described to play a role in promoting protein clearance in yeast cells expressing human αSyn [Tenreiro *et al*, 2014a], might constitute a primary evidence of a synergic protective effect between the S129 and S87 simultaneous phosphorylation on αSyn aggregation and toxicity.

Important to notice is the observation that at 24 hours after αSyn expression induction, the phenotypes of inclusion formation, and more importantly the toxic phenotype of the S87E mutant, was lost. To explain this fact, two possible reasons were hypothesized: the first one, the toxicity induced by the S87E mutation was so high that the surviving cells were cells able to developed mechanisms to cope with αSyn expression or the second one, intrinsic to the culture growth. To shed a light on this issue, the cellular quality-control mechanisms of proteasome function and autophagy activation, which are conserved from yeast to higher eukaryotes [Tenreiro *et al*, 2014b], were assessed at both time points (7 and 24 hours). Interestingly, the S87E phospho-mutant showed high proteasome impairment after 24 hours of protein expression, which is consistent with a scenario of cell death. To support this hypothesis, it is the observation of intermediary degradation species of αSyn, due to the failure of cells to cope with the high inclusion formation detected for this mutant, as the proteasome was already described as being able to degrade monomeric aberrant αSyn but not higher molecular species, as oligomers and fibrils [Lashuel *et al*, 2013]. Once again, when the S87E and S129D mutations are coupled, proteasome is functional at both time points tested, as well as for the single mutant S129D. This is consistent with an already described prevailing protective effect of the S129 residue phosphorylation in promoting protein degradation [Tenreiro *et al*, 2014a] over the impairment of clearance induced by the S87 mutation phosphorylation.

Regarding autophagy function evaluation, this was assessed by inducing Atg8 overexpression in yeast cells, a protein essential to target proteins to the autophagosome and promote protein degradation [Lopes da Fonseca *et al*, 2015]. Overall, autophagy upregulation lead to a decrease of αSyn levels after 24 hours of protein expression induction for all phospho-mutants analyzed and the activation of autophagy is considerably higher for the S87E mutant at both time points of 7 and 24 hours of protein expression induction. Notably, at 7 hours of protein expression, the activation of autophagy correlated with the degradation of protein through this mechanism. This is in key with two major concepts: the first one, the higher molecular species, as the high number of αSyn inclusions observed for the S87E mutant, are degraded through an autophagic mechanism [Lee *et al*, 2004] and, the second one, since it was observed that for this phospho-mutant the proteasome was impaired 7 hours following protein expression, it would be expected that the complementary mechanism to maintain cell homeostasis would be upregulated: autophagy [Lopes da Fonseca, 2015]. Furthermore, supporting the scenario of cell death for the mutant S87E, following 24 hours of protein expression induction, is the fact that autophagy activation is not translated in autophagy-mediated degradation of proteins, evidencing the highly toxic effect of the single phosphorylation of the S87 residue for yeast cells. Regarding the double mutant phosphorylated both at S87 and S129, autophagy was not upregulated, which is possibly due to the fact that most of the αSyn protein species are monomers, therefore are degraded through the proteasome, which was shown to be functional for this mutant at either of the time points of protein expression induction tested.

On the contrary to what was exposed in a previous study expressing human αSyn in yeast cells [Tenreiro *et al*, 2014a], the effect amongst the expression of the S129A, S129D and WT protein were somehow indistinguishable. It was previously reported that the integrative transformed yeast strain carrying the αSyn mutation S129A increased toxicity, as opposed to its homologous S129D, that was found to minimize αSyn toxicity to cells and promote protein degradation [Tenreiro *et al*, 2014a]. However, these differences in the phenotypes obtained between the previous study and this one, are acceptably explained by the differences in the experimental conditions used in this study: by growing yeast cells in poor media, the phenotypes caused by the phospho-mutants were expected to be less severe and, therefore, more similar amongst them. However, in this study it was still possible to detect a slight less toxicity when S129D αSyn was expressed and an increased percentage of cells with inclusions, as well as bigger sized and more heterogeneous nature of these inclusions observed for the mutant S129A, accordingly to what was previously described [Tenreiro *et al*, 2014a]. Furthermore, the toxic effect previously reported for the S129A mutant on cell quality control impairment [Tenreiro *et al*, 2014a] was also recapitulated in this study, namely in impairment of proteasome function and up-regulation of autophagy.

Overall, the results obtained by the analysis of the αSyn phospho-mutants, support the concept of a neuroprotective effect of the phosphorylation at the S129 residue, in preventing inclusion formation and promoting protein degradation and clearance, in accordance with the results obtained in other model organisms, such as *C. elegans*, mice and other rodents [Yin *et al*, 2014], [Wu *et al*, 2011], [Kuwahara *et al*, 2012] and for the first time, suggests an important interplay between the phosphorylation at the residues S87 and S129 in αSyn inclusion formation and induced cellular toxicity.

6. General Conclusions and Future Perspectives

The major contribution of this work relies on the usage of a simple model organism in the understanding of the etiology of complex human diseases, such as the second most common and incurable neurodegenerative disease, PD [Marques *et al*, 2011]. In fact, by using the simple budding yeast *S. cerevisiae*, this project was able not only to provide a characterization of the effect of the most recent PD linked mutation of αSyn, A53E, but also provide insights into the cross-talk between the phosphorylation of the major residues associated with LB formation, the S87 and S129 residues [Fujiwara *et al*, 2002], [Paleologou *et al*, 2010]. In conclusion, the most important take-home evidences provided during this project are the following:

A) In yeast cells, the A53E PD-linked mutation of αSyn induced toxicity and inclusion formation comparable to the WT protein and both show comparable phosphorylation at S129 and nature of the inclusions formed;
B) In a yeast cell model, mimicking phosphorylation at the S87 residue of αSyn protein dramatically increased toxicity and inclusion formation, causing an impairment of UPS function and up-regulating autophagy when compared to the WT protein;
C) When both S87 and S129 residues are phosphorylated, αSyn expression is less toxic, forming less inclusions and being more easily cleared when compared to the expression of WT protein, prevailing a protective effect of S129 phosphorylation over the phosphorylation on S87 or even both phosphorylated residues playing a synergic neuroprotective effect.

Overall, the phenotypic characterization of the A53E mutant was in accordance to what was previously described in *in vitro* and *in vivo* studies regarding this mutant [Rutherford *et al*, 2015], [Lázaro *et al*, 2016], [Ghosh *et al*, 2014], [Pasanen *et al*, 2014] suggesting that the early-onset PD phenotype caused by this and other different αSyn familial-PD linked mutations lead to cell toxicity through different mechanisms. Therefore, exploring specific cellular mechanisms as well as differences in the initial steps of the aggregation process (dimerization/oligomerization) of α αSyn, and not the later steps that culminate with the formation of the mature inclusions, are pivotal paths to follow in the understanding of the role of αSyn missense mutations in its toxicity.

Concerning the phosphorylation role of αSyn in PD pathogenesis, this study shed a light on the concept that the phenotype induced by PTMs depends mostly on a cross-talk between the different residues. This study supports a neuroprotective effect of the phosphorylation at S129 of αSyn and when coupled to the phosphorylation at S87. However, different approaches regarding the effects of coupling phosphorylation with tyrosine residues, such as Y125, Y133 and Y136, as well as a role of different phosphorylation patterns and other PTMs effect on different cellular organelles ought to be followed in the future, to better understand αSyn induced toxicity.

Taken together, the contribution of this work and a future effort on a deeper understanding of the effect of αSyn and its alterations on the protein behavior, including new strategies to modulate phosphorylation (namely at residues S87 and S129), as well as cellular proteostase and overall homeostasis play a major key role in the development of new therapeutic avenues for PD and other synucleinopathies.

7. References

Agarraberes, F.A., Terlecky, S.R. & Dice, J.F. An intralysosomal hsp70 is required for a selective pathway of lysosomal protein degradation. *J Cell Biol* 137, 825-834 (1997).

Ahn, B.H., *et al* alpha-Synuclein interacts with phospholipase D isozymes and inhibits pervanadate-induced phospholipase D activation in human embryonic kidney-293 cells. *J Biol Chem* 277, 12334-12342 (2002).

Albuquerque, E.X., Pereira, E.F., Alkondon, M. & Rogers, S.W. Mammalian nicotinic acetylcholine receptors: from structure to function. *Physiol Rev* 89, 73-120 (2009).

Alvarez-Erviti, L., *et al* Chaperone-mediated autophagy markers in Parkinson disease brains. *Arch Neurol* 67, 1464-1472 (2010).

Anderson, J.P., *et al* Phosphorylation of Ser-129 is the dominant pathological modification of alpha-synuclein in familial and sporadic Lewy body disease. *J Biol Chem* 281, 29739-29752 (2006).

Appel-Cresswell, S., *et al* Alpha-synuclein p.H50Q, a novel pathogenic mutation for Parkinson's disease. *Mov Disord* 28, 811-813 (2013).

Auluck, P.K., Caraveo, G. & Lindquist, S. α-Synuclein: membrane interactions and toxicity in Parkinson's disease. *Annu Rev Cell Dev Biol* 26, 211-233 (2010).

Azeredo da Silveira, S., *et al* Phosphorylation does not prompt, nor prevent, the formation of alpha-synuclein toxic species in a rat model of Parkinson's disease. *Hum Mol Genet* 18, 872-887 (2009).

Beal, M.F. Mitochondria take center stage in aging and neurodegeneration. *Ann Neurol* 58, 495-505 (2005).

Bedford, L., Paine, S., Sheppard, P.W., Mayer, R.J. & Roelofs, J. Assembly, structure, and function of the 26S proteasome. *Trends Cell Biol* 20, 391-401 (2010).

Bence, N.F., Sampat, R.M. & Kopito, R.R. Impairment of the ubiquitin-proteasome system by protein aggregation. *Science* 292, 1552-1555 (2001).

Bender, A., *et al* TOM40 mediates mitochondrial dysfunction induced by α-synuclein accumulation in Parkinson's disease. *PLoS One* 8, e62277 (2013).

Bender, A., *et al* High levels of mitochondrial DNA deletions in substantia nigra neurons in aging and Parkinson disease. *Nat Genet* 38, 515-517 (2006).

Bennett, M.C., *et al* Degradation of alpha-synuclein by proteasome. *J Biol Chem* 274, 33855-33858 (1999).

Berg, D., *et al* Alpha-synuclein and Parkinson's disease: implications from the screening of more than 1,900 patients. *Mov Disord* 20, 1191-1194 (2005).

Bergeron, M., *et al* In vivo modulation of polo-like kinases supports a key role for PLK2 in Ser129 α-synuclein phosphorylation in mouse brain. *Neuroscience* 256, 72-82 (2014).

Bertoncini, C.W., Fernandez, C.O., Griesinger, C., Jovin, T.M. & Zweckstetter, M. Familial mutants of alpha-synuclein with increased neurotoxicity have a destabilized conformation. *J Biol Chem* 280, 30649-30652 (2005).

Bertram, L. & Tanzi, R.E. The genetic epidemiology of neurodegenerative disease. *J Clin Invest* 115, 1449-1457 (2005).

Beyer, K. Alpha-synuclein structure, posttranslational modification and alternative splicing as aggregation enhancers. *Acta Neuropathol* 112, 237-251 (2006).

Beyer, K. & Ariza, A. α-Synuclein posttranslational modification and alternative splicing as a trigger for neurodegeneration. *Mol Neurobiol* 47, 509-524 (2013).

Bhattacharyya, S., Yu, H., Mim, C. & Matouschek, A. Regulated protein turnover: snapshots of the proteasome in action. *Nat Rev Mol Cell Biol* 15, 122-133 (2014).

Bi, W., *et al* Serine 129 Phosphorylation of α-Synuclein Cross-Links with Tissue Transglutaminase to Form Lewy Body-Like Inclusion Bodies. *ISRN Neurol* 2011, 732879 (2011).

Bill, J., Ronchese, F., Germain, R.N. & Palmer, E. The contribution of mutant amino acids to alloantigenicity. *J Exp Med* 170, 739-750 (1989).

Bonifacino, J.S. & Glick, B.S. The mechanisms of vesicle budding and fusion. *Cell* 116, 153-166 (2004).

Bose, A. & Beal, M.F. Mitochondrial dysfunction in Parkinson's disease. *J Neurochem* 139 Suppl 1, 216-231 (2016).

Bowman, A.B., Yoo, S.Y., Dantuma, N.P. & Zoghbi, H.Y. Neuronal dysfunction in a polyglutamine disease model occurs in the absence of ubiquitin-proteasome system impairment and inversely correlates with the degree of nuclear inclusion formation. *Hum Mol Genet* 14, 679-691 (2005).

Braak, H. & Braak, E. Pathoanatomy of Parkinson's disease. *J Neurol* 247 Suppl 2, II3-10 (2000).

Braak, H., *et al* Staging of brain pathology related to sporadic Parkinson's disease. *Neurobiol Aging* 24, 197-211 (2003a).

Braak, H., Rüb, U., Gai, W.P. & Del Tredici, K. Idiopathic Parkinson's disease: possible routes by which vulnerable neuronal types may be subject to neuroinvasion by an unknown pathogen. *J Neural Transm (Vienna)* 110, 517-536 (2003b).

Braun, R.J. Mitochondrion-mediated cell death: dissecting yeast apoptosis for a better understanding of neurodegeneration. *Front Oncol* 2, 182 (2012).

Braun, R.J., Büttner, S., Ring, J., Kroemer, G. & Madeo, F. Nervous yeast: modeling neurotoxic cell death. *Trends Biochem Sci* 35, 135-144 (2010).

Burré, J., Sharma, M. & Südhof, T.C. α-Synuclein assembles into higher-order multimers upon membrane binding to promote SNARE complex formation. *Proc Natl Acad Sci U S A* 111, E4274-4283 (2014).

Burré, J., *et al* Alpha-synuclein promotes SNARE-complex assembly in vivo and in vitro. *Science* 329, 1663-1667 (2013).

Büttner, S., *et al* Functional mitochondria are required for alpha-synuclein toxicity in aging yeast. *J Biol Chem* 283, 7554-7560 (2013).

Calì, T., Ottolini, D., Negro, A. & Brini, M. α-Synuclein controls mitochondrial calcium homeostasis by enhancing endoplasmic reticulum-mitochondria interactions. *J Biol Chem* 287, 17914-17929 (2012).

Cardenas, M.E., Cutler, N.S., Lorenz, M.C., Di Como, C.J. & Heitman, J. The TOR signaling cascade regulates gene expression in response to nutrients. *Genes Dev* 13, 3271-3279 (1999).

Chandra, S., Gallardo, G., Fernández-Chacón, R., Schlüter, O.M. & Südhof, T.C. Alpha-synuclein cooperates with CSPalpha in preventing neurodegeneration. *Cell* 123, 383-396 (2005).

Chartier-Harlin, M.C., *et al* Alpha-synuclein locus duplication as a cause of familial Parkinson's disease. *Lancet* 364, 1167-1169 (2004).

Chaturvedi, R.K. & Beal, M.F. Mitochondrial approaches for neuroprotection. *Ann N Y Acad Sci* 1147, 395-412 (2008).

Chau, K.Y., Ching, H.L., Schapira, A.H. & Cooper, J.M. Relationship between alpha synuclein phosphorylation, proteasomal inhibition and cell death: relevance to Parkinson's disease pathogenesis. *J Neurochem* 110, 1005-1013 (2009).

Chaudhuri, K.R., Bhidayasiri, R. & van Laar, T. Unmet needs in Parkinson's disease: New horizons in a changing landscape. *Parkinsonism Relat Disord* 33 Suppl 1, S2-S8 (2016).

Chen, L., *et al* Tyrosine and serine phosphorylation of alpha-synuclein have opposing effects on neurotoxicity and soluble oligomer formation. *J Clin Invest* 119, 3257-3265 (2009).

Chen, L., Thiruchelvam, M.J., Madura, K. & Richfield, E.K. Proteasome dysfunction in aged human alpha-synuclein transgenic mice. *Neurobiol Dis* 23, 120-126 (2006).

Chen, Q., Thorpe, J. & Keller, J.N. Alpha-synuclein alters proteasome function, protein synthesis, and stationary phase viability. *J Biol Chem* 280, 30009-30017 (2005).

Chen, L. & Feany, M.B. Alpha-synuclein phosphorylation controls neurotoxicity and inclusion formation in a Drosophila model of Parkinson disease. *Nat Neurosci* 8, 657-663 (2005).

Chen, R.H., *et al* α-Synuclein membrane association is regulated by the Rab3a recycling machinery and presynaptic activity. *J Biol Chem* 288, 7438-7449 (2013).

Chi, Y.C., Armstrong, G.S., Jones, D.N., Eisenmesser, E.Z. & Liu, C.W. Residue histidine 50 plays a key role in protecting α-synuclein from aggregation at physiological pH. *J Biol Chem* 289, 15474-15481 (2014).

Chiang, H.L., Terlecky, S.R., Plant, C.P. & Dice, J.F. A role for a 70-kilodalton heat shock protein in lysosomal degradation of intracellular proteins. *Science* 246, 382-385 (1989).

Chinta, S.J., Mallajosyula, J.K., Rane, A. & Andersen, J.K. Mitochondrial α-synuclein accumulation impairs complex I function in dopaminergic neurons and results in increased mitophagy in vivo. *Neurosci Lett* 486, 235-239 (2010).

Choi, B.K., *et al* Large α-synuclein oligomers inhibit neuronal SNARE-mediated vesicle docking. *Proc Natl Acad Sci U S A* 110, 4087-4092 (2013).

Choubey, V., *et al* Mutant A53T alpha-synuclein induces neuronal death by increasing mitochondrial autophagy. *J Biol Chem* 286, 10814-10824 (2011).

Christie, K.R., Hong, E.L. & Cherry, J.M. Functional annotations for the Saccharomyces cerevisiae genome: the knowns and the known unknowns. *Trends Microbiol* 17, 286-294 (2009).

Chu, C.T. Diversity in the regulation of autophagy and mitophagy: lessons from Parkinson's disease. *Parkinsons Dis* 2011, 789431 (2011).

Ciechanover, A. & Brundin, P. The ubiquitin proteasome system in neurodegenerative diseases: sometimes the chicken, sometimes the egg. *Neuron* 40, 427-446 (2003).

Cieri, D., Brini, M. & Calì, T. Emerging (and converging) pathways in Parkinson's disease: keeping mitochondrial wellness. *Biochem Biophys Res Commun* (2016).

Colla, E., *et al* Accumulation of toxic α-synuclein oligomer within endoplasmic reticulum

occurs in α-synucleinopathy in vivo. *J Neurosci* 32, 3301-3305 (2012).

Conway, K.A., Harper, J.D. & Lansbury, P.T. Accelerated in vitro fibril formation by a mutant alpha-synuclein linked to early-onset Parkinson disease. *Nat Med* 4, 1318-1320 (1998).

Conway, K.A., *et al* Accelerated oligomerization by Parkinson's disease linked alpha-synuclein mutants. *Ann N Y Acad Sci* 920, 42-45 (2000).

Cook, C., Stetler, C. & Petrucelli, L. Disruption of protein quality control in Parkinson's disease. *Cold Spring Harb Perspect Med* 2, a009423 (2012).

Cookson, M.R. The biochemistry of Parkinson's disease. *Annu Rev Biochem* 74, 29-52 (2005).

Cooper, A.A., *et al* Alpha-synuclein blocks ER-Golgi traffic and Rab1 rescues neuron loss in Parkinson's models. *Science* 313, 324-328 (2006).

Corti, O., Lesage, S. & Brice, A. What genetics tells us about the causes and mechanisms of Parkinson's disease. *Physiol Rev* 91, 1161-1218 (2011).

Costanzo, M. & Zurzolo, C. The cell biology of prion-like spread of protein aggregates: mechanisms and implication in neurodegeneration. *Biochem J* 452, 1-17 (2013).

Crews, L., *et al* Selective molecular alterations in the autophagy pathway in patients with Lewy body disease and in models of alpha-synucleinopathy. *PLoS One* 5, e9313 (2010).

Cuervo, A.M. & Dice, J.F. A receptor for the selective uptake and degradation of proteins by lysosomes. *Science* 273, 501-503 (1996).

Cuervo, A.M. & Dice, J.F. Age-related decline in chaperone-mediated autophagy. *J Biol Chem* 275, 31505-31513 (2000).

Cuervo, A.M., Stefanis, L., Fredenburg, R., Lansbury, P.T. & Sulzer, D. Impaired degradation of mutant alpha-synuclein by chaperone-mediated autophagy. *Science* 305, 1292-1295 (2004).

Cummings, C.J., *et al* Chaperone suppression of aggregation and altered subcellular proteasome localization imply protein misfolding in SCA1. *Nat Genet* 19, 148-154 (1998).

Dantuma, N.P., & Bott, L.C., The ubiquitin-proteasome system in neurodegenerative diseases: precipitating factor, yet part of the solution., *Front Mol Neurosci*. 7(70), 1-18 (2014)

Dantuma, N.P., Lindsten, K., Glas, R., Jellne, M. & Masucci, M.G. Short-lived green fluorescent proteins for quantifying ubiquitin/proteasome-dependent proteolysis in living cells. *Nat Biotechnol* 18, 538-543 (2000).

Danzer, K.M., *et al* Exosomal cell-to-cell transmission of alpha synuclein oligomers. *Mol Neurodegener* 7, 42 (2012).

Dauer, W. & Przedborski, S. Parkinson's disease: mechanisms and models. *Neuron* 39, 889-909 (2003).

de Lau, L.M. & Breteler, M.M. Epidemiology of Parkinson's disease. *Lancet Neurol* 5, 525-535 (2006).

Desplats, P., *et al* Inclusion formation and neuronal cell death through neuron-to-neuron transmission of alpha-synuclein. *Proc Natl Acad Sci U S A* 106, 13010-13015 (2009).

Devi, L., Raghavendran, V., Prabhu, B.M., Avadhani, N.G. & Anandatheerthavarada, H.K. Mitochondrial import and accumulation of alpha-synuclein impair complex I in human dopaminergic neuronal cultures and Parkinson disease brain. *J Biol Chem* 283, 9089-9100 (2008).

Di Maio, R., *et al* α-Synuclein binds to TOM20 and inhibits mitochondrial protein import in Parkinson's disease. *Sci Transl Med* 8, 342ra378 (2016).

Dice, J.F. Peptide sequences that target cytosolic proteins for lysosomal proteolysis. *Trends Biochem Sci* 15, 305-309 (1990).

Dorval, V. & Fraser, P.E. Small ubiquitin-like modifier (SUMO) modification of natively unfolded proteins tau and alpha-synuclein. *J Biol Chem* 281, 9919-9924 (2006).

Doyle, K.M., *et al* Unfolded proteins and endoplasmic reticulum stress in neurodegenerative disorders. *J Cell Mol Med* 15, 2025-2039 (2011).

Ebrahimi-Fakhari, D., *et al* Distinct roles in vivo for the ubiquitin-proteasome system and the autophagy-lysosomal pathway in the degradation of α-synuclein. *J Neurosci* 31, 14508-14520 (2011).

Edwards, T.L., *et al* Genome-wide association study confirms SNPs in SNCA and the MAPT region as common risk factors for Parkinson disease. *Ann Hum Genet* 74, 97-109 (2010).

El-Agnaf, O.M., *et al* Aggregates from mutant and wild-type alpha-synuclein proteins and NAC peptide induce apoptotic cell death in human neuroblastoma cells by formation of beta-sheet and amyloid-like filaments. *FEBS Lett* 440, 71-75 (1998a).

El-Agnaf, O.M., Jakes, R., Curran, M.D. & Wallace, A. Effects of the mutations Ala30 to Pro and Ala53 to Thr on the physical and morphological properties of alpha-synuclein protein implicated in Parkinson's disease. *FEBS Lett* 440, 67-70 (1998b).

Elbaz, A. & Moisan, F. Update in the epidemiology of Parkinson's disease. *Curr Opin Neurol* 21, 454-460 (2008).

Emamzadeh, F.N. Alpha-synuclein structure, functions, and interactions. *J Res Med Sci* 21, 29 (2016).

Emanuele, M. & Chieregatti, E. Mechanisms of alpha-synuclein action on neurotransmission: cell-autonomous and non-cell autonomous role. *Biomolecules* 5, 865-892 (2015).

Escobar, V.D., Kuo, Y.M., Orrison, B.M., Giasson, B.I. & Nussbaum, R.L. Transgenic mice expressing S129 phosphorylation mutations in α-synuclein. *Neurosci Lett* 563, 96-100 (2014).

Eskelinen, E.L., *et al* Unifying nomenclature for the isoforms of the lysosomal membrane protein LAMP-2. *Traffic* 6, 1058-1061 (2005).

Fares, M.B., *et al* The novel Parkinson's disease linked mutation G51D attenuates in vitro aggregation and membrane binding of α-synuclein, and enhances its secretion and nuclear localization in cells. *Hum Mol Genet* 23, 4491-4509 (2014).

Feany, M.B. & Bender, W.W. A Drosophila model of Parkinson's disease. *Nature* 404, 394-398 (2000).

Febbraro, F., *et al* Ser129D mutant alpha-synuclein induces earlier motor dysfunction while S129A results in distinctive pathology in a rat model of Parkinson's disease. *Neurobiol Dis* 56, 47-58 (2013).

Feng, Y., Jankovic, J. & Wu, Y.C. Epigenetic mechanisms in Parkinson's disease. *J Neurol Sci* 349, 3-9 (2015).

Fleming, J., Outeiro, T.F., Slack, M., Lindquist, S.L. & Bulawa, C.E. Detection of compounds that rescue Rab1-synuclein toxicity. *Methods Enzymol* 439, 339-351 (2008).

Flower, T.R., Chesnokova, L.S., Froelich, C.A., Dixon, C. & Witt, S.N. Heat shock prevents alpha-synuclein-induced apoptosis in a yeast model of Parkinson's disease. *J Mol Biol* 351, 1081-1100 (2005).

Franco-Iborra, S., Vila, M. & Perier, C. The Parkinson Disease Mitochondrial Hypothesis: Where Are We at? *Neuroscientist* 22, 266-277 (2016).

Fu, H., Subramanian, R.R. & Masters, S.C. 14-3-3 proteins: structure, function, and regulation. *Annu Rev Pharmacol Toxicol* 40, 617-647 (2000).

Fuchs, J., *et al* Phenotypic variation in a large Swedish pedigree due to SNCA duplication and triplication. *Neurology* 68, 916-922 (2007).

Fuchs, J., *et al* Genetic variability in the SNCA gene influences alpha-synuclein levels in the blood and brain. *FASEB J* 22, 1327-1334 (2008).

Fujioka, S., *et al* Update on novel familial forms of Parkinson's disease and multiple system atrophy. *Parkinsonism Relat Disord* 20 Suppl 1, S29-34 (2014).

Fujita, N., *et al* The Atg16L complex specifies the site of LC3 lipidation for membrane biogenesis in autophagy. *Mol Biol Cell* 19, 2092-2100 (2008).

Fujiwara, H., *et al* alpha-Synuclein is phosphorylated in synucleinopathy lesions. *Nat Cell Biol* 4, 160-164 (2002).

Gasser, T. Mendelian forms of Parkinson's disease. *Biochim Biophys Acta* 1792, 587-596 (2010).

Geng, X., *et al* α-Synuclein binds the K(ATP) channel at insulin-secretory granules and inhibits insulin secretion. *Am J Physiol Endocrinol Metab* 300, E276-286 (2011).

Ghosh, D., *et al* The Parkinson's disease-associated H50Q mutation accelerates α-Synuclein aggregation in vitro. *Biochemistry* 52, 6925-6927 (2013).

Ghosh, D., *et al* The newly discovered Parkinson's disease associated Finnish mutation (A53E) attenuates α-synuclein aggregation and membrane binding. *Biochemistry* 53, 6419-6421 (2014).

Giasson, B.I., *et al* Oxidative damage linked to neurodegeneration by selective alpha-synuclein nitration in synucleinopathy lesions. *Science* 290, 985-989 (2000).

Giasson, B.I., Murray, I.V., Trojanowski, J.Q. & Lee, V.M. A hydrophobic stretch of 12 amino acid residues in the middle of alpha-synuclein is essential for filament assembly. *J Biol Chem* 276, 2380-2386 (2001).

Gitler, A.D. Beer and bread to brains and beyond: can yeast cells teach us about neurodegenerative disease? *Neurosignals* 16, 52-62 (2008).

Gitler, A.D., *et al* Alpha-synuclein is part of a diverse and highly conserved interaction network that includes PARK9 and manganese toxicity. *Nat Genet* 41, 308-315 (2009).

Goers, J., *et al* Nuclear localization of alpha-synuclein and its interaction with histones. *Biochemistry* 42, 8465-8471 (2003).

Goffeau, A., *et al* Life with 6000 genes. *Science* 274, 546, 563-547 (1996).

Gonçalves, S. & Outeiro, T.F. Assessing the subcellular dynamics of alpha-synuclein using photoactivation microscopy. *Mol Neurobiol* 47, 1081-1092 (2013).

Gorbatyuk, O.S., *et al* The phosphorylation state of Ser-129 in human alpha-synuclein

determines neurodegeneration in a rat model of Parkinson disease. *Proc Natl Acad Sci U S A* 105, 763-768 (2008).

Griffioen, G., *et al* A yeast-based model of alpha-synucleinopathy identifies compounds with therapeutic potential. *Biochim Biophys Acta* 1762, 312-318 (2006).

Guardia-Laguarta, C., *et al* α-Synuclein is localized to mitochondria-associated ER membranes. *J Neurosci* 34, 249-259 (2014).

Gui, Y.X., *et al* Extracellular signal-regulated kinase is involved in alpha-synuclein-induced mitochondrial dynamic disorders by regulating dynamin-like protein 1. *Neurobiol Aging* 33, 2841-2854 (2012).

Gupta, V.B., Hegde, M.L. & Rao, K.S. Role of protein conformational dynamics and DNA integrity in relevance to neuronal cell death in neurodegeneration. *Curr Alzheimer Res* 3, 297-309 (2006).

Hansen, C., *et al* α-Synuclein propagates from mouse brain to grafted dopaminergic neurons and seeds aggregation in cultured human cells. *J Clin Invest* 121, 715-725 (2011).

Harding, T.M., Morano, K.A., Scott, S.V. & Klionsky, D.J. Isolation and characterization of yeast mutants in the cytoplasm to vacuole protein targeting pathway. *J Cell Biol* 131, 591-602 (1995).

Hashimoto, M., *et al* alpha-Synuclein protects against oxidative stress via inactivation of the c-Jun N-terminal kinase stress-signaling pathway in neuronal cells. *J Biol Chem* 277, 11465-11472 (2002).

Hayashi, T., Rizzuto, R., Hajnoczky, G. & Su, T.P. MAM: more than just a housekeeper. *Trends Cell Biol* 19, 81-88 (2009).

Hegde, M.L. & Jagannatha Rao, K.S. Challenges and complexities of alpha-synuclein toxicity: new postulates in unfolding the mystery associated with Parkinson's disease. *Arch Biochem Biophys* 418, 169-178 (2003).

Hegde, M.L., Vasudevaraju, P. & Rao, K.J. DNA induced folding/fibrillation of alpha-synuclein: new insights in Parkinson's disease. *Front Biosci (Landmark Ed)* 15, 418-436 (2010).

Hershko, A. & Ciechanover, A. The ubiquitin system. *Annu Rev Biochem* 67, 425-479 (1998).

Hindle, J.V. Ageing, neurodegeneration and Parkinson's disease. *Age Ageing* 39, 156-161 (2010).

Hofer, A. & Gasser, T. New aspects of genetic contributions to Parkinson's disease. *J Mol Neurosci* 24, 417-424 (2004).

Högen, T., *et al* Two different binding modes of α-synuclein to lipid vesicles depending on its aggregation state. *Biophys J* 102, 1646-1655 (2012).

Huang, W.P., Scott, S.V., Kim, J. & Klionsky, D.J. The itinerary of a vesicle component, Aut7p/Cvt5p, terminates in the yeast vacuole via the autophagy/Cvt pathways. *J Biol Chem* 275, 5845-5851 (2000).

Huang, Y., Cheung, L., Rowe, D. & Halliday, G. Genetic contributions to Parkinson's disease. *Brain Res Brain Res Rev* 46, 44-70 (2004).

Hughes, R.E., *et al* Altered transcription in yeast expressing expanded polyglutamine. *Proc Natl Acad Sci U S A* 98, 13201-13206 (2001).

Ibanez, P., *et al* Alpha-synuclein gene rearrangements in dominantly inherited parkinsonism:

frequency, phenotype, and mechanisms. *Arch Neurol* 66, 102-108 (2009).

Ikeuchi, T., *et al* Patients homozygous and heterozygous for SNCA duplication in a family with parkinsonism and dementia. *Arch Neurol* 65, 514-519 (2008).

Jakes, R., Spillantini, M.G. & Goedert, M. Identification of two distinct synucleins from human brain. *FEBS Lett* 345, 27-32 (1994).

Jang, A., *et al* Non-classical exocytosis of alpha-synuclein is sensitive to folding states and promoted under stress conditions. *J Neurochem* 113, 1263-1274 (2010).

Jensen, M.B., *et al* Membrane curvature sensing by amphipathic helices: a single liposome study using α-synuclein and annexin B12. *J Biol Chem* 286, 42603-42614 (2011).

Jensen, P.H., Nielsen, M.S., Jakes, R., Dotti, C.G. & Goedert, M. Binding of alpha-synuclein to brain vesicles is abolished by familial Parkinson's disease mutation. *J Biol Chem* 273, 26292-26294 (1998).

Jiang, M., *et al* Baicalein reduces E46K alpha-synuclein aggregation in vitro and protects cells against E46K alpha-synuclein toxicity in cell models of familiar Parkinsonism. *J Neurochem* 114, 419-429 (2010).

Jin, H., *et al* α-Synuclein negatively regulates protein kinase Cδ expression to suppress apoptosis in dopaminergic neurons by reducing p300 histone acetyltransferase activity. *J Neurosci* 31, 2035-2051 (2011).

Kabeya, Y., *et al* LC3, a mammalian homologue of yeast Apg8p, is localized in autophagosome membranes after processing. *EMBO J* 19, 5720-5728 (2000).

Kamp, F., *et al* Inhibition of mitochondrial fusion by α-synuclein is rescued by PINK1, Parkin and DJ-1. *EMBO J* 29, 3571-3589 (2010).

Karpinar, D.P., *et al* Pre-fibrillar alpha-synuclein variants with impaired beta-structure increase neurotoxicity in Parkinson's disease models. *EMBO J* 28, 3256-3268 (2009).

Keyser, R.J., Lombard, D., Veikondis, R., Carr, J. & Bardien, S. Analysis of exon dosage using MLPA in South African Parkinson's disease patients. *Neurogenetics* 11, 305-312 (2010).

Khalaf, O., *et al* The H50Q mutation enhances α-synuclein aggregation, secretion, and toxicity. *J Biol Chem* 289, 21856-21876 (2014).

Kiely, A.P., *et al* α-Synucleinopathy associated with G51D SNCA mutation: a link between Parkinson's disease and multiple system atrophy? *Acta Neuropathol* 125, 753-769 (2013).

Kim, E.J., *et al* Dyrk1A phosphorylates alpha-synuclein and enhances intracellular inclusion formation. *J Biol Chem* 281, 33250-33257 (2006).

Kim, T.D., Choi, E., Rhim, H., Paik, S.R. & Yang, C.H. Alpha-synuclein has structural and functional similarities to small heat shock proteins. *Biochem Biophys Res Commun* 324, 1352-1359 (2004).

Kim, W.S., Kågedal, K. & Halliday, G.M. Alpha-synuclein biology in Lewy body diseases. *Alzheimers Res Ther* 6, 73 (2014).

Kleiger, G. & Mayor, T. Perilous journey: a tour of the ubiquitin-proteasome system. *Trends Cell Biol* 24, 352-359 (2014).

Klein, C. & Westenberger, A. Genetics of Parkinson's disease. *Cold Spring Harb Perspect Med* 2, 2:a008888 (2012)

Klionsky, D.J., Abdalla, F.C., Abeliovich, H., Abraham, R.T. & Acevedo-Arozena, A., *et al* Guidelines for the use and interpretation of assays for monitoring autophagy. *Autophagy* 8, 445–544 (2012).

Klionsky, D.J., *et al* A unified nomenclature for yeast autophagy-related genes. *Dev Cell* 5, 539-545 (2003).

Komander, D. & Rape, M. The ubiquitin code. *Annu Rev Biochem* 81, 203-229 (2012).

Kontopoulos, E., Parvin, J.D. & Feany, M.B. Alpha-synuclein acts in the nucleus to inhibit histone acetylation and promote neurotoxicity. *Hum Mol Genet* 15, 3012-3023 (2006).

Kraft, C. & Martens, S. Mechanisms and regulation of autophagosome formation. *Curr Opin Cell Biol* 24, 496-501 (2012).

Kraft, C., Peter, M. & Hofmann, K. Selective autophagy: ubiquitin-mediated recognition and beyond. *Nat Cell Biol* 12, 836-841 (2010).

Kragh, C.L., Ubhi, K., Wyss-Coray, T., Wyss-Corey, T. & Masliah, E. Autophagy in dementias. *Brain Pathol* 22, 99-109 (2012).

Kraytsberg, Y., *et al* Mitochondrial DNA deletions are abundant and cause functional impairment in aged human substantia nigra neurons. *Nat Genet* 38, 518-520 (2006).

Kruger, R., *et al* Ala30Pro mutation in the gene encoding alpha-synuclein in Parkinson's disease. *Nat Genet* 18, 106-108 (2001).

Kuwahara, T., Tonegawa, R., Ito, G., Mitani, S. & Iwatsubo, T. Phosphorylation of α-synuclein protein at Ser-129 reduces neuronal dysfunction by lowering its membrane binding property in Caenorhabditis elegans. *J Biol Chem* 287, 7098-7109 (2012).

Lakso, M., *et al* Dopaminergic neuronal loss and motor deficits in Caenorhabditis elegans overexpressing human alpha-synuclein. *J Neurochem* 86, 165-172 (2003).

Lang, T., *et al* Aut2p and Aut7p, two novel microtubule-associated proteins are essential for delivery of autophagic vesicles to the vacuole. *EMBO J* 17, 3597-3607 (1998).

Lashuel, H.A., Overk, C.R., Oueslati, A. & Masliah, E. The many faces of α-synuclein: from structure and toxicity to therapeutic target. *Nat Rev Neurosci* 14, 38-48 (2013).

Latchoumycandane, C., *et al* Protein kinase Cdelta is a key downstream mediator of manganese-induced apoptosis in dopaminergic neuronal cells. *J Pharmacol Exp Ther* 313, 46-55 (2005).

Lavedan, C. The synuclein family. *Genome Res* 8, 871-880 (1998).

Lázaro, D.F., *et al* The effects of the novel A53E alpha-synuclein mutation on its oligomerization and aggregation, *Acta Neuropathol Comm* 4, 128 (2016)

Lázaro, D.F., *et al* Systematic comparison of the effects of alpha-synuclein mutations on its oligomerization and aggregation. *PLoS Genet* 10, e1004741 (2014).

Lee, H.J., Khoshaghideh, F., Patel, S. & Lee, S.J. Clearance of alpha-synuclein oligomeric intermediates via the lysosomal degradation pathway. *J Neurosci* 24, 1888-1896 (2004).

Lee, J.W., Kim, W.H., Yeo, J. & Jung, M.H. ER stress is implicated in mitochondrial dysfunction-induced apoptosis of pancreatic beta cells. *Mol Cells* 30, 545-549 (2010).

Lee, V.M. & Trojanowski, J.Q. Mechanisms of Parkinson's disease linked to pathological alpha-synuclein: new targets for drug discovery. *Neuron* 52, 33-38 (2006).

Lees, A.J., Hardy, J. & Revesz, T. Parkinson's disease. *Lancet* 373, 2055-2066 (2009).

Leger, J., Kempf, M., Lee, G. & Brandt, R. Conversion of serine to aspartate imitates phosphorylation-induced changes in the structure and function of microtubule-associated protein tau. *J Biol Chem* 272, 8441-8446 (1997).

Lesage, S., *et al* G51D α-synuclein mutation causes a novel parkinsonian-pyramidal syndrome. *Ann Neurol* 73, 459-471 (2013).

Li, W., *et al* Aggregation promoting C-terminal truncation of alpha-synuclein is a normal cellular process and is enhanced by the familial Parkinson's disease-linked mutations. *Proc Natl Acad Sci U S A* 102, 2162-2167 (2005).

Li, X., *et al* Generation of destabilized green fluorescent protein as a transcription reporter. *J Biol Chem* 273, 34970-34975 (1998).

Lim, J.H., Lee, H.J., Ho Jung, M. & Song, J. Coupling mitochondrial dysfunction to endoplasmic reticulum stress response: a molecular mechanism leading to hepatic insulin resistance. *Cell Signal* 21, 169-177 (2009).

Lin, M.T. & Beal, M.F. Mitochondrial dysfunction and oxidative stress in neurodegenerative diseases. *Nature* 443, 787-795 (2006).

Lindholm, D., Wootz, H. & Korhonen, L. ER stress and neurodegenerative diseases. *Cell Death Differ* 13, 385-392 (2002).

Liu, C.W.; Corboy, M.J.; DeMartino, G.N. & Thomas, P.J. Endoproteolytic activity of the proteasome. *Science* 87, 299, 408–411. 87 (2003).

Lopes da Fonseca, T., Villar-Pique, A. & Outeiro, T.F. The Interplay between Alpha-Synuclein Clearance and Spreading. *Biomolecules* 5, 435-471 (2015).

Luk, K.C., *et al* Pathological α-synuclein transmission initiates Parkinson-like neurodegeneration in nontransgenic mice. *Science* 338, 949-953 (2012).

Mahul-Mellier, A.L., *et al* c-Abl phosphorylates α-synuclein and regulates its degradation: implication for α-synuclein clearance and contribution to the pathogenesis of Parkinson's disease. *Hum Mol Genet* 23, 2858-2879 (2014).

Maraganore, D.M., *et al* Collaborative analysis of alpha-synuclein gene promoter variability and Parkinson disease. *JAMA* 296, 661-670 (2006).

Maroteaux, L., Campanelli, J.T. & Scheller, R.H. Synuclein: a neuron-specific protein localized to the nucleus and presynaptic nerve terminal. *J Neurosci* 8, 2804-2815 (1988).

Marques, S.C., Oliveira, C.R., Pereira, C.M. & Outeiro, T.F. Epigenetics in neurodegeneration: a new layer of complexity. *Prog Neuropsychopharmacol Biol Psychiatry* 35, 348-355 (2011).

Marsh, J.A., Singh, V.K., Jia, Z. & Forman-Kay, J.D. Sensitivity of secondary structure propensities to sequence differences between alpha- and gamma-synuclein: implications for fibrillation. *Protein Sci* 15, 2795-2804 (2006).

Martin, L.J., *et al* Parkinson's disease alpha-synuclein transgenic mice develop neuronal mitochondrial degeneration and cell death. *J Neurosci* 26, 41-50 (2006).

Martinez, J., Moeller, I., Erdjument-Bromage, H., Tempst, P. & Lauring, B. Parkinson's disease-associated alpha-synuclein is a calmodulin substrate. *J Biol Chem* 278, 17379-17387 (2003).

Martinez-Vicente, M., *et al* Dopamine-modified alpha-synuclein blocks chaperone-mediated autophagy. *J Clin Invest* 118, 777-788 (2008).

Masliah, E., *et al* Dopaminergic loss and inclusion body formation in alpha-synuclein mice: implications for neurodegenerative disorders. *Science* 287, 1265-1269 (2000).

Mayer, R.J., *et al* Intermediate filament-ubiquitin diseases: implications for cell sanitization. *Biochem Soc Symp* 55, 193-201 (1989).

Mbefo, M.K., *et al* Parkinson disease mutant E46K enhances α-synuclein phosphorylation in mammalian cell lines, in yeast, and in vivo. *J Biol Chem* 290, 9412-9427 (2015).

McCormack, A.L., Mak, S.K. & Di Monte, D.A. Increased α-synuclein phosphorylation and nitration in the aging primate substantia nigra. *Cell Death Dis* 3, e315 (2012).

McFarland, N.R., *et al* Alpha-synuclein S129 phosphorylation mutants do not alter nigrostriatal toxicity in a rat model of Parkinson disease. *J Neuropathol Exp Neurol* 68, 515-524 (2009).

McLean, P.J., Kawamata, H., Ribich, S. & Hyman, B.T. Membrane association and protein conformation of alpha-synuclein in intact neurons. Effect of Parkinson's disease-linked mutations. *J Biol Chem* 275, 8812-8816 (2000a).

McLean, P.J., Ribich, S. & Hyman, B.T. Subcellular localization of alpha-synuclein in primary neuronal cultures: effect of missense mutations. *J Neural Transm Suppl*, 53-63 (2000b).

Menezes, R., *et al*, From the baker to the bedside: yeast models of Parkinson's disease, *Microbial Cell* 2(8), 262-279 (2015).

Middleton, E.R. & Rhoades, E. Effects of curvature and composition on α-synuclein binding to lipid vesicles. *Biophys J* 99, 2279-2288 (2010).

Mizushima, N. & Klionsky, D.J. Protein turnover via autophagy: implications for metabolism. *Annu Rev Nutr* 27, 19-40 (2007).

Mizushima, N., Noda, T. & Ohsumi, Y. Apg16p is required for the function of the Apg12p-Apg5p conjugate in the yeast autophagy pathway. *EMBO J* 18, 3888-3896 (1999).

Mizushima, N., *et al* A protein conjugation system essential for autophagy. *Nature* 395, 395-398 (1998).

Mizuta, I., *et al* Multiple candidate gene analysis identifies alpha-synuclein as a susceptibility gene for sporadic Parkinson's disease. *Hum Mol Genet* 15, 1151-1158 (2006).

Mori, F., Tanji, K., Yoshimoto, M., Takahashi, H. & Wakabayashi, K. Immunohistochemical comparison of alpha- and beta-synuclein in adult rat central nervous system. *Brain Res* 941, 118-126 (2002).

Mumberg, D., Müller R & Funk, M., Yeast vectors for the controlled expression of heterologous proteins in different genetic backgrounds. *Gene* 156(1),119-22 (1995).

Muntane, G., Dalfo, E., Martinez, A. & Ferrer, I. Phosphorylation of tau and alpha-synuclein in synaptic-enriched fractions of the frontal cortex in Alzheimer's disease, and in Parkinson's disease and related alpha-synucleinopathies. *Neuroscience* 152, 913-923 (2008).

Nakamura, K., *et al* Direct membrane association drives mitochondrial fission by the Parkinson

disease-associated protein alpha-synuclein. *J Biol Chem* 286, 20710-20726 (2011).

Nakamura, T., Yamashita, H., Takahashi, T. & Nakamura, S. Activated Fyn phosphorylates alpha-synuclein at tyrosine residue 125. *Biochem Biophys Res Commun* 280, 1085-1092 (2001).

Neefjes, J. & Dantuma, N.P. Fluorescent probes for proteolysis: tools for drug discovery. *Nat Rev Drug Discov* 3, 58-69 (2004).

Noda, T., Suzuki, K. & Ohsumi, Y. Yeast autophagosomes: de novo formation of a membrane structure. *Trends Cell Biol* 12, 231-235 (2002).

Nubling, G.S., *et al* Modelling Ser129 phosphorylation inhibits membrane binding of pore-forming alpha-synuclein oligomers. *PLoS One* 9, e98906 (2014).

Nussbaum, R.L. & Ellis, C.E. Alzheimer's disease and Parkinson's disease. *N Engl J Med* 348, 1356-1364 (2003).

O'Donnell, K.C., *et al* Axon degeneration and PGC-1α-mediated protection in a zebrafish model of α-synuclein toxicity. *Dis Model Mech* 7, 571-582 (2014).

Okochi, M., *et al* Constitutive phosphorylation of the Parkinson's disease associated alpha-synuclein. *J Biol Chem* 275, 390-397 (2000).

Orsi, A., *et al* Dynamic and transient interactions of Atg9 with autophagosomes, but not membrane integration, are required for autophagy. *Mol Biol Cell* 23, 1860-1873 (2012).

Ostrerova, N., *et al* alpha-Synuclein shares physical and functional homology with 14-3-3 proteins. *J Neurosci* 19, 5782-5791 (1999).

Otomo, C., Metlagel, Z., Takaesu, G. & Otomo, T. Structure of the human ATG12~ATG5 conjugate required for LC3 lipidation in autophagy. *Nat Struct Mol Biol* 20, 59-66 (2013).

Oueslati, A., Fournier, M. & Lashuel, H.A. Role of post-translational modifications in modulating the structure, function and toxicity of alpha-synuclein: implications for Parkinson's disease pathogenesis and therapies. *Prog Brain Res* 183, 115-145 (2010).

Outeiro, T.F., *et al* Small heat shock proteins protect against alpha-synuclein-induced toxicity and aggregation. *Biochem Biophys Res Commun* 351, 631-638 (2006).

Outeiro, T.F. & Lindquist, S. Yeast cells provide insight into alpha-synuclein biology and pathobiology. *Science* 302, 1772-1775 (2003).

Padmaraju, V., Bhaskar, J.J., Prasada Rao, U.J., Salimath, P.V. & Rao, K.S. Role of advanced glycation on aggregation and DNA binding properties of α-synuclein. *J Alzheimers Dis* 24 Suppl 2, 211-221 (2011).

Paleologou, K.E., *et al* Phosphorylation at S87 is enhanced in synucleinopathies, inhibits alpha-synuclein oligomerization, and influences synuclein-membrane interactions. *J Neurosci* 30, 3184-3198 (2010).

Paleologou, K.E., *et al* Phosphorylation at Ser-129 but not the phosphomimics S129E/D inhibits the fibrillation of alpha-synuclein. *J Biol Chem* 283, 16895-16905 (2008).

Park, S.M., *et al* Distinct roles of the N-terminal-binding domain and the C-terminal-solubilizing domain of alpha-synuclein, a molecular chaperone. *J Biol Chem* 277, 28512-28520 (2002).

Pasanen, P., *et al* Novel α-synuclein mutation A53E associated with atypical multiple system atrophy and Parkinson's disease-type pathology. *Neurobiol Aging* 35, 2180.e2181-2185 (2014).

Pasanen, P., *et al* SNCA mutation p.Ala53Glu is derived from a common founder in the Finnish population. *Neurobiol Aging* 50, 168.e165-168.e168 (2017).

Paxinou, E., *et al* Induction of alpha-synuclein aggregation by intracellular nitrative insult. *J Neurosci* 21, 8053-8061 (2001).

Peng, X., *et al* Alpha-synuclein activation of protein phosphatase 2A reduces tyrosine hydroxylase phosphorylation in dopaminergic cells. *J Cell Sci* 118, 3523-3530 (2005).

Perfeito, R., Lázaro, D.F., Outeiro, T.F. & Rego, A.C. Linking alpha-synuclein phosphorylation to reactive oxygen species formation and mitochondrial dysfunction in SH-SY5Y cells. *Mol Cell Neurosci* 62, 51-59 (2014).

Perier, C., *et al* Apoptosis-inducing factor deficiency sensitizes dopaminergic neurons to parkinsonian neurotoxins. *Ann Neurol* 68, 184-192 (2010).

Petroi, D., *et al* Aggregate clearance of α-synuclein in Saccharomyces cerevisiae depends more on autophagosome and vacuole function than on the proteasome. *J Biol Chem* 287, 27567-27579 (2012).

Petrucci, S., Ginevrino, M. & Valente, E.M. Phenotypic spectrum of alpha-synuclein mutations: New insights from patients and cellular models. *Parkinsonism Relat Disord* 22 Suppl 1, S16-20 (2016).

Pickart, C.M. Mechanisms underlying ubiquitination. *Annu Rev Biochem* 70, 503-533 (2001).

Poehler, A.M., *et al* Autophagy modulates SNCA/α-synuclein release, thereby generating a hostile microenvironment. *Autophagy* 10, 2171-2192 (2014).

Polymeropoulos, M.H., *et al* Mutation in the alpha-synuclein gene identified in families with Parkinson's disease. *Science* 276, 2045-2047 (1997).

Porcari, R., *et al* The H50Q mutation induces a 10-fold decrease in the solubility of α-synuclein. *J Biol Chem* 290, 2395-2404 (2015).

Pringsheim, T., Jette, N., Frolkis, A. & Steeves, T.D. The prevalence of Parkinson's disease: a systematic review and meta-analysis. *Mov Disord* 29, 1583-1590 (2014).

Proukakis, C., *et al* A novel α-synuclein missense mutation in Parkinson disease. *Neurology* 80, 1062-1064 (2013).

Puschmann, A. Monogenic Parkinson's disease and parkinsonism: clinical phenotypes and frequencies of known mutations. *Parkinsonism Relat Disord* 19, 407-415 (2013).

Ranjan, P., *et al.* Differential copper binding to alpha-synuclein and its disease-associated mutants affect the aggregation and amyloid formation. *Biochim Biophys Acta* 1861, 365-374 (2016).

Rappold, P.M., *et al* Drp1 inhibition attenuates neurotoxicity and dopamine release deficits in vivo. *Nat Commun* 5, 5244 (2014).

Reeve, A.K., *et al* Aggregated α-synuclein and complex I deficiency: exploration of their relationship in differentiated neurons. *Cell Death Dis* 6, e1820 (2015).

Reggiori, F., Shintani, T., Nair, U. & Klionsky, D.J. Atg9 cycles between mitochondria and the pre-autophagosomal structure in yeasts. *Autophagy* 1, 101-109 (2005).

Reggiori, F., Tucker, K.A., Stromhaug, P.E. & Klionsky, D.J. The Atg1-Atg13 complex regulates Atg9 and Atg23 retrieval transport from the pre-autophagosomal structure. *Dev Cell* 6, 79-90 (2004).

Reits, E., *et al* Peptide diffusion, protection, and degradation in nuclear and cytoplasmic

compartments before antigen presentation by MHC class I. *Immunity* 18, 97-108 (2003).

Rinaldi, T., Dallabona, C., Ferrero, I., Frontali, L. & Bolotin-Fukuhara, M. Mitochondrial diseases and the role of the yeast models. *FEMS Yeast Res* 10, 1006-1022 (2010).

Rodriguez-Araujo, G., *et al* Low alpha-synuclein levels in the blood are associated with insulin resistance. *Sci Rep* 5, 12081 (2015).

Rodriguez-Araujo, G., Nakagami, H., Hayashi, H., Mori, M., Shiuchi, T. & Minokoshi, Y., *et al*, Alpha-synuclein elicits glucose uptake and utilization in adipocytes through the Gab1/PI3K/Akt transduction pathway, *Cell Mol Life Sci* 70, 1123-1133 (2013).

Romanov, J., *et al* Mechanism and functions of membrane binding by the Atg5-Atg12/Atg16 complex during autophagosome formation. *EMBO J* 31, 4304-4317 (2009).

Ross, O.A., *et al* Genomic investigation of alpha-synuclein multiplication and parkinsonism. *Ann Neurol* 63, 743-750 (2008).

Ruipérez, V., Darios, F. & Davletov, B. Alpha-synuclein, lipids and Parkinson's disease. *Prog Lipid Res* 49, 420-428 (2010).

Rutherford, N.J. & Giasson, B.I. The A53E α-synuclein pathological mutation demonstrates reduced aggregation propensity in vitro and in cell culture. *Neurosci Lett* 597, 43-48 (2015).

Rutherford, N.J., Moore, B.D., Golde, T.E. & Giasson, B.I. Divergent effects of the H50Q and G51D SNCA mutations on the aggregation of α-synuclein. *J Neurochem* 131, 859-867 (2014).

Ryu, E.J., *et al* Endoplasmic reticulum stress and the unfolded protein response in cellular models of Parkinson's disease. *J Neurosci* 22, 10690-10698 (2002).

Saito, Y., *et al* Accumulation of phosphorylated alpha-synuclein in aging human brain. *J Neuropathol Exp Neurol* 62, 644-654 (2003).

Salazar, C. & Hofer, T. Multisite protein phosphorylation--from molecular mechanisms to kinetic models. *FEBS J* 276, 3177-3198 (2009).

Salvador, N., Aguado, C., Horst, M. & Knecht, E. Import of a cytosolic protein into lysosomes by chaperone-mediated autophagy depends on its folding state. *J Biol Chem* 275, 27447-27456 (2000).

Sampaio-Marques, B., *et al* SNCA (α-synuclein)-induced toxicity in yeast cells is dependent on sirtuin 2 (Sir2)-mediated mitophagy. *Autophagy* 8, 1494-1509 (2012).

Sancenon, V., *et al* Suppression of α-synuclein toxicity and vesicle trafficking defects by phosphorylation at S129 in yeast depends on genetic context. *Hum Mol Genet* 21, 2432-2449 (2012).

Satake, W., *et al* Genome-wide association study identifies common variants at four loci as genetic risk factors for Parkinson's disease. *Nat Genet* 41, 1303-1307 (2009).

Schreurs, S., *et al* In vitro phosphorylation does not influence the aggregation kinetics of WT α-synuclein in contrast to its phosphorylation mutants. *Int J Mol Sci* 15, 1040-1067 (2014).

Scott, S.V., *et al* Cytoplasm-to-vacuole targeting and autophagy employ the same machinery to deliver proteins to the yeast vacuole. *Proc Natl Acad Sci U S A* 93, 12304-12308 (1996).

Seidel, K., *et al* First appraisal of brain pathology owing to A30P mutant alpha-synuclein. *Ann Neurol* 67, 684-689 (2010).

Sevlever, D., Jiang, P. & Yen, S.H. Cathepsin D is the main lysosomal enzyme involved in the degradation of alpha-synuclein and generation of its carboxy-terminally truncated species. *Biochemistry*

47, 9678-9687 (2008).

Sharma, N., *et al* alpha-Synuclein budding yeast model: toxicity enhanced by impaired proteasome and oxidative stress. *J Mol Neurosci* 28, 161-178 (2006).

Sharma, S.K., *et al* Insulin-degrading enzyme prevents α-synuclein fibril formation in a nonproteolytical manner. *Sci Rep* 5, 12531 (2015).

Sharon, R., *et al* The formation of highly soluble oligomers of alpha-synuclein is regulated by fatty acids and enhanced in Parkinson's disease. *Neuron* 37, 583-595 (2003).

Shimura, H., *et al*. Ubiquitination of a new form of alpha-synuclein by parkin from human brain: implications for Parkinson's disease. *Science* 293, 263-269 (2001).

Shintani, T.& Klionsky, D.J., Cargo proteins facilitate the formation of transport vesicles in the cytoplasm to vacuole targeting pathway. *J Biol Chem* 279, 29889–29894. (2004).

Simuni, T. & Sethi, K. Nonmotor manifestations of Parkinson's disease. *Ann Neurol* 64 Suppl 2, S65-80 (2008).

Singleton, A.B., *et al* alpha-Synuclein locus triplication causes Parkinson's disease. *Science* 302, 841 (2003).

Smith, W.W., *et al* Alpha-synuclein phosphorylation enhances eosinophilic cytoplasmic inclusion formation in SH-SY5Y cells. *J Neurosci* 25, 5544-5552 (2005).

Snyder, H., *et al* Aggregated and monomeric alpha-synuclein bind to the S6' proteasomal protein and inhibit proteasomal function. *J Biol Chem* 278, 11753-11759 (2003).

Sode, K. *et al*, Effect of reparation of repeat sequences in the human α-synuclein on fibrillation ability, *Bio Sci* 3, 1-7 (2007)

Soper, J.H., *et al* Alpha-synuclein-induced aggregation of cytoplasmic vesicles in Saccharomyces cerevisiae. *Mol Biol Cell* 19, 1093-1103 (2008).

Specht, C.G., *et al* Subcellular localisation of recombinant alpha- and gamma-synuclein. *Mol Cell Neurosci* 28, 326-334 (2005).

Spencer, B., *et al* Beclin 1 gene transfer activates autophagy and ameliorates the neurodegenerative pathology in alpha-synuclein models of Parkinson's and Lewy body diseases. *J Neurosci* 29, 13578-13588 (2009).

Spillantini, M.G., Divane, A. & Goedert, M. Assignment of human alpha-synuclein (SNCA) and beta-synuclein (SNCB) genes to chromosomes 4q21 and 5q35. *Genomics* 27, 379-381 (1995).

Spillantini, M.G., *et al* Alpha-synuclein in Lewy bodies. *Nature* 388, 839-840 (1997).

Stefanis, L., Larsen, K.E., Rideout, H.J., Sulzer, D. & Greene, L.A. Expression of A53T mutant but not wild-type alpha-synuclein in PC12 cells induces alterations of the ubiquitin-dependent degradation system, loss of dopamine release, and autophagic cell death. *J Neurosci* 21, 9549-9560 (2001).

Stefanovic, A.N., Lindhoud, S., Semerdzhiev, S.A., Claessens, M.M. & Subramaniam, V. Oligomers of Parkinson's Disease-Related α-Synuclein Mutants Have Similar Structures but Distinctive Membrane Permeabilization Properties. *Biochemistry* 54, 3142-3150 (2015).

Stichel, C.C., *et al* Mono- and double-mutant mouse models of Parkinson's disease display severe mitochondrial damage. *Hum Mol Genet* 16, 2377-2393 (2007).

Su, L.J., *et al* Compounds from an unbiased chemical screen reverse both ER-to-Golgi trafficking defects and mitochondrial dysfunction in Parkinson's disease models. *Dis Model Mech* 3, 194-208 (2010).

Sugeno, N., *et al* Serine 129 phosphorylation of alpha-synuclein induces unfolded protein response-mediated cell death. *J Biol Chem* 283, 23179-23188 (2008).

Suter, B., Auerbach, D. & Stagljar, I. Yeast-based functional genomics and proteomics technologies: the first 15 years and beyond. *Biotechniques* 40, 625-644 (2006).

Sundal, C., Fujioka, S., Uitti, R.J.& Wszolek, Z.K., Autosomal dominant Parkinson's disease. *Parkinsonism Relat Disord* 18 Suppl 1, S7–10 (2012).

Takahashi, M., *et al* Phosphorylation of alpha-synuclein characteristic of synucleinopathy lesions is recapitulated in alpha-synuclein transgenic Drosophila. *Neurosci Lett* 336, 155-158 (2003).

Takahashi, M., *et al* Oxidative stress-induced phosphorylation, degradation and aggregation of alpha-synuclein are linked to upregulated CK2 and cathepsin D. *Eur J Neurosci* 26, 863-874 (2007).

Tanida, I., *et al* HsAtg4B/HsApg4B/autophagin-1 cleaves the carboxyl termini of three human Atg8 homologues and delipidates microtubule-associated protein light chain 3- and GABAA receptor-associated protein-phospholipid conjugates. *J Biol Chem* 279, 36268-36276 (2004).

Tanida, I., Tanida-Miyake, E., Komatsu, M., Ueno, T. & Kominami, E. Human Apg3p/Aut1p homologue is an authentic E2 enzyme for multiple substrates, GATE-16, GABARAP, and MAP-LC3, and facilitates the conjugation of hApg12p to hApg5p. *J Biol Chem* 277, 13739-13744 (2002).

Tanida, I., Tanida-Miyake, E., Ueno, T. & Kominami, E. The human homolog of Saccharomyces cerevisiae Apg7p is a Protein-activating enzyme for multiple substrates including human Apg12p, GATE-16, GABARAP, and MAP-LC3. *J Biol Chem* 276, 1701-1706 (2001).

Tanik, S.A., Schultheiss, C.E., Volpicelli-Daley, L.A., Brunden, K.R. & Lee, V.M. Lewy body-like α-synuclein aggregates resist degradation and impair macroautophagy. *J Biol Chem* 288, 15194-15210 (2013).

Taschenberger, G., *et al* Aggregation of αSynuclein promotes progressive in vivo neurotoxicity in adult rat dopaminergic neurons. *Acta Neuropathol* 123, 671-683 (2012).

Taymans, J.M. & Baekelandt, V. Phosphatases of α-synuclein, LRRK2, and tau: important players in the phosphorylation-dependent pathology of Parkinsonism. *Front Genet* 5, 382 (2014).

Tenreiro, S., *et al* Phosphorylation modulates clearance of alpha-synuclein inclusions in a yeast model of Parkinson's disease, *PLOS Gen* 10(5), e1004302 (2014a)

Tenreiro, S., Eckermann, K. & Outeiro, T.F. Protein phosphorylation in neurodegeneration: friend or foe? *Front Mol Neurosci* 7, 42 (2014b).

Tenreiro, S., Munder, M.C., Alberti, S. & Outeiro, T.F. Harnessing the power of yeast to unravel the molecular basis of neurodegeneration. *J Neurochem* 127, 438-452 (2013).

Tenreiro, S. & Outeiro, T.F. Simple is good: yeast models of neurodegeneration. *FEMS Yeast Res* 10, 970-979 (2010).

Thomas, B.J., & Rothstein, R, Elevated recombination rates in transcriptionally active DNA. *Cell* 56, 619–630 (1989)

Thumm, M., *et al* Isolation of autophagocytosis mutants of Saccharomyces cerevisiae. *FEBS Lett* 349, 275-280 (1994).

Tobin, J.E., *et al* Haplotypes and gene expression implicate the MAPT region for Parkinson disease: the GenePD Study. *Neurology* 71, 28-34 (2008).

Todorova, A., Jenner, P. & Ray Chaudhuri, K. Non-motor Parkinson's: integral to motor Parkinson's, yet often neglected. *Pract Neurol* 14, 310-322 (2014).

Tofaris, G.K., *et al* Ubiquitin ligase Nedd4 promotes alpha-synuclein degradation by the endosomal-lysosomal pathway. *Proc Natl Acad Sci U S A* 108, 17004-17009 (2011).

Tokui, K., *et al* 17-DMAG ameliorates polyglutamine-mediated motor neuron degeneration through well-preserved proteasome function in an SBMA model mouse. *Hum Mol Genet* 18, 898-910 (2009).

Tsukada, M. & Ohsumi, Y. Isolation and characterization of autophagy-defective mutants of Saccharomyces cerevisiae. *FEBS Lett* 333, 169-174 (1994).

Twig, G. & Shirihai, O.S. The interplay between mitochondrial dynamics and mitophagy. *Antioxid Redox Signal* 14, 1939-1951 (2011).

Ueda, K., *et al* Molecular cloning of cDNA encoding an unrecognized component of amyloid in Alzheimer disease. *Proc Natl Acad Sci U S A* 90, 11282-11286 (1993).

Vargas, K.J., *et al* Synucleins Have Multiple Effects on Presynaptic Architecture. *Cell Rep* 18, 161-173 (2017).

Vasudevaraju, P., *et al* New evidence on α-synuclein and Tau binding to conformation and sequence specific GC* rich DNA: Relevance to neurological disorders. *J Pharm Bioallied Sci* 4, 112-117 (2012).

Vekrellis, K., Xilouri, M., Emmanouilidou, E., Rideout, H.J. & Stefanis, L. Pathological roles of α-synuclein in neurological disorders. *Lancet Neurol* 10, 1015-1025 (2011).

Venda, L.L., Cragg, S.J., Buchman, V.L. & Wade-Martins, R. α-Synuclein and dopamine at the crossroads of Parkinson's disease. *Trends Neurosci* 33, 559-568 (2006).

Villar-Pique, A., *et al.* Environmental and genetic factors support the dissociation between α-synuclein aggregation and toxicity. *Proc Natl Acad Sci U S A* 113, E6506-E6515 (2016).

Visanji, N.P., *et al* Effect of Ser-129 phosphorylation on interaction of α-synuclein with synaptic and cellular membranes. *J Biol Chem* 286, 35863-35873 (2011).

Vogiatzi, T., Xilouri, M., Vekrellis, K. & Stefanis, L. Wild type alpha-synuclein is degraded by chaperone-mediated autophagy and macroautophagy in neuronal cells. *J Biol Chem* 283, 23542-23556 (2008).

Wales, P., Pinho, R., Lázaro, D.F. & Outeiro, T.F. Limelight on alpha-synuclein: pathological and mechanistic implications in neurodegeneration. *J Parkinsons Dis* 3, 415-459 (2013).

Waxman, E.A. & Giasson, B.I. Specificity and regulation of casein kinase-mediated phosphorylation of alpha-synuclein. *J Neuropathol Exp Neurol* 67, 402-416 (2008).

Waxman, E.A. & Giasson, B.I. Characterization of kinases involved in the phosphorylation of aggregated α-synuclein. *J Neurosci Res* 89, 231-247 (2011).

Webb, J.L., Ravikumar, B., Atkins, J., Skepper, J.N. & Rubinsztein, D.C. Alpha-Synuclein is degraded by both autophagy and the proteasome. *J Biol Chem* 278, 25009-25013 (2003).

Weintraub, D., Comella, C.L. & Horn, S. Parkinson's disease--Part 1: Pathophysiology,

symptoms, burden, diagnosis, and assessment. *Am J Manag Care* 14, S40-48 (2008).

Willingham, S., Outeiro, T.F., DeVit, M.J., Lindquist, S.L. & Muchowski, P.J. Yeast genes that enhance the toxicity of a mutant huntingtin fragment or alpha-synuclein. *Science* 302, 1769-1772 (2003).

Winslow, A.R., *et al* α-Synuclein impairs macroautophagy: implications for Parkinson's disease. *J Cell Biol* 190, 1023-1037 (2010).

Witt, S.N. Molecular chaperones, α-synuclein, and neurodegeneration. *Mol Neurobiol* 47, 552-560 (2013).

Witt, S.N. & Flower, T.R. alpha-Synuclein, oxidative stress and apoptosis from the perspective of a yeast model of Parkinson's disease. *FEMS Yeast Res* 6, 1107-1116 (2006).

Wood, S.J., *et al* alpha-synuclein fibrillogenesis is nucleation-dependent. Implications for the pathogenesis of Parkinson's disease. *J Biol Chem* 274, 19509-19512 (1999).

Wu, B., *et al* Phosphorylation of α-synuclein upregulates tyrosine hydroxylase activity in MN9D cells. *Acta Histochem* 113, 32-35 (2011).

Xilouri, M., Vogiatzi, T., Vekrellis, K., Park, D. & Stefanis, L. Abberant alpha-synuclein confers toxicity to neurons in part through inhibition of chaperone-mediated autophagy. *PLoS One* 4, e5515 (2009).

Xu, Y., Deng, Y. & Qing, H. The phosphorylation of α-synuclein: development and implication for the mechanism and therapy of the Parkinson's disease. *J Neurochem* 135, 4-18 (2015).

Yan, J.Q., *et al* Overexpression of human E46K mutant α-synuclein impairs macroautophagy via inactivation of JNK1-Bcl-2 pathway. *Mol Neurobiol* 50, 685-701 (2014).

Yang, F., *et al* Crosstalk between the proteasome system and autophagy in the clearance of α-synuclein. *Acta Pharmacol Sin* 34, 674-680 (2013a).

Yang, W., Wang, X., Duan, C., Lu, L. & Yang, H. Alpha-synuclein overexpression increases phospho-protein phosphatase 2A levels via formation of calmodulin/Src complex. *Neurochem Int* 63, 180-194 (2013b).

Yeger-Lotem, E., *et al* Bridging high-throughput genetic and transcriptional data reveals cellular responses to alpha-synuclein toxicity. *Nat Genet* 41, 316-323 (2009).

Yin, G., *et al* α-Synuclein interacts with the switch region of Rab8a in a Ser129 phosphorylation-dependent manner. *Neurobiol Dis* 70, 149-161 (2014).

Young, A.R., *et al* Starvation and ULK1-dependent cycling of mammalian Atg9 between the TGN and endosomes. *J Cell Sci* 119, 3888-3900 (2006).

Ysselstein, D., *et al* Effects of impaired membrane interactions on α-synuclein aggregation and neurotoxicity. *Neurobiol Dis* 79, 150-163 (2015).

Yu, S., *et al* Extensive nuclear localization of alpha-synuclein in normal rat brain neurons revealed by a novel monoclonal antibody. *Neuroscience* 145, 539-555 (2007).

Zabrocki, P., *et al* Phosphorylation, lipid raft interaction and traffic of alpha-synuclein in a yeast model for Parkinson. *Biochim Biophys Acta* 1783, 1767-1780 (2008).

Zarranz, J.J., *et al* The new mutation, E46K, of alpha-synuclein causes Parkinson and Lewy body dementia. *Ann Neurol* 55, 164-173 (2004).

Zeng, X., Overmeyer, J.H. & Maltese, W.A. Functional specificity of the mammalian Beclin-

Vps34 PI 3-kinase complex in macroautophagy versus endocytosis and lysosomal enzyme trafficking. *J Cell Sci* 119, 259-270 (2006).

Zhou, J., *et al* Changes in the solubility and phosphorylation of α-synuclein over the course of Parkinson's disease. *Acta Neuropathol* 121, 695-704 (2011).

Zhou, W., Hurlbert, M.S., Schaack, J., Prasad, K.N. & Freed, C.R. Overexpression of human alpha-synuclein causes dopamine neuron death in rat primary culture and immortalized mesencephalon-derived cells. *Brain Res* 866, 33-43 (2000).

Zhu, M., Qin, Z.J., Hu, D., Munishkina, L.A. & Fink, A.L. Alpha-synuclein can function as an antioxidant preventing oxidation of unsaturated lipid in vesicles. *Biochemistry* 45, 8135-8142 (2006).

8. Annexes

Table 8.1. List of yeast plasmids used in this study.

Plasmid Type	Yeast Plasmid Designation	Reference
Multicopy (or 2µ)	p426GAL	[Mumberg *et al*, 1995]
	p426GAL_WT_ αSyn-GFP	[Outeiro and Lindquist, 2003]
	p426GAL_A53E_ αSyn-GFP	This study
	p426GAL_S87E_ αSyn-GFP	Host Laboratory
Centromeric	p413GPD_uGFP	Host Laboratory
	p415GAL_ATG8-GFP	Host Laboratory

Table 8.2. List of yeast strains used in this study.

	Yeast Strain Description	References
	Wild-Type Yeast Strains	
W303-1A	MATa; can1-100; his3-11,15; leu2-3,112; trp1-1; ura3-1; ade2-1	[Thomas and Rothstein, 1989]
	Integrative Phosphorylation αSyn Mutations Yeast Strains (Haploid Genomic Double Insertions)	
VSY71	W303-1A trp1-1::pRS304 TRP1+; ura3-1:: pRS306 URA3+	[Sancenon *et al*, 2012]
VSY72	W303-1A trp1-1:: pRS304 GAL1pr-SNCA(WT)-GFP TRP1+; ura3-1:: pRS306 pRS306GAL1pr-SNCA(WT)-GFP::URA3+	[Sancenon *et al*, 2012]
VSY73	W303-1A trp1-1::pRS304 GAL1pr-SNCA(S129A)-GFP TRP1+; ura3-1:: pRS306 GAL1pr-SNCA(S129A)-GFP::URA3+	[Sancenon *et al*, 2012]
VSY74	W303-1A trp1-1:: pRS304 GAL1pr-SNCA(S129D)-GFP TRP1+; ura3-1::pRS306 pRS306GAL1pr-SNCA(S129D)-GFP::URA3+	[Sancenon *et al*, 2012]
SC658	W303-1A trp1-1::pRS304 GAL1pr-SNCA(S87E_S129D)-GFP TRP1+; ura3-1::pRS306 pRS306GAL1pr-SNCA(S87E_S129D)-GFP::URA3+	Host Laboratory
SC663	W303-1A trp1-1::pRS304 GAL1pr-SNCA(S87E)-GFP TRP1+; ura3-1::pRS306 pRS306GAL1pr-SNCA(S87E)-GFP::URA3+	Host Laboratory
SC665	W303-1A trp1-1::pRS304 GAL1pr-SNCA(S87E)-GFP TRP1+; ura3-1::pRS306 pRS306GAL1pr-SNCA(S87E)-GFP::URA3+	Host Laboratory

Table 8.3 List of yeast growth media composition used in this study.

Type of Growth Media	Media Designation	Media Composition
Complete/Enriched	YPD	Glucose 2% (Sigma-Aldrich®, Steinheim, Germany) Peptone 1% (HiMedia®, Lisbon, Portugal) Yeast Extract 2% (HiMedia®, Lisbon, Portugal) Agar 3% (only for solid culture media) (Sigma-Aldrich®, Steinheim, Germany)
	YEP-Raffinose* OR YEP-Galactose**	Raffinose 1%* OR Galactose 1%** (Sigma-Aldrich®, Steinheim, Germany) Yeast extract 1% (HiMedia®, Lisbon, Portugal) Peptone 2% (HiMedia®, Lisbon, Portugal)
Minimum Selective	SC-Glucose* OR SC-Raffinose** OR SC-Galactose***	Glucose 2%* OR Raffinose 1%** OR Galactose 1%*** (Sigma-Aldrich®, Steinheim, Germany) Yeast Nitrogen Base (YNB) without amino acids 0.67% (BD®, MD, USA) Complete Supplement Mixture (CSM) – to complement auxotrophies -TRP (0.074%) OR -URA (0.078%) OR -TRP-URA (0.072%) OR -TRP-URA-LEU (0.062%) OR -TRP-HIS (0.075%) (MP®, CA, USA) Agar 3% (only for solid culture media) (Sigma-Aldrich®, Steinheim, Germany)

(A)

```
CLUSTAL O(1.2.1) multiple sequence alignment

α-Synuclein WT   ATGGATGTATTCATGAAAGGACTTTCAAAGGCCAAGGAGGGAGTTGTGGCTGCTGCTGAG
A53E+P15         ------------------------AAAAGG--AGTAAAGGAATTGTGGCTGCTGCTGAG
                                         .*****  *. .*.***.******************

α-Synuclein WT   AAAACCAAACAGGGTGTGGCAGAAGCAGCAGGAAAGACAAAAGAGGGTGTTCTCTATGTA
A53E+P15         AA-ACCAAACAGGGTGTGGCAGAAGCAGCAGGAAAGACAAAAGAGGGTGTTCTCTATGTA
                 ** ************************************************************

α-Synuclein WT   GGCTCCAAAACCAAGGAGGGAGTGGTGCATGGTGTGGCACAGTGGCTGAGAAGACCAAA
A53E+P15         GGCTCCAAAACCAAGGAGGGAGTGGTGCATGGTGTGGAAACAGTGGCTGAGAAGACCAAA
                 ****************************************.*********************

α-Synuclein WT   GAGCAAGTGACAAATGTTGGAGGAGCAGTGGTGACGGGTGTGACAGCAGTAGCCCAGAAG
A53E+P15         GAGCAAGTGACAAATGTTGGAGGAGCAGTGGTGACGGGTGTGACAGCAGTAGCCCAGAAG
                 ************************************************************

α-Synuclein WT   ACAGTGGAGGGAGCAGGGAGCATTGCAGCAGCCACTGGCTTTGTCAAAAAGGACCAGTTG
A53E+P15         ACAGTGGAGGGAGCAGGGAGCATTGCAGCAGCCACTGGCTTTGTCAAAAAGGACCAGTTG
                 ************************************************************

α-Synuclein WT   GGCAAGAATGAAGAAGGAGCCCCACAGGAAGGAATTCTGGAAGATATGCCTGTGGATCCT
A53E+P15         GGCAAGAATGAAGAAGGAGCCCCACAGGAAGGAATTCTGGAAGATATGCCTGTGGATCCT
                 ************************************************************

α-Synuclein WT   GACAATGAGGCTTATGAAATGCCTTCTGAGGAAGGGTATCAAGACTACGAACCTGAAGCC
A53E+P15         GACAATGAGGCTTATGAAATGCCTTCTGAGGAAGGGTATCAAGACTACGAACCTGAAGCC
                 ************************************************************

α-Synuclein WT   TAA---------------------------------------------------------
A53E+P15         AAGCTTATCGATAGCAAGGGCGAGGAGCTGTTCACCGGGGTGGTGCCCATCCTGGTCGAG
                 :*.

α-Synuclein WT   ------------------------------------------------------------
A53E+P15         CTGGACGGCGACGTAAACGGCCACAAGTTCAGCGTGTCCGGCGAGGGCGAGGGCGATGCC

α-Synuclein WT   ------------------------------------------------------------
A53E+P15         ACCTACGGCAAGCTGACCCTGAAGTTCATCTGCACCACCGGCAAGCTGCCCGTGCCCTGG

α-Synuclein WT   ------------------------------------------------------------
A53E+P15         CCCACCCTCGTGACCACCCTGACCTACGGCGTGCAGTGCTTCAGCCGCTACCCCGACCAC

α-Synuclein WT   ------------------------------------------------------------
A53E+P15         ATGAAGCAGCACGACTTCTTCAAGTCCGCCATGCCCGAAGGCTACGTCCAGGAGCGCACC

α-Synuclein WT   ------------------------------------------------------------
A53E+P15         ATCTTCTTCAAGGACGACGGCAACTACAAGACCCGCGCCGAGGTGAAGTTCGAGGGCGAC

α-Synuclein WT   ------------------------------------------------------------
A53E+P15         ACCCTGGTGAACCGCATCGAGCTGAAGGGCATCGACTTCAAGGAGGACGGCAACATCCTG

α-Synuclein WT   ------------------------------------------------------------
A53E+P15         GGGCACAAGCTGGAGTACAACTACAACAGCCACAACGTCTATATCATGCCCGACAAGCAG

α-Synuclein WT   ------------------------------------------------------------
A53E+P15         AAGAACGGCATCAAGGTGAACTTCAAGATCCGCCACAACATCCAAGGACGGCAGCCGTGC

α-Synuclein WT   ------------------------------------------------------------
A53E+P15         ACCTCGCCCGACCACTACCAGCAGAACACCCCCCATCGGGCGACGGCCCCGTTGCTGCTG

α-Synuclein WT   ------------------------------------------------------------
A53E+P15         GCCCGACAACCCCCTACCTTGAGCACCCAGTCCGGCCCTGAAACAAAAAACCCCCAACG

α-Synuclein WT   ------------------------------------------------------------
A53E+P15         AAGAAACCCCGATTCCCTTGGTCCCTGCTGGGATTTCCGTGACCCGCCGCCCGGGATTCC
```

(B)

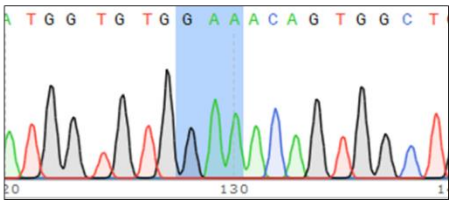

Figure 8.1. Identity confirmation of the multi-copy yeast plasmid encoding for A53E αSyn by DNA sequencing. (A) Results from the DNA sequencing (Sanger sequencing) sequence obtained full aligned with WT αSyn coding gene sequence, using *ClustalOmega* bioinformatics tool. The presence of the desired mutation is highlighted in yellow (substitution of the GCA codon – encoding for the amino acid A – for the GAA codon – encoding for the amino acid E) and (B) Degree of confidence on the presence of the desired amino acid substitution obtained from the DNA sequencing (highlighted in blue).

(A)

```
CLUSTAL O(1.2.1) multiple sequence alignment

α-Synuclein WT      ATGGATGTATTCATGAAAG-GACTTTCAAAGGCCAAGGAGGGAGTTGTGGCTGCTGCTGA
SC_663+P99          NNNGATGGATTCNNGGGAANNANNTTNAAANNCCAAN-NAGNNGGNGTGGCTGCTGNNGA
                     . **** **** .*..*.  * .** ***  ****   .*  * .********** .**

α-Synuclein WT      GAAAACCAAACAGGGTGTGGCAGAAGCAGCAGGAAAGACAAAAGAGGGTGTTCTCTATGT
SC_663+P99          GAAAACCAAACAGGGTGTGGCANAAGCAGCAGGAAAGACAAAAGAGGGTGTTGTNTANNG
                    ********************** ***************************** * **.

α-Synuclein WT      AGGCTCCAAAACCAAGGAGGGAGTGGTGCATGGTGTGGCAACAGTGGCTGAGAAGACCAA
SC_663+P99          GGGCTCCAAAACCAAGGAGGGAGTGGTNCAGGGTGTGGCAACAGTGGCTGAGAAGACCAA
                    .************************** ** ****************************

α-Synuclein WT      AGAGCAAGTGACAAATGTTGGAGGAGCAGTGGTGACGGGTGTGACAGCAGTAGCCCAGAA
SC_663+P99          AGAGCAAGTGACAAATGTTGGAGGAGCAGTGGTGACGGGTGTGACAGCAGTAGGCCAGAA
                    ************************************************************

α-Synuclein WT      GACAGTGGAGGGAGCAGGGAGCATTGCAGCAG-CCACTGGCTTTGTCAAAAAGGACCAGT
SC_663+P99          GACAGTGGAGGGAGCAGGGGAAATTGCAGCAGGGCACTGGCTTTGTCAAAAAGGACCAGG
                    ******************...**********  *************************

α-Synuclein WT      TGGGCAAGAATGAAGAAGGAGCCCCACAGGAAGGAATTCTGGAAGATATGCCTGTGGATC
SC_663+P99          GGAGCAAGAATGAAGAA-GNGCCCCACAGGAAGGAATTCTGGAAGATATGCCTGTGGATC
                     *.************** * ****************************************

α-Synuclein WT      CTGACAATGAGGCTTATGAAATGCCTTCTGAGGAAGGGTATCAAGACTACGAACCTGAAG
SC_663+P99          CTGACAATGGGGCTTATGA-AAGCCTTGTGAGGAAGGGTATCGAGACTACGAACCTGAAG
                    *********.********* *:***** **************.*****************

α-Synuclein WT      CCTAA-------------------------------------------------------
SC_663+P99          GCAAGGTTATCGGTAGCAAGGGCGGGGAGCTGTTCGCCNGGTGGTGCCCATCCTGTCGNN
                     *:*.

α-Synuclein WT      -------------------------------------------------------------
SC_663+P99          CTGNACGGCGAGCGTAAACGGCCACAAGTCAGCGNNNGGGNGNNNNNNNGNNNNNNNNNN

α-Synuclein WT      ---
SC_663+P99          NNN
```

(B)

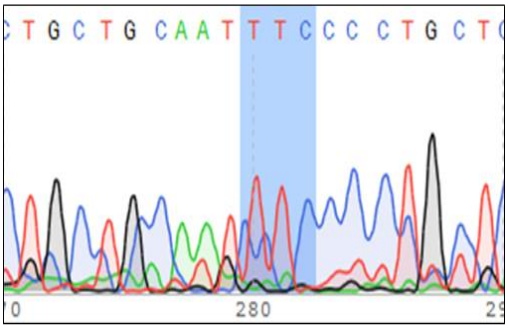

(C)

```
CLUSTAL O(1.2.1) multiple sequence alignment

α-Synuclein WT      ---------------------------------------------ATGGATGTATTCATGA
SC_658+P99          GAGGGAATTTTAAGGATGTATTCATGAAAGGACTTTCAAAGGTTATGGATGTATTCATGA
                                                                 ****************

α-Synuclein WT      AAGGACTTTCAAAGGCCAAGGAGGGAGTTGTGGCTGCTGCTGAGAAAACCAAACAGGGTG
SC_658+P99          AAGGACTTTCAAAGGCCAAGGAGGGAGTTGTGGATGCTGCTGAGAAAACCAAACAGGGTG
                    ************************************.************************

α-Synuclein WT      TGGCAGAAGCAGCAGGAAAGACAAAAGAGGGTGTTCTCTATGTAGGCTCCAAAACCAAGG
SC_658+P99          TGGCAGAAGCAGCAGGAAAGACAAAAGAGGGTGTTCTGTATGTAGGCTCCAAAACCAAGG
                    ************************************ ************************

α-Synuclein WT      AGGGAGTGGTGCATGGTGTGGCAACAGTGGCTGAGAAGACCAAAGAGCAAGTGACAAATG
SC_658+P99          AGGGAGTGGTGCATGGTGTGGCAACAGTGGCTGAGAAGACCAAAGAGCAAGTGACAAATG
                    ************************************************************

α-Synuclein WT      TTGGAGGAGCAGTGGTGACGGGTGTGACAGCAGTAGCCCAGAAGACAGTGGAGGGAGCAG
SC_658+P99          TTGGAGGAGCAGCGGTGACGGGTGTGACAGCAGTAGCCCAGAAGACAGTGGAGGGAGCAG
                    ************ ************************************************

α-Synuclein WT      GGAGCATTGCAGCAGCCACTGGCTTTGTCAAAAAGGACCAGTTGGGCAAGAATGAAGAAG
SC_658+P99          GGGAAATTGCAGCCGCCACTGGGTTTGTCAAAAAGGACCAGTTGGGCAAGAATGAAGAAG
                    **...********.******** ************************************

α-Synuclein WT      GAGCCCCACAGGAAGGAATTCTGGAAGATATGCCTGTGGATCCTGACAATGAGGCTTATG
SC_658+P99          GAGCCCCACAGGAAGGAATTGTGGAAGATATGCCTGTGGATCCTGACAATGAGGCTTATG
                    ******************** ****************************************

α-Synuclein WT      AAATGCCTTCTGAGGAAGGGTATCAAGACTACGAACCTGAAGCCTAA-------------
SC_658+P99          AAATGCCTGATGAGGAAGGGTATCAAGACTACGAACCTGAAGCCAAGCTTATCGATAGCA
                    ******** .**********************************:*.

α-Synuclein WT      ------------------------------------------------------------
SC_658+P99          AGGGCGAGGAGCTGTTCACCGGGGAGGTGCCCATCCTGGTCGAGGTGTGACGGCGAGCGT

α-Synuclein WT      ----------------------------------
SC_658+P99          AAACGGCCCATCAAGTCAGCGTTCCCGGGGACGG
```

(D)

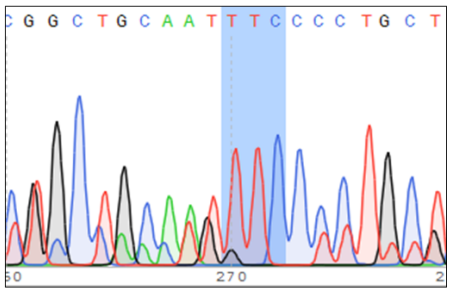

(E)

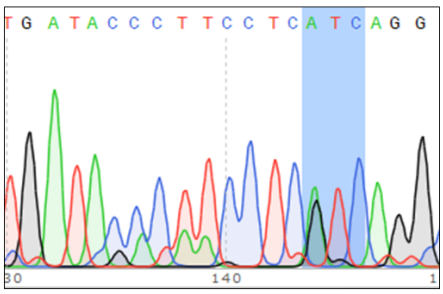

Figure 8.2. Identity confirmation of the phospho-mutant yeast strains encoding for S87E αSyn and S87E_S129D αSyn. (A) and (C) Results from the DNA sequencing (Sanger sequencing) sequences obtained full aligned with WT αSyn coding gene sequence, using *ClustalOmega* bioinformatics tool. (A) The presence of the desired mutation is highlighted in green (substitution of the AGC codon – encoding for the amino acid S – for the GAA codon – encoding for the amino acid E), confirming the identity of the SC_663 yeast strain (encoding for S87E_αSyn) and (C) The presence of the desired mutations are highlighted in green (substitution of the AGC codon – encoding for the amino acid S – for the GAA codon – encoding for the amino acid E) and yellow (substitution of the TCT codon – encoding for the amino acid S – for the GAT codon – encoding for the amino acid D) confirming the identity of the SC_658 yeast strain (encoding for S87E_S129D αSyn). (B), (D) and (E) Degree of confidence on the presence of the desired amino acid substitution obtained from the DNA sequencing (highlighted

in blue) of the (B) S87E substitution of the SC_663 yeast strain (encoding S87E αSyn), (D) S87E and (E) S129 substitutions of the SC_658 yeast strain (encoding S87E_S129D αSyn) (highlighted in blue).

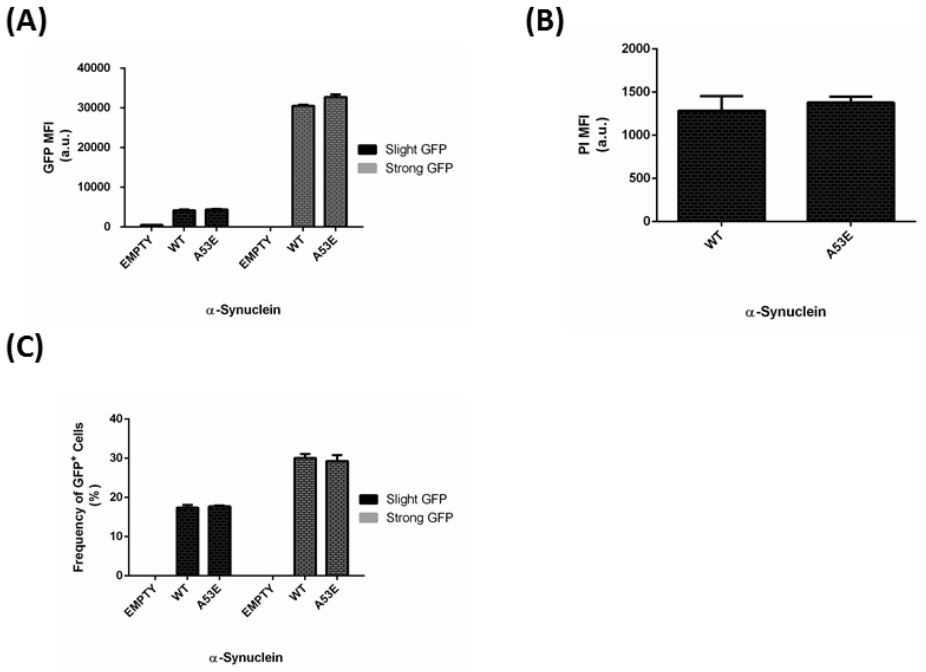

Figure 8.3. Validation of the results for the toxicity induced by the A53E αSyn mutant. (A) GFP MFI of the two distinct subpopulations expressing GFP (slight and strong GFP) for the Empty, WT and A53E assays (B) PI MFI comparison between cells expressing WT and A53E αSyn and (C) Percentage of cells expressing αSyn protein (GFP^+ cells), assessed by flow cytometry analysis. A representative result is shown from at least three independent experiments. Values represent the mean ± SD and statistical analysis were performed by One-Way ANOVA with Bonferroni's multiple comparison test.

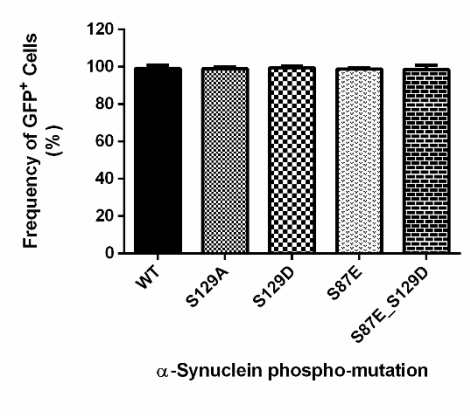

Figure 8.4. Validation of the results for toxicity assessment of the αSyn phospho-mutations expression for yeast cells. Frequency of percentage of cells expressing αSyn (GFP^+ cells) assessed by flow cytometry analysis as a control for αSyn expression homogeneity amongst the phospho-mutants. A representative result is shown from at least three independent experiments. Values represent the mean ± SD and statistical analysis were performed by One-Way ANOVA with Bonferroni's multiple comparison test.

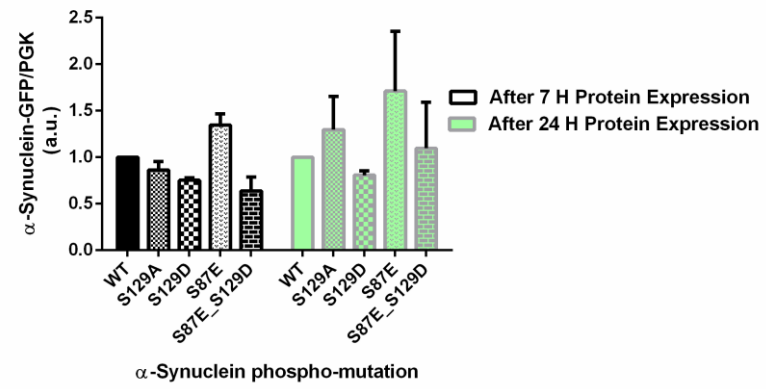

Figure 8.5. Validation of the results for the effect of the phospho-mutations on uGFP levels, for proteasome function evaluation. Densitometric analysis of the immunodetection of αSyn relative to the intensity obtained for PGK, used as loading control, presented in arbitrary units (a.u.). Results shown are representative of one experiment containing three biological replicates. Values represent the mean ± SD and statistical analysis were performed by One-Way ANOVA with Bonferroni's multiple comparison test.